DYNAMICAL CONTROL OF THE COHERENT FORWARD SCATTERING OF XUV AND X-RAY RADIATION

A Dissertation

by

TIMUR RINATOVICH AKHMEDZHANOV

Submitted to the Office of Graduate and Professional Studies of
Texas A&M University
in partial fulfillment of the requirements for the degree of

DOCTOR OF PHILOSOPHY

Chair of Committee,	Olga Kocharovskaya
Committee Members,	Alexey A. Belyanin
	Alexei V. Sokolov
	Philip R. Hemmer
Head of Department,	Peter McIntyre

May 2017

Major Subject: Physics

ABSTRACT

This work aims at development of new dynamical methods to control a resonant light-matter interaction as well as at their application for producing new sources of coherent intense sub-fs radiation in x-ray range. The dynamical control is based on modulation in time and in space of the parameters of the atomic transition (coupled to the resonant high-frequency field) by means of sufficiently strong off-resonant low-frequency control field. In particular, it may result in efficient transfer of quasi-monochromatic VUV or XUV radiation into ultrashort pulses via its resonant interaction with atomic hydrogen gas or plasma of hydrogen-like ions respectively by means of two different techniques: time and space dependent linear Stark effect or interruption of resonant interaction by the tunneling ionization, as shown in previous works of our group.

In this thesis, I further develop these ideas and demonstrate their important potential applications. First of all, both techniques are extended to arbitrary (non-hydrogen-like) atomic medium. Furthermore, advanced analytical and numerical solutions describing a process of pulses formation are found and shown to be in excellent agreement with each other. A deep physical analogy between the processes of coherent forward scattering of γ-ray radiation in the vibrated quasi-resonant nuclear absorber and the XUV field propagation in the quasi-resonant atomic medium in the presence of the moderately strong IR field is established.

Finally, the application of the developed techniques for production of intense coherent attosecond sources of soft X-ray radiation, including so-called “water window”

range (2.2-4.3nm) (especially promising for dynamical imaging of the proteins in a living cell) is proposed. Two different paths towards production of intense coherent attosecond pulses in a soft X-ray range are suggested: (i) via efficient transformation of the picosecond radiation of the high energy pulses of the existing x-ray plasma lasers into the trains of attosecond pulses in the resonant passive plasma, and (ii) via amplification of the low energy pulses of the existing high harmonic sources in the resonant active plasma of x-ray lasers.

DEDICATION

To

My wife Fechukwu Chudy-Onwugaje

With love

ACKNOWLEDGEMENTS

I would like to thank my advisor Prof. Olga Kocharovskaya for her support and guidance during all the years that I was a graduate student at Texas A&M University. I learned a lot from her and got numerous insights into physical problems during our conversations.

It was a great pleasure to work on the research in collaboration with my colleagues and mentors. Especially I would like to thank Dr. Vladimir Antonov, whose advices and support helped me a lot during all the stages of my PhD studies. I really appreciated the time Dr. Farit Vagizov has dedicated to teaching me the basics of the experiments he is doing in the lab. Fruitful discussions with Dr. Y. Radeonychev, Dr. M. Emelin, Dr. M. Ryabikin, Dr. S. Suckewer and Dr. A. Goltsov has always been motivating and encouraging. Their advices helped me to move forward much faster and broadened my understanding of physics of many processes. Dr. Alexei Sokolov, Dr. Alexey Belaynin and Dr. Philip Hemmer, who are my committee members, helped and motivated me with their suggestions, questions and advices during all the stages of this work.

I am really grateful to Dr. Marlan Scully for his participation in our discussions, his fresh ideas and the fantastic atmosphere of the Institute of Quantum Science and Engineering. His support allowed me to participate in a lot of wonderful events, including PQEs and TAMU-Casper Summer Schools.

Thanks also go to my friends and classmates at Texas A&M University who made my student years such a fun experience. Roman Chyzh, Roman Kogan, Pavel Lapa, Sasha

Zhdanova, Petr Zhokhov, Aysen Tatarinov, Oleks Tansky, Anton Shutov, Masha Shutova and many other – thank you, friends!

Finally, I am very grateful to my wife and her family, my parents and my brother for their continuous unconditional support.

CONTRIBUTORS AND FUNDING SOURCES

Contributors

This work was supervised by a dissertation committee consisting of Professor Olga Kocharovskaya of the Department of Physics and Astronomy (advisor), Professor Alexey Belyanin of the Department of the Department of Physics and Astronomy, Professor Alexey Sokolov of the Department of Physics and Astronomy and Professor Philip Hemmer of the Department of Electrical and Computer Engineering.

All work for the dissertation was completed by the student, in collaboration with Professor Olga Kocharovskaya of the Department of Physics and Astronomy, Dr. Farit Vagizov of the Department of Physics and Astronomy, Dr. Vladimir Antonov of Institute of Applied Physics of Russian Academy of Sciences (Nizhny Novgorod, Russia) and Dr. Evgeny Radeonychev of Institute of Applied Physics of Russian Academy of Sciences (Nizhny Novgorod, Russia).

Funding Sources

Graduate studies were supported by Herman F. Heep and Minnie Belle Heep Texas A&M University Endowed Fund held/administrated by Texas A&M Foundation. The research was supported by the National Science Foundation (NSF) grant PHY-1307346 and PHY-1506467 and the Robert A. Welch Foundation (Award A-1261). I acknowledge Texas A&M High Performance Research Computing for the use of supercomputer time.

TABLE OF CONTENTS

Page

LIST OF FIGURES

Page

CHAPTER I[1]

INTRODUCTION

All fundamental optical processes (absorption, emission, propagation, refraction, fluorescence, and scattering of light) are greatly enhanced near atomic resonances. Such resonant processes have been widely used both to probe matter and to manipulate light itself. Recently much attention has been paid to the possibilities to control the interaction of the signal typically high-frequency field with a resonant medium by means of a strong low-frequency coherent control field. Such coherent control of resonant light-matter interaction may be implemented under two essentially different scenarios. The first one is the situation when both the signal and control field resonantly interact with the adjacent transitions and became coupled to each other through the excitation of two photon coherence (Figure 1(a)). The second one when control field is off-resonant with any atomic transition but it is strong enough to modulate in time and/or in space the parameters

[1] Partially reprinted with permission from "Formation of ultrashort pulses from quasimonochromatic XUV radiation via infrared-field-controlled forward scattering" by T.R. Akhmedzhanov, V.A. Antonov and O. Kocharovskaya, 2016, Phys. Rev. A, vol. 94, pp. 023821, Copyright [2016] by American Physical Society; "Attosecond pulse formation via switching of resonant interaction by tunnel ionization" by V.A. Antonov, T.R. Akhmedzhanov, Y.V. Radeonychev and O. Kocharovskaya, 2015, Phys. Rev. A, vol. 91, pp. 023830, Copyright [2015] by American Physical Society; "Attosecond pulse formation via switching of resonant interaction by tunnel ionization" by T.R. Akhmedzhanov, V.A. Antonov, Y.V. Radeonychev and O. Kocharovskaya, 2015, *Proc. SPIE* 9589, X-Ray Lasers and Coherent X-Ray Sources: Development and Applications XI, 95890W, Copyright [2015] by SPIE; "Ultimate capabilities for few-cycle pulse formation via resonant interaction of XUV radiation with IR-field-dressed atoms" by T. R. Akhmedzhanov, M.Yu. Emelin, V. A. Antonov, Y. V. Radeonychev, M.Yu. Ryabikin, and Olga Kocharovskaya, 2017, accepted to Phys. Rev. A, Copyright [2017] by American Physical Society; "Coherent forward scattering of gamma-ray and XUV radiation in the medium with the modulated quasi-resonant transition" by T.R. Akhmedzhanov, V.A. Antonov and O. Kocharovskaya, 2016, J. Phys. B: At. Mol. Opt. Phys., vol. 49**,** pp. 205602, Copyright [2016] by IOP Publishing; the related work "Formation and amplification of sub-femtosecond X-ray pulses in a plasma medium of the hydrogen-like ions with a modulated resonant transition" by T.R. Akhmedzhanov et al. will be submitted to journal publication soon.

of atomic transition resonant to the signal field (Figure 1(b)). Both approaches are united by using induced quantum interference.

The first approach based on resonant interaction of the control field with a transition adjacent to the transition resonant to the signal field proved to be very fruitful. Such phenomena as coherent population trapping (CPT), electromagnetically induced transparency (EIT), lasing without inversion (LWI) (based on control of resonant absorption) and slow and stored light (based on the control of the refraction index) have been intensively studied both theoretically and experimentally in many laboratories around the world (for reviews see [1-9]). An enormous interest in this field of research has been motivated by a high potential for applications, including spectroscopy, metrology and magnetometry [10,11], resonant nonlinear optics [12-15], controllable optical delay lines [16,17], quantum memories [18-21], etc.

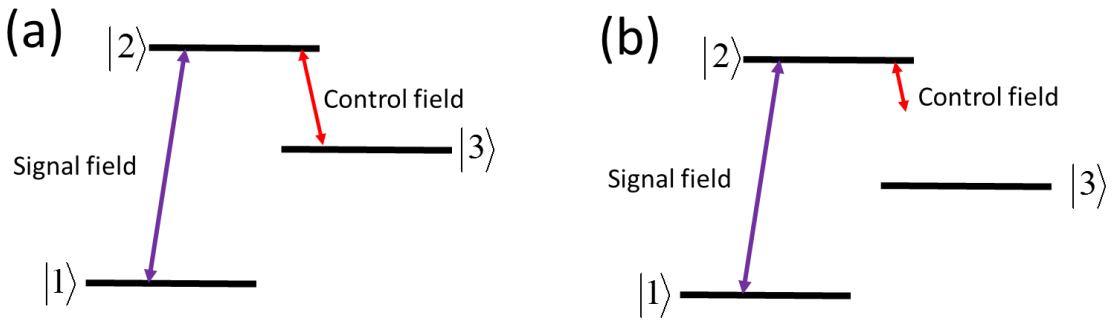

Figure 1. Two scenarios of coherent control of resonant light-matter interaction. Signal field, shown by violet arrow, is interacting with resonant atomic transition. This interaction is controlled by low-frequency control field, shown by red arrow. (a) both the signal and control field resonantly interact with the adjacent transitions and became coupled to each other through the excitation of two photon coherence. (b) control field is off-resonant with any atomic transition but it is strong enough to modulate in time and/or in space the parameters of atomic transition resonant to the signal field

Recently the second approach based on dynamical control of the resonant interaction has become a topic of active theoretical and experimental studies In particular, interaction of VUV and XUV radiation produced via high harmonic generation (HHG) with the atomic or molecular medium that is simultaneously coupled to the strong far-off-resonant infrared or visible laser radiation has been intensively studied [22-33]. The properties of the medium and, thus, the way it interacts with the VUV and XUV radiation, can be dynamically controlled by changing the parameters of the control IR field, such as its frequency and intensity. The applications of such dynamical control of forward scattering of VUV and XUV radiation such as modulation of both ionization yield [22,34,35] and absorption of the individual spectral components of XUV field as a function of the IR field delay [24,26,36], as well as suppression or enhancement of some spectral components of the incoming radiation [27,33] have been widely discussed. Another promising application, namely, the possibility of efficient transformation of quasi-monochromatic VUV or XUV into the train or individual sub-femtosecond pulses in the hydrogen atomic gas or plasma of the hydrogen-like ions has been proposed and developed in a series of works of our group [37-42].

Two regimes of pulse formation were suggested: (i) via the linear Stark effect caused by the nonionizing z-polarized IR field propagating in x-direction [38,41], and (ii) via interruption of the resonant interaction due to rapid excited-state tunneling ionization [37,40,42]. In the first case, the pulse formation relies on adiabatic (quasi-static) splitting of the degenerate resonant excited atomic energy level in space and time due to the linear AC Stark effect. Namely, under the action of modulating field the instantaneous energies

of the excited energy sub-levels (dressed by IR field) linearly depend on the instantaneous value of modulating field at the considered moment of time and point in space. This modulation results in appearance of Stokes and anti-Stokes sidebands of an incident field in the coherently forward scattered radiation. The phases of these sidebands can be matched with the proper choice of the modulation index.

The second regime is based on sudden interruption of the resonant interaction of the XUV field with the medium twice within IR field cycle due to depletion of the resonant excited state by ionization near the peaks of absolute value of the IR field. It requires stronger IR field providing large ionization rate compared to the maximum value of the Stark shift and may lead to formation of extremely short isolated pulses [37]. The theoretical analysis of pulse formation in the optically thin medium in both regimes was conducted by different methods: i) numerical solution of density matrix equation within a three-level and two-level models (for the first and second regimes, accordingly), including time and space-dependent Stark shifts and excited state ionization rates [37,38,40-42]; ii) approximate analytical solution of those equations in the first regime [38,40].

It is worth to emphasize that the proposed mechanisms hold a promise for a very important application, namely, for producing the intense coherent sub-fs sources of soft-X-ray radiation, which presents the major motivation for this work.

Indeed, such coherent intense sub-femtosecond soft x-ray pulses would open extremely wide applications for dynamical, element-specific microscopy and diffraction imaging in chemistry, biology, medicine, nanoscience and material science, providing unique combination of the unprecedented high spatial and temporal resolution, ultimately

determined by the nm carrier wavelength and attosecond pulse duration accordingly (see reviews on x-ray lasers [43-52] and attosecond physics [53-61]). Production of the bright ultrafast coherent sources in a "water window" range (between the C and O K-shell absorption edges at 284–540 eV, i.e. 4.4–2.3 nm), is considered to be especially important for imaging of the protein dynamics in the living cells [44-68].

Currently there are three types of coherent sources in the soft x-ray wavelength range: free-electron lasers [69-76], x-ray plasma-based lasers [46-48,50,77,78] and high harmonic generation (HHG) sources [64-68]. Free-electron lasers produce high energy pulses, but the pulse duration is currently limited by fs and pulses are typically not transform limited due to the short noise. Such lasers present themselves large-scale state-of-the-art expensive facilities and there are only few of them available in the world. Table-top soft x-ray plasma-based lasers produce relatively high energy pulses (up to several mJ) but of rather long pico-second duration. The HHG sources allow producing thousands of high harmonics stretching into x-ray range. Potentially, they can constitute the attosecond x-ray pulses (under condition of atto-chirp compensation), but the harmonics energy in the soft x-ray range, in particular, in a water window range, does not exceed nJ due to the low (less than 10^{-7}) conversion efficiency.

This dissertation aims at the following goals:

1. To generalize the regime of pulses formation, based on modulation of the resonant excited atomic state by the nonionizing IR field from the hydrogen-like to the non-hydrogen-like medium.

2. To clarify the physics beyond the second regime of pulses formation and to get an analytical solution describing this regime.

3. To get an analytical solution describing the transition from the first to the second regime with an increase of the intensity of the control field.

4. To determine the ultimate capabilities and the limits of applicability of both methods of pulses formation based on direct simulation of the time-dependent Schrodinger equation and its comparison with the approximate analytical solutions of the simplified three-level model.

5. To establish a close physical analogy between coherent forward scattering of γ-ray radiation in the vibrating quasi-resonant nuclear absorber and the XUV field propagation in the quasi-resonant atomic medium in the presence of the moderately strong IR field.

6. To develop the new application of the proposed technique for producing of intense coherent attosecond sources of soft-X-ray radiation via two different paths, namely, (i) via efficient compression of picosecond radiation of x-ray plasma lasers into attosecond pulse trains without essential loss of the energy; (ii) via amplification of an individual high-harmonic radiation in an active medium of x-ray lasers accompanied by formation of attosecond pulses.

The structure of the thesis is as follows.

In Chapter II, a highly efficient method of ultrashort pulse formation from the resonant XUV radiation due to sub-laser-cycle modulation of the excited state of non-hydrogen-like atoms by a nonionizing IR laser field is suggested. This modulation results

in formation of the Raman Stokes and anti-Stokes sidebands in coherently forward scattered radiation, which, in turn, leads to formation of short pulses, when the phases of the sidebands are matched. This method is a generalization of recently suggested technique [38] to non-hydrogen-like medium. Possibility to form 2 fs XUV pulses in the gas of helium atoms and 990 as XUV pulses in the plasma of Li+ ions with efficiencies over 80% is shown.

In Chapter III, an analytical solution uncovering the origin of few-cycle attosecond pulse formation from vacuum-ultraviolet (VUV) radiation in an atomic gas simultaneously irradiated by a moderately strong infrared (IR) laser field, which does not perturb atoms in the ground state, but induces rapid quasistatic ionization from the excited states [42], is derived. The derived solution shows that the pulses are produced due to periodic switching of the resonant interaction between the incident VUV radiation and the atoms: turning it off near the crests of the IR-field strength and switching it back on near the IR field zero-crossings. The method originally proposed in [42] is extended to non-hydrogenlike media and it is shown that the pulses can be produced from resonant VUV radiation in a variety of atomic gases. The pulses are nearly bandwidth-limited without external adjustment of phases of the generated sidebands. Proximity of the carrier frequency of the produced pulses to intra-atomic resonances may allow their utilization for nondestructive steering of ultrafast dynamics of the bound electrons. The experimental possibilities for attosecond pulse formation from 58.4 nm VUV radiation in helium and from 73.6 nm VUV radiation in neon dressed by the 3.9 μm laser field, as well as from 122 nm VUV radiation in atomic hydrogen dressed by CO_2-laser field are discussed.

In Chapter IV, possibility to form a single attosecond pulse using the ionization switching mechanism in He atoms is shown. Formation of a train of attosecond of attosecond pulses manifests multifrequency response of atoms to XUV field. In order to form a single pulse, one needs to restrict such a response to an ultrashort period of time. This can be done using IR pulse with steep front edge [37]. In this approach XUV field resonantly excites resonance coherence which is then ionized by the coming IR field in less than its period. Thus, multifrequency response of atoms is effectively limited to an ultrashort period of time, which allows formation of a single attosecond pulse.

In Chapter V, an *ab initio* study of the ultimate capabilities and limits of applicability of the method for few-cycle pulse formation via the resonant interaction of an extreme ultraviolet (XUV) radiation with atoms dressed by moderately strong infrared (IR) laser field is performed. Taking into account all the multiphoton processes in the systems under consideration on the basis of numerical solution of the three-dimensional time-dependent Schrödinger equation (TDSE) in the single-active-electron approximation, the possibility to produce 1.1 fs pulses from 124.6 nm XUV radiation via linear Stark effect in atomic hydrogen, as well as 500 as pulses from 58.4 nm XUV radiation via excited-state ionization in helium is shown. A generalized analytical solution, which takes into account the interplay between sub-laser-cycle Stark effect and excited-state ionization and allows to analyze the results of TDSE calculations is derived. It is found that the ultimate intensity of the IR field suitable for few-cycle pulse formation via the linear Stark effect or excited-state-ionization is limited by the threshold for atomic ionization from the resonant excited state or the ground state, respectively.

In Chapter VI, a close physical analogy between coherent forward scattering of γ-ray radiation in the vibrating quasi-resonant nuclear absorber and the XUV field propagation in the quasi-resonant atomic medium in the presence of the moderately strong IR field is established. Both processes, under certain conditions, are described by similar Maxwell-Bloch equations for a two-level medium with modulated parameters of the resonant transition. It results in similar transformation of both γ-ray and XUV fields at the exit from the medium, fully determined by the characteristics of applied modulation and spectral content of the incident fields. An appropriate analytical solution describing transformation of the electromagnetic field as a result of its propagation in the modulated medium is derived. It is shown, in particular, that recently observed effects of (i) suppressed resonant absorption in coherent γ-ray scattering of vibrating absorber and (ii) ionization rate modulation in IR pump - XUV probe experiments, present themselves as different manifestations of the same general physical phenomenon of modulation induced transparency (MIT). That transparency is induced by modulating the parameters of the resonant transition. While only partial MIT was observed so far, certain conditions for conducting some realistic experiments, which should demonstrate nearly 100% transparency in both processes, are suggested.

In Chapter VII, a technique to form amplified trains of sub-femtosecond pulses from an incident weak X-ray radiation in the active medium of such lasers via modulation of the frequency of an operating transition by a moderately strong IR or optical laser field is suggested. Such modulation leads to appearance of the number of sidebands of the X-ray radiation accompanied by its amplification in the inverted resonant medium. With the

proper choice of the parameters of the system, most of sidebands are in phase with each other, which results in a formation of a train of strong sub-femtosecond X-ray pulses at the output of the medium. Experimental realizations of the suggested technique in the active media of Li III ions modulated by the mid-IR laser and of C VI ions modulated by the optical laser is proposed.

CHAPTER II

FORMATION OF ULTRASHORT PULSES FROM QUASI-MONOCHROMATIC XUV RADIATION VIA INFRARED-FIELD-CONTROLLED FORWARD SCATTERING[2]

II.1 Introduction

Sub-femtosecond XUV pulses provide a unique combination of high spatial and time resolution and find numerous applications to capture the motion of electrons, atoms, and molecules in real time, to observe element-specific dynamics at the M- and L- shells absorption edges of magnetic materials, etc. [27,61,79-82]. The conventional way of producing such ultrashort XUV pulses in table-top setup is high harmonic generation (HHG) in gases [65,83]. This method allows formation of very short pulses (up to 67 as [84]). However, the efficiency of conversion of visible or IR laser radiation into high harmonics is low. In particular, in the water window 2.3-4.4nm, it is 10^{-8}-10^{-9} [66,67]. It results in low total energy of the generated pulse trains (on the order of nJ) which limits their applications. Much higher energy per pulse can be achieved at XFELS in a few femtosecond regime, but there are only few such facilities in the world [70,76,85,86]. Modern table-top X-ray lasers are able to generate high energy (in the mJ range) X-ray pulses, but with relatively long duration in the range of few picoseconds [63,78,87]. Thus,

[2] Reprinted with permission from "Formation of ultrashort pulses from quasimonochromatic XUV radiation via infrared-field-controlled forward scattering" by T.R. Akhmedzhanov, V.A. Antonov and O. Kocharovskaya, 2016, Phys. Rev. A, vol. 94, pp. 023821, Copyright [2016] by American Physical Society.

a highly efficient method of transformation of an output pulse of X-ray laser into the sub-femtosecond pulses would be very desirable.

Recently, a technique for production of ultrashort pulses from a quasi-monochromatic XUV radiation via the resonant interaction with atoms, dressed by a moderately strong IR laser field was suggested [41,42] and studied [37,38,40]. The two regimes of pulse formation were considered: (i) via the linear Stark effect in hydrogen-like medium, irradiated by the nonionizing IR field, and (ii) via rapid excited-state-ionization in arbitrary atomic gas. In the first case, the pulse formation relies on adiabatic (quasi-static) splitting of the resonant excited atomic energy level in space and time due to the linear AC Stark effect. Namely, under the action of modulating field the instantaneous values of transition frequencies from the ground to excited energy levels linearly depend on the instantaneous value of modulating field at the considered moment of time and point in space. The degeneracy of the first excited energy level of hydrogen (or a hydrogen-like ion) and the anti-phase shift of its relevant sublevels under the action of the IR field play a key role in the pulses formation. The second regime is based on sudden interruption of the resonant interaction of the XUV field with the medium due to the complete atomic ionization from the resonant excited state within each half-cycle of the IR field. In this case, the produced pulses are extremely short. However, since the pulse formation is essentially based on ionization, this regime can't be realized in the active media of X-ray plasma lasers. Besides, its efficiency is essentially lower than that in the first, nonionizing, regime, which is characterized by the very high efficiency of transformation of an incident XUV radiation into the ultrashort pulse trains (close to unity)

and can be potentially realized in the active media of X-ray lasers. But, since it essentially relies on the degeneracy of the first excited state of hydrogen-like atoms, the possibility of its generalization and realization in the other atomic gases remains questionable.

In the present chapter we suggest the generalization of the technique, based on modulation of the resonant excited atomic state by the nonionizing IR field. This approach is not restricted to the atoms of hydrogen and hydrogen-like ions with degenerate excited energy levels. Below, we consider its implementation in the medium of helium or helium like ions, but it can be realized in a variety of atomic gases, which makes its experimental realization more feasible and promising for wider potential applications. By using Floquet formalism [88], we study the formation of a train of ultrashort pulses from quasi-monochromatic XUV radiation in the gas of IR-field-dressed He atoms. We investigate the case of not too strong IR field, when the role of ionization is negligible in comparison with mixing and modulation of the excited atomic states. Under the action of IR field the excited states of atoms are properly described in Floquet basis [88], rather than in the bare one. It is shown, that the parameters of the IR field can be optimized in a way that one of the Floquet states produces a few in-phase sidebands of an incident field with comparable amplitudes. If the incident XUV field is tuned in resonance with this state, the scattered XUV field contains a few sidebands in phase with each other, which, after attenuation of an incident spectral component to the level of generated sidebands, leads to formation of a train of ultrashort pulses. Firstly, within a three-level model of He atom, we show that the pulses with time duration of 2 fs can be produced at the output of an optically thin medium of He atoms. Secondly, we verify that neither the presence of higher lying discrete

excited states nor ionization affect the possibility of pulse formation. Thirdly, we consider the propagation problem and show that the efficiency of transformation of an incident quasi-monochromatic XUV field into the train of femtosecond pulses in the optically thick medium of helium may exceed 80%. Finally, we show that with proper scaling of the parameters of an IR field, the suggested method allows formation of the train of sub-femtosecond pulses in the plasma of He-like ions with an efficiency 87.4%.

The chapter is structured as follows. In Section II.2, we analyze the spectral and temporal properties of the XUV field scattered by an optically thin layer of He atoms within a three-level approximation, using Floquet approach [88]. We show that for the properly chosen dressing IR field wavelength and intensity, a train of ultrashort pulses can be produced at the output of the medium. In Section II.3, we study an influence of the higher lying excited states and ionization from the excited states on the pulse formation. At first, we consider 5 level model of He and show that taking into account of the two extra excited states does not change the pulse shape appreciably. After that we confirm the possibility of the pulse formation by solving the full time dependent Schrodinger equation (TDSE), taking into account all the bound and continuum states of an atom in a single active electron approximation. In Section II.4 we numerically study the propagation of an XUV field in the optically thick medium and demonstrate high efficiency of transformation of the incident radiation into the train of ultrashort pulses. In Section II.5 we discuss a possibility to reduce the pulse duration using plasma of He-like ions and derive the scaling law which allows immediately find the IR field parameters required for

pulse formation in He-like media. In Section II.6, we summarize the main results of the chapter. Atomic units are used throughout the chapter, unless specified otherwise.

II.2 Three-level model

Let us consider the linearly polarized quasi-monochromatic XUV radiation, propagating along *x*-axis through the atomic gas with quasi-resonant atomic transition from the ground state, $|1\rangle$, to an excited state, $|2\rangle$. At the input of the medium ($x = 0$), the field is given by:

$$\vec{E}(x,t) = \vec{z}_0 \frac{1}{2} \tilde{E}(x,t) \exp\{-i\omega\tau\} + \text{c.c.}, \qquad \text{(II.1)}$$

where $\vec{z}_0$ is the unit vector directed along the polarization of the field, $\tilde{E}(x,t)$ is an amplitude of the field, ω is its carrier frequency, *c* is the speed of light in vacuum, and **c.c.** stands for complex conjugation. $\tau = t - x/c$ is the local time in the reference frame, co-moving with the X-ray radiation wave. The XUV field is considered to be sufficiently weak so that it does not change the population of the ground and excited states during the interaction time. We consider an interaction of the XUV field with the atomic gas in the presence of an additional linearly polarized IR field, propagating in the same direction as the XUV radiation:

$$\vec{E}_{IR}(x,t) = \vec{z}_0 \tilde{E}_{IR} \cos(\omega_{IR}\tau), \qquad \text{(II.2)}$$

where $\tilde{E}_{IR}$ is amplitude of IR field, ω_{IR} is its frequency. The IR field is moderately strong: it does not couple the ground state to the excited states, but it couples the state $|2\rangle$ to another excited state $|3\rangle$.

Mixing of the states $|2\rangle$ and $|3\rangle$ by the IR field leads to appearance of two Floquet states [88]. The wave function of the IR-field-dressed atom can be represented in the Floquet basis as follows [24]:

$$|\psi\rangle = c_1|1\rangle + \sum_{i=1,2} c_{\lambda_i} \exp(-i\lambda_i\tau)|\Phi_{\lambda_i}(\tau)\rangle, \tag{II.3}$$

where energy of the ground state is chosen to be zero. Here λ_i is the quasi-energy of the i^{th} Floquet state $|\Phi_{\lambda_i}\rangle$, which periodically depends on time and constitutes the Fourier series:

$$|\Phi_{\lambda_i}(\tau)\rangle = \sum_{m=-\infty}^{+\infty} \exp(-im\omega_{IR}\tau)\sum_{\alpha} a_m^{i;\alpha}|\alpha\rangle, \tag{II.4}$$

and c_{λ_i} is an amplitude of this Floquet state. The amplitudes $a_m^{i;\alpha}$ of Fourier components of Floquet states (II.4) and quasi-energies λ_i of these states are determined by the intensity and the frequency of the IR field and can be expressed analytically in terms of the infinite continued fractions (see, e.g. [89]). In general case $a_m^{i;\alpha}$ are the complex numbers. For the field (II.2) they can be chosen to be real. The index α enumerates excited states of a bare atom (an atom in the absence of the IR field), that is, $|2\rangle$ and $|3\rangle$ states. It is worth noting that quasi-energy of Floquet state is defined up to integral number of ω_{IR} since Floquet state $|\Phi_{\lambda_i - n\omega_{IR}}(\tau)\rangle = \sum_{m=-\infty}^{+\infty} \exp\left(-i(m+n)\omega_{IR}\tau\right)\sum_{\alpha} a_m^{i;\alpha}|\alpha\rangle$ with quasi-energy $\lambda_i - n\omega_{IR}$ is physically the same as state $|\Phi_{\lambda_i}(\tau)\rangle = \sum_{m=-\infty}^{+\infty} \exp\left(-im\omega_{IR}\tau\right)\sum_{\alpha} a_m^{i;\alpha}|\alpha\rangle$ with quasi-energy λ_i

[88]. In the following we choose the quasi-energies in a way that $m=0$ corresponds to the levels, nearest to the unperturbed energy of the 1s2p state. Another important property of Floquet states is that coefficients $a_m^{i;2}$ are not zeroes only for even m, and $a_m^{i;3}$ are not zeroes only for odd m (or vice versa – depending on the choice of the quasi-energy) [24,88,90], that is, with our choice of quasi-energies, $a_{2m+1}^{i;2}=0$ and $a_{2m}^{i;3}=0$.

If the XUV field is tuned close to the exact resonance with the transition from the ground state $|1\rangle$ to the only step with $m=k$ one Floquet state i, then, within the framework of perturbation theory, the slowly-varying amplitude of the XUV field at the output of an optically thin medium can be found as [24,90]:

$$\begin{aligned}&\tilde{E}(x,t)=\tilde{E}(0,t)+\tilde{E}_{Scatt}=\\&=\tilde{E}(0,t)-x\frac{2\pi\omega N\left|d_{2,1}\right|^2}{c\hbar}e^{-i(\lambda_i-\omega)\tau}\times\\&\times\left(\sum_{m=-\infty}^{+\infty}a_{2m}^{i,2}\exp(-2im\omega_{IR}\tau)\right)\int_{-\infty}^{\tau}\exp(i(\lambda_i-\omega)\tau')\tilde{E}(\tau')\left(a_k^{i,2}\right)^*d\tau',\end{aligned}\qquad\text{(II.5)}$$

Excitation of another Floquet state by XUV field is negligible as long as the bandwidth of incident XUV pulse is small as compared to the frequency separation between the two neighboring Floquet states (i.e. the pulse duration is sufficiently large). As it is seen from (II.5), the properties of the output field are controlled by the amplitudes $a_{2m}^{i;2}$ of Fourier components of Floquet states, which are determined by the parameters of the IR field. In order to form a train of ultrashort pulses we need to find the wavelength and intensity of the IR field that correspond to a Floquet state where the majority of coefficients $a_{2m}^{i;2}$ will have comparable amplitudes and nearly the same phases. Within the

framework of Hermitian Floquet theory, this optimization can be quickly done numerically for some specific atom. The $a_{2m}^{i;2}$ are determined by the two dimensionless parameters, namely by the ratios of the IR field frequency, ω_{IR}, and the Rabi frequency of the IR field, $\tilde{E}_{IR}d_{2,3}$ (where $d_{2,3}$ is dipole moment of transition $|2\rangle \leftrightarrow |3\rangle$), to the frequency of transition $|2\rangle \leftrightarrow |3\rangle$, those are ω_{IR}/ω_{23} and $\tilde{E}_{IR}d_{2,3}/\omega_{23}$.

Let us consider, in particular, a gas of helium atoms under the following conditions. The XUV field is weak and its frequency is close to the frequency of transition from the ground state $1s^2$ to 1s2p state. So it couples only these states, exciting polarization at the transition $1s^2 \leftrightarrow 1s2p$. The IR field is low frequency (as compared to the frequencies of transitions from the resonantly populated 1s2p state to the other states of helium) and not too strong. Taking into account that the dipole moment of transition 1s2s↔1s2p is a few times larger than those of transitions from the resonant1s2p state to the other excited states, while the frequency of transition 1s2s↔1s2p is a few times smaller, it is reasonable to consider coupling of the IR field only to 1s2s↔1s2p transition. The corresponding transition wavelengths are shown in Figure 2(a). Thus, the three-level model, including $1s^2$, 1s2s and 1s2p states (which are the states $|1\rangle$, $|3\rangle$ and $|2\rangle$ in our notation, correspondingly) is well justified in the case under consideration (the role of other excited discrete states and continuum will be investigated in the next sections).

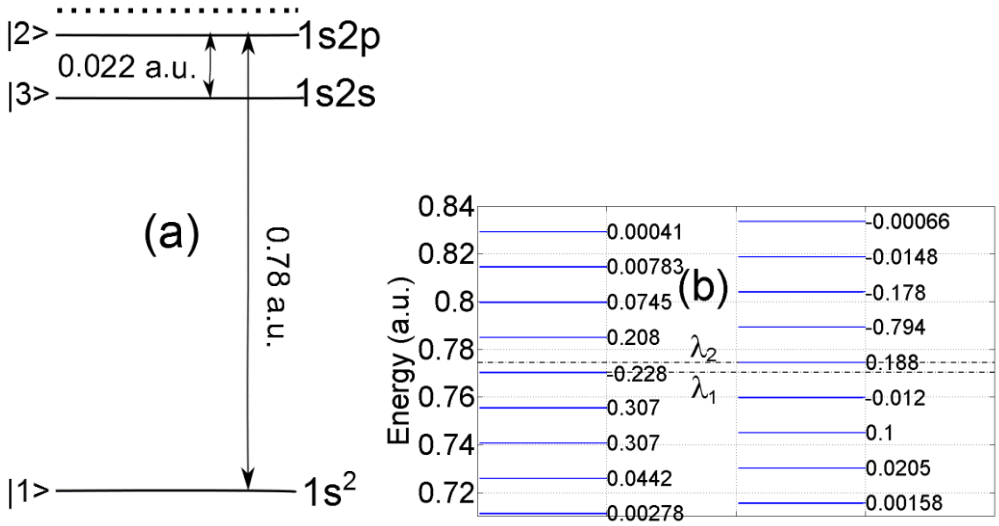

Figure 2. (a) Three level model and its implementation in helium. Vertical arrows correspond to the transition wavelengths. Transition energies are shown in atomic units. (b) Coupling of 1s2s and 1s2p states of He by the IR field leads to formation of the two Floquet states. Each state corresponds to the energy ladder with the steps separated by the IR field frequency. However, the steps containing the same state ($|2\rangle$ or $|3\rangle$) are separated by the doubled photon energy of the IR field. Only the steps containing 2p state are shown. Note that these steps don't contain 2s state, since $a_{2m}^{i;2s} = 0$ (vice versa, the steps containing 2s state don't contain 2p state, since $a_{2m+1}^{i;2p} = 0$, and hence they are not coupled to the XUV field). The vertical axis corresponds to energy in atomic units, while numbers near the steps correspond to the amplitudes $a_{2m}^{i;2p}$. The quasi-energies λ_1 and λ_2 are shown by the dashed black horizontal lines. The IR field parameters are λ=6176 nm, $I=2.5\times10^{12} W/cm^2$.

As it was already mentioned, mixing of 1s2s and 1s2p states by the IR field leads to appearance of two Floquet states. We optimize the IR field parameters in order for one of the Floquet states to have a few $a_{2m}^{i;2p}$'s of the same phase and comparable amplitudes. The result of optimization is shown in Figure 2(b). As it can be seen, the first Floquet state (the left ladder in Figure 2(b)) contains 6 sidebands of the same order of magnitude, with 5 of them having the same sign. The IR field producing this Floquet states has wavelength

6176 nm (corresponding to $\omega_{IR}/\omega_{23} \approx 1/3$) and intensity $I=2.5\times10^{12} W/cm^2$ (corresponds to $\tilde{E}_{IR} d_{23}/\omega_{23} \approx 1.11$).

The spectral structure of the resonantly scattered field is fully defined by the structure of the Floquet ladder itself. However, the XUV radiation at the output of an optically thin medium is a sum of the incident and scattered fields. In an absorbing medium, the resonant component of scattered field is always in antiphase to the incident field. Therefore, if the resonant component is in anti-phase to the others, then all the other spectral components will be in-phase with the incident XUV field, resulting in pulse formation, while if the resonant component is in-phase with the others, then most of the sidebands will be in anti-phase with the incident field, and the pulses will not be produced. Thus, the XUV field should be tuned in resonance with the step of Floquet ladder with $a_2^{1;2p} = -0.228$, which has opposite sign in comparison to the other steps. In the considered case, it corresponds to wavelength 59.16 nm. It is worth noting that in general, when the excited-state-ionization is taken into account, the quasi-energies λ_i are complex numbers [88]. In order to take into account the finite lifetime of the excited states $|2\rangle$ and $|3\rangle$ within the three-level model, we add a small complex part γ_i to both λ_1 and λ_2, $\gamma_i \ll \omega_{IR}$, $|\lambda_1 - \lambda_2|$, artificially. The value γ_i determines the half-linewidths of transitions to the ground atomic state, $|1\rangle \leftrightarrow |2\rangle$ and $|1\rangle \leftrightarrow |3\rangle$. In its turn, the bandwidth of an incident XUV field is considered to be smaller than this linewidth. Under such conditions the XUV field, scattered by atoms under the simultaneous action of monochromatic XUV and IR fields, is given by

$$\tilde{E}_{scatt} = -xA\tilde{E}_0 \frac{a_2^{1,2p}}{\gamma}\left(\sum_m a_{2m}^{1,2p} \exp(-2im\omega_{IR}\tau)\right), \tag{II.6}$$

where $A = \dfrac{2\pi\omega N \left|d_{2p1s}\right|^2}{c\hbar}$ and $\tilde{E}_0$ is incident XUV field amplitude. The validity of these assumptions is justified in the next sections via numerical solution of the full TDSE. The spectral structure of this field corresponds to the left Floquet ladder in Figure 2(b). The XUV radiation at the output of thin medium is given by the sum of scattered field and the incident field:

$$\begin{aligned}\tilde{E}(x,t) &= \tilde{E}_0 - xA\tilde{E}_0 \frac{a_2^{1,2p}}{\gamma}\left(\sum_m a_{2m}^{1,2p} \exp(-2im\omega_{IR}\tau)\right) \approx \\ &\approx \tilde{E}_0 - x\tilde{E}_0 A\frac{a_2^{1,2p}}{\gamma}\left(\sum_{m\neq 0} a_{2m}^{1,2p} \exp(-2im\omega_{IR}\tau)\right).\end{aligned} \tag{II.7}$$

Summation of the incident and the resonantly scattered fields results in phase matching of the central frequency component with the sidebands. To produce the pulses of shortest duration, the amplitude of the incident XUV field spectral component at the output of the medium should be attenuated to the level of the generated sidebands. In such a case, the output XUV field takes the form:

$$\tilde{E}(x,t) = -xA\tilde{E}_0 \frac{a_2^{1,2p}}{\gamma}\left(\sum_{m\neq 0} a_{2m}^{1,2p} \exp(-2im\omega_{IR}\tau) - a_2^{1,2p}\right). \tag{II.8}$$

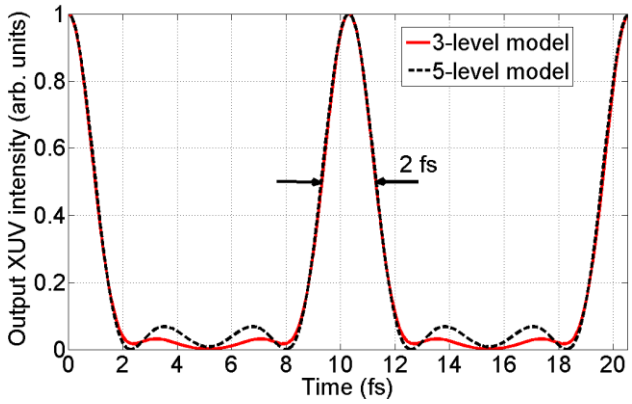

Figure 3. Intensity of the 59.16 nm XUV field at the exit of an optically thin layer of helium, irradiated by 6176 nm IR field with intensity $I=2.5\times10^{12} W/cm^2$. The solid red line corresponds to three-level model, dash black line corresponds to five-level model. The incident XUV frequency component is attenuated according to (II.8).

This field corresponds to the train of well-shaped pulses with pulse duration 2 fs, shown in Figure 3 by solid red line. An attenuation can be produced by frequency selective multilayer mirrors with half of FWHM of reflectivity curve less than $2\omega_{IR}$ [91,92]. On the other hand, it is not necessary to attenuate the incident XUV spectral component with the additional tools. Instead, one may simply increase the optical thickness of the resonant absorbing modulated medium. In the last case, the produced pulses will be slightly longer, but the efficiency of transformation of the incident XUV radiation into the pulse train can exceed 80%. The possible experimental realizations of the last approach are discussed in Sections IV and V.

It is worth noting that the pulse formation does not require exact tuning of wavelength of the IR and XUV fields, which may vary in the ranges 6100-6200 nm and 59.05-59.25 nm, respectively (although, a larger pedestal up to 0.2 of peak pulse intensity might appear).

The choice of modulation field parameters, presented above, is not unique. Namely, the proper Floquet state with comparable amplitudes and nearly the same phases of the spectral components, resulting in ultrashort pulses formation, can be produced with different choices of frequency and intensity of the IR field. For example, in Figure 4 we show the train of pulses with duration 1.2 fs and carrier wavelength 59.24 nm, formed in optically thin layer of helium atoms irradiated by 4117 nm IR field with intensity $I=8.0\times10^{12}W/cm^2$ (the incident XUV spectral component is attenuated according to (II.8)). However, in general, with further increase of intensity or shortening of wavelength of the IR field, the three-level approximation becomes invalid, so that more levels need to be taken into account. Moreover, the linewidth of the resonant XUV transition becomes broader due to the increased excited-state-ionization rate, making the selective interaction of the XUV field with the only one specific Floquet state impossible.

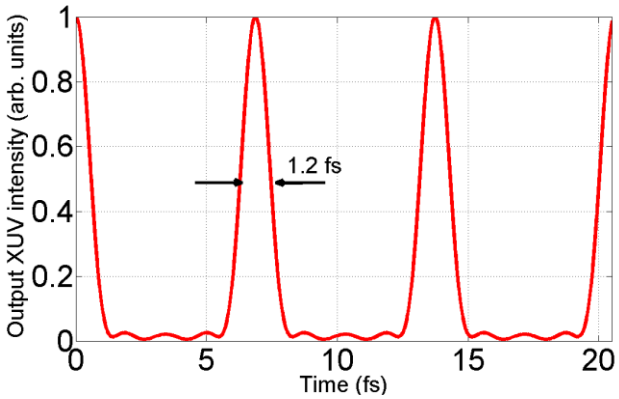

Figure 4. Intensity of the 59.24 nm field at the exit of an optically thin layer of helium irradiated by 4117 nm IR field with intensity $I=8.0\times10^{12}W/cm^2$. The incident XUV spectral component is attenuated according to (II.8).

II.3 Role of higher lying states and ionization

In this section, we study the influence of higher lying bound energy levels of helium, as well as ionization, on the spectral and temporal properties of the output XUV radiation and prove that the results, derived in previous section for the three level model, still hold within more accurate models of helium atom.

Firstly, we repeat the Floquet state calculation, taking into account five unperturbed states of helium atom, namely, $1s^2$, 1s2s, 1s2p, 1s3s and 1s3d states. We have added 1s3s and 1s3d states, since they correspond to the strongest dipole allowed transitions from 1s2p state (with an exception of the 1s2s↔1s2p transition) and are the closest to it in energy. The excited states 1s2s, 1s2p, 1s3s and 1s3d are coupled to each other by the IR field. The IR field with the same parameters, as considered in the previous section (those are wavelength 6176 nm and intensity $I=2.5\times10^{12} W/cm^2$) produces four Floquet states. One of these states has the amplitudes of the "steps" $a_{2m}^{i;2p}$'s, which are very similar to $a_{2m}^{i;2p}$'s of the one of two Floquet states, calculated within the three-level model (the corresponding ladder looks similar to the one on the left in Figure 2(b)). Excitation of this state by the resonant XUV field with the wavelength 59.23 nm (which is slightly different from the value 59.16 nm, given by the three-level model) and subsequent attenuation of the incident XUV spectral component to the level of the sidebands according to (II.8) leads to formation of the ultrashort pulse train shown in Figure 3 by dashed black line. As it can be seen, the agreement between the predictions of 3-level and 5-level models is excellent, except minor difference in pedestal shape.

Secondly, we study the influence of the higher-lying bound atomic states as well as ionization on pulse formation on the basis of numerical solution of full TDSE for helium atom simultaneously interacting with XUV and IR field. We use the numerical scheme first introduced in [93], and the model potential [94]. In order to find the proper frequency of the incident XUV field for TDSE calculation, we firstly repeat the Floquet states calculation within the five-level model of with parameters of the states $1s^2$, 1s2s, 1s2p, 1s3s and 1s3d, defined by the model potential [94]. The XUV field, quasi-resonant to the required Floquet state, has wavelength 59.24 nm. We perform TDSE calculation for He atoms placed in this XUV field along with 6176 nm IR field with intensity $I=2.5\times10^{12} W/cm^2$. As a result, we numerically find the induced dipole moment $d(t)=\langle z(t)\rangle$. The XUV field at the output of the optically thin medium is given by:

$$\tilde{E}_{XUV}(x,\tau)=\tilde{E}_{XUV}(0,\tau)-\frac{2\pi x}{c}\frac{dP}{dt},\quad P=Nd(t). \tag{II.9}$$

The squared modulus of this field after attenuation of the incident XUV spectral component to the level of the adjacent sidebands is shown in Figure 5 by the thin blue line. As it can be seen, the pulses are clearly formed and are in a rather good agreement with predictions of the three-level model, shown in Figure 5 by the bold red line. Thus, the performed calculations confirm validity of the simple three level model of He and open up the prospects for experimental realization of the suggested method.

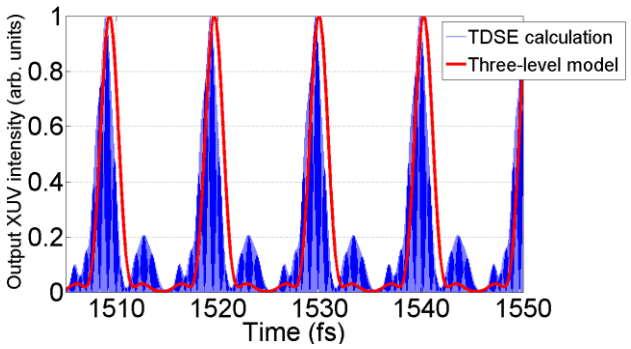

Figure 5. The results of TDSE calculation. Intensity of the 59.24 nm XUV radiation after propagation through an optically thin medium of helium, irradiated by 6176 nm IR field with intensity $I=2.5\times10^{12}W/cm^2$. The spectral component at the incident XUV radiation frequency is attenuated to the level of the adjacent sidebands.

II.4 Propagation effects and efficiency of the method

In this section we analyze the effects of propagation of the XUV radiation through the optically thick medium of helium, dressed by the IR field, on the shape of produced pulses and determine the efficiency of transformation of the incident XUV radiation into the pulse train.

Propagation of the resonant XUV field through an optically thick gas of helium irradiated by the strong IR field is described by the wave equation for the XUV field and the density matrix equations for the helium atoms. Use of the density matrix allows taking into account both ionization- and collisional-broadening of the atomic transition lines. Within the previously formulated three-level model, in the slowly varying amplitude approximation for the XUV field and the resonant polarization of the medium, as well as the rotating-wave approximation for the elements of the density matrix, and the approximation of the given amplitude of the IR field, the equations take the form

$$
\begin{cases}
\dfrac{\partial \tilde{E}}{\partial x} = i\dfrac{2\pi\omega}{c}\tilde{P} \\
\tilde{P} = 2Nd_{1s,2p}\tilde{\rho}_{2p,1s} \\
\dfrac{\partial \tilde{\rho}_{1s,1s}}{\partial \tau} = -\gamma_{1s}\tilde{\rho}_{1s,1s} + \dfrac{id_{1s,2p}}{2}\left(\tilde{E}^{*}\tilde{\rho}_{2p,1s} - \tilde{E}\tilde{\rho}_{1s,2p}\right) \\
\dfrac{\partial \tilde{\rho}_{2s,2s}}{\partial \tau} = -\gamma_{2s}\tilde{\rho}_{2s,2s} + i\tilde{E}_{IR}\cos(\omega_{IR}\tau)d_{2s,2p}\left(\tilde{\rho}_{2p,2s} - \tilde{\rho}_{2s,2p}\right) \\
\dfrac{\partial \tilde{\rho}_{2p,2p}}{\partial \tau} = -\gamma_{2p}\tilde{\rho}_{2p,2p} - \dfrac{id_{1s,2p}}{2}\left(\tilde{E}^{*}\tilde{\rho}_{2p,1s} - \tilde{E}\tilde{\rho}_{1s,2p}\right) - i\tilde{E}_{IR}\cos(\omega_{IR}\tau)d_{2s,2p}\left(\tilde{\rho}_{2p,2s} - \tilde{\rho}_{2s,2p}\right) \\
\dfrac{\partial \tilde{\rho}_{2p,1s}}{\partial \tau} = -\left(\gamma_{2p,1s} + i(\omega_{2p} - \omega)\right)\tilde{\rho}_{2p,1s} + \dfrac{id_{1s,2p}\tilde{E}}{2}\left(\tilde{\rho}_{1s,1s} - \tilde{\rho}_{2p,2p}\right) + i\tilde{E}_{IR}\cos(\omega_{IR}\tau)d_{2s,2p}\tilde{\rho}_{2s,1s} \\
\dfrac{\partial \tilde{\rho}_{2s,1s}}{\partial \tau} = -\left(\gamma_{2s,1s} + i(\omega_{2s} - \omega)\right)\tilde{\rho}_{2s,1s} - \dfrac{id_{1s,2p}\tilde{E}}{2}\tilde{\rho}_{2s,2p} + i\tilde{E}_{IR}\cos(\omega_{IR}\tau)d_{2s,2p}\tilde{\rho}_{2p,1s} \\
\dfrac{\partial \tilde{\rho}_{2p,2s}}{\partial \tau} = -\left(\gamma_{2p,2s} + i(\omega_{2p} - \omega_{2s})\right)\tilde{\rho}_{2p,2s} + \dfrac{id_{1s,2p}\tilde{E}}{2}\tilde{\rho}_{1s,2s} + i\tilde{E}_{IR}\cos(\omega_{IR}\tau)d_{2s,2p}\left(\tilde{\rho}_{2s,2s} - \tilde{\rho}_{2p,2p}\right)
\end{cases}, \qquad \text{(II.10)}
$$

where $\tilde{\rho}_{ij}$ are the slowly-varying amplitudes of the density matrix elements, $\tilde{P}$ is slowly varying atomic polarization, $\omega_{2s,1s} = (E_{2s} - E_{1s})/\hbar$ and $\omega_{2p,1s} = (E_{2p} - E_{1s})/\hbar$ are the frequencies of transitions 1s2s↔1s2p and $1s^2$↔1s2p, respectively, while γ_i and $\gamma_{i,j}$ are decay rates of the diagonal and non-diagonal elements of the density matrix. The population decay rate γ_i is estimated as ionization rate from the corresponding i^{th} atomic state under the action of the IR field, which is determined from auxiliary numerical calculation (by numerically solving time-dependent Schrodinger equation with He model potential [94]). For the considered parameters of the IR field, those are wavelength 6176 nm and intensity $\mathrm{I}=2.5\times10^{12} W/cm^2$, $\gamma_{2p} \approx 2\times 0.11\omega_{IR}$, $\gamma_{2s} = 2\times 0.055\omega_{IR}$, and $\gamma_{1s} \approx 0$. Since in a rare atomic gas, exposed to a strong laser field, the collisional and Doppler broadenings are negligible in comparison with the ionization one, the off-diagonal decay rates can be calculated as $\gamma_{i,j} = \left(\gamma_j + \gamma_i\right)/2$. The initial and boundary conditions are:

$$\begin{cases} \tilde{E}(0,t) = \tilde{E}_0 f(t) \\ \rho_{1s,1s}(x,0) = 1 \\ \rho_{2s,2s}(x,0) = 0, \\ \rho_{2p,2p}(x,0) = 0, \\ \rho_{i,j}(x,0) = 0, i \neq j \end{cases}, \qquad \text{(II.11)}$$

where $f(t)$ is an envelope of the incident XUV field. These equations are written and numerically solved in the basis of bare atomic states using a fourth order Runge-Kutta scheme for time step and a second order Adams-Bashforth scheme for step in x [95].

Let us consider a propagation of an incident XUV pulse with carrier wavelength 59.16 nm and Gaussian envelope with FWHM 145 fs and peak intensity $I=10^{10} W/cm^2$ through the gas of helium with atomic density $10^{17} cm^{-3}$, irradiated by 6176 nm IR field with intensity $I=2.5\times10^{12} W/cm^2$. The bandwidth of the incident XUV pulse is $0.01eV$, which is much less than the energy separation between the Floquet states, $\lambda_1 - \lambda_2 \approx 0.58\omega_{IR} \approx 0.12eV$. The XUV field with such wavelength and pulse duration might be produced via the resonantly enhanced high-harmonic generation in InP plasma plume [96,97]. Another way to generate it is frequency doubling of 355 nm radiation in a nonlinear crystal, followed by its frequency tripling in a gas. The time-dependence of the output XUV intensity strongly depends on whether the output spectral component at the frequency of the incident XUV radiation is attenuated, or not, see Figure 6. In the presence of attenuation to the level of the generated sidebands the well-shaped pulses with duration 2 fs and peak intensity, equal to 0.87 maximum intensity of the incident XUV radiation are produced at the output of the medium with the *optimal* propagation length 4.00 mm,

Figure 6(a). It is worth noting, that an optical thickness, defined as a ratio of medium length to characteristic length at which an intensity of the resonant field is decreased by $e \approx 2.718$ times, in the medium of IR-dressed-atoms is smaller, than in the unperturbed medium. Namely, additional multiplier $a_2^{1,2p} \sum_{m \neq 0} a_{2m}^{1,2p} \exp(-2im\omega_{IR}\tau)$ appears in (II.7). Thus the effective optical thickness for perturbed medium might be roughly estimated as $2\left|a_2^{1,2p}\right|^2 \frac{2\pi\omega x N \left|d_{2p,1s}\right|^2}{c\hbar\gamma_{1s,2p}}$. For the considered parameters of the medium and the IR field, it is equal to 0.87. Under these conditions, the efficiency of transformation, defined as a ratio of the incident XUV radiation energy to the energy contained in the pulse train, equals 19.3%. For shorter propagation lengths a form of pulses is almost identical, while their intensity (and, thus, the transformation efficiency) is smaller. For longer propagation distances, the peak intensity of the produced pulses is no longer increasing, while their duration becomes larger. In the absence of attenuation, both the peak pulse intensity and the efficiency of transformation are substantially increased at the cost of increased pulse duration and pedestal. Thus, for the same parameters of the incident XUV and IR fields and the medium in the absence of attenuation the peak intensity of the pulses is 2.7 times larger than peak intensity of the incident XUV radiation, while the efficiency of transformation reaches 80.6%, Figure 6(b).

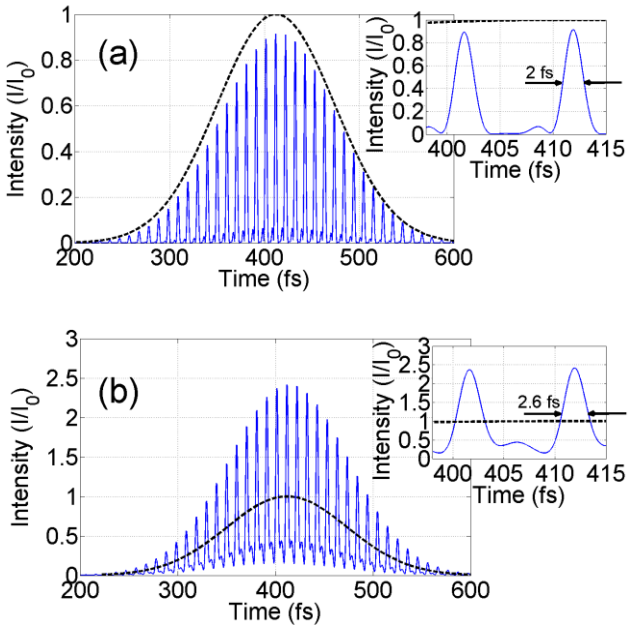

Figure 6. (a) The XUV pulse at the entrance to the medium (black dashed line) and after propagation through 4 mm of helium gas with atomic density $10^{17} cm^{-3}$ irradiated by 6176 nm IR field with intensity $I=2.5\times10^{12} W/cm^2$ (blue solid line). The resonant component of the output XUV radiation (corresponding to the incident field) is attenuated to the level of adjacent sidebands. Inset: a couple of pulses from the train shown in the main figure. (b) The same as in (a), but the resonant XUV spectral component is not attenuated.

II.5 Scaling to other atomic systems

The suggested method is easily scalable to an arbitrary three-level system with one high frequency (say, XUV) dipole-allowed transition and one low frequency (say, IR) dipole-allowed transition. Such a scalability potentially allows to adjust the carrier frequency and duration of the produced pulses of XUV radiation via the proper choice of the generating medium. Let us consider an atomic system with some IR transition with frequency ω_{23}. Choosing the frequency and the amplitude of the IR field according to the criteria presented in Section II, that is $\omega_{IR}/\omega_{23}=1/3$ and $\tilde{E}_{IR}d_{2,3}/\omega_{23}\approx1.11$, leads to

creation of Floquet states with the same coefficients $a^m_{i;\alpha_0}$ as in Section II and allows pulse train formation from the resonant XUV radiation. Suppose we choose three-level atoms with IR transition frequency X times bigger than 2s2p transition in He and set the frequency and the Rabi frequency of the IR field to be X times bigger as well (the incident XUV radiation frequency has to be properly adjusted). In this case, the sideband separation, $2\omega_{IR}$, will also be X times bigger than in case of He atoms, which means that the *pulses duration (as well as the repetition period) will be X times smaller*. It opens up the possibility for efficient conversion of an XUV radiation into a train of sub-femtosecond pulses.

Let us consider, for example, Li+ ions. The energy level diagram of Li+ ion is the same as for helium, but the transition wavelengths for $1s^2 \leftrightarrow 1s2p$ and $1s2s \leftrightarrow 1s2p$ transitions are 19.928 nm and 958.4 nm, correspondingly. The other relevant parameters of Li+ ions can be found in [98]. It is worth noting that 19.9 nm Li+-based X-ray laser was theoretically suggested and investigated [99-101]. An emission at 19.9 nm was experimentally observed from lithium plasma XUV sources [102,103]. Applying the described scaling approach, we immediately find the wavelength and intensity of the IR field, required for the ultrashort pulse formation, which are $3 \times 958.4 \sim 2875$ nm and $I = 4.4 \times 10^{13} W/cm^2$, respectively. Using Floquet approach, we find that XUV field resonant to the first Floquet state has wavelength 20.1 nm. In order to estimate an efficiency of transformation of the XUV radiation into the pulse train we simulate propagation of both XUV and IR fields in an optically thick Li+ plasma layer taking into

account the plasma dispersion, as well as the collisional broadening of the relevant transition lines. The plasma dispersion for the IR field is taken into account in Eqs. (10) by replacing $\cos(\omega_{IR}\tau)$ with $\cos(\omega_{IR}(t - xn_{plasma}/c))$, where $n_{plasma} = \sqrt{1-\omega_p^2/\omega_{IR}^2}$ is the plasma refractive index, ω_p is plasma frequency; the plasma dispersion for the XUV field is negligible. For the typical temperature and concentration of plasma ~ 5000 K and $10^{18} cm^{-3}$, the linewidths $\gamma_{1s2p}, \gamma_{1s2s}, \gamma_{2s2p}$ are mainly determined by collisional broadening and are in the range of a few meV [104,105]. Since the ionization potentials of 1s2s and 1s2p states are much higher in Li+ than in He (while the required intensity of the IR field is just an order of magnitude higher), a contribution of the ionization rates is negligible. As it follows from the numerical solution of Eqs. (10), at the output of the medium with the length 80 μm (which corresponds to the effective optical thickness $2\left|a_2^{1,2p}\right|^2 \frac{2\pi\omega x N \left|d_{2p,1s}\right|^2}{c\hbar\gamma_{1s,2p}} \approx 3.9$), a train of pulses will be produced with the pulse duration 0.99 fs (which is remarkably close to the prediction of the scaling law, $2\,fs \times 2875/6176 \approx 0.93\,fs$), see Figure 7. The efficiency of transformation into the pulse train equals 26.6%. The output pulses are delayed with respect to incident one due to the resonant dispersion of Li+ ions, which turns out to be important, since bandwidth of the incident XUV radiation exceeds linewidth of the resonant transition $1s^2 \leftrightarrow 1s2p$. Similar to the case of He atoms, without attenuation of the resonant output XUV spectral component both the peak pulse intensity and the efficiency of transformation are substantially increased at the cost of increased pulse duration and pedestal. Thus, for the same

parameters of the medium in the absence of attenuation the peak intensity of the pulses is 2 times larger than the peak intensity of the incident XUV field, while efficiency of transformation reaches 87.4%, see Figure 7(b).

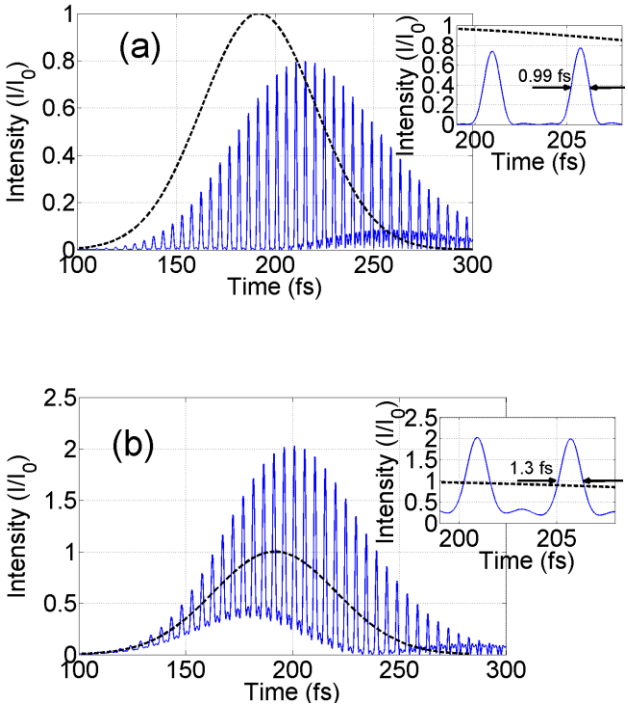

Figure 7. Intensity of the 20.1 nm XUV field at the entrance to the medium (black dashed line) and after propagation through 80 μm of Li+ plasma along with 2875 nm IR field with intensity $I=4.4\times10^{13} W/cm^2$ (blue solid line). (a) The resonant frequency of the XUV field at the exit of the medium is attenuated. Ion density is $10^{18} cm^{-3}$. Inset: a couple of the pulses from the train shown in the main figure. (b) The same as (a), but the resonant XUV spectral component is not attenuated.

II.6 Conclusion

In the present chapter, we have shown the possibility to produce the ultrashort femto- and sub-femtosecond pulses of XUV radiation via its resonant interaction with the medium of IR-field-dressed non-hydrogen-like atoms. The mechanism of pulse formation

is based on mixing and modulating of the excited atomic states by the nonionizing relatively low frequency IR field. Using Floquet formalism within the three-level model of He atoms and He-like Li+ ions, we found the optimal parameters (frequency and amplitude) of the IR field, providing formation of well-shaped pulses with duration 2 fs and 990 as, correspondingly. We verified that the presence of the other bound atomic states and ionization results in only slight changes in the shape of produced pulses. We found a simple scalability law which can be used for determination of the optimal parameters of the IR field providing the ultrashort pulse formation in various non-hydrogen-like media under conditions when the three-level model approximation is applicable. Under the optimal conditions, the efficiency of pulse formation reaches 80-90%, which makes the suggested technique very favorable for time shaping of picosecond pulses of X-ray lasers. Since this method does not imply ionization neither from the ground, nor from the excited states of the generating medium, it can be potentially used directly in the active media of X-ray lasers.

CHAPTER III

ATTOSECOND PULSE FORMATION VIA SWITCHING OF RESONANT INTERACTION BY TUNNEL IONIZATION[3]

III.1 Introduction

The first decade of the millennium was marked by the birth of attosecond science - the branch of physics devoted to direct investigation and control of the motion of charged particles in atoms, molecules, clusters, and solids, unfolding on the attosecond time scale [52,54,56-59].

In recent years, there has been a growing interest in investigation of the ultrafast dynamics of atoms, simultaneously irradiated by an intense low-frequency (LF) laser field, far detuned from all the atomic resonances, and a high-frequency (HF) radiation, quasi-resonant to a transition from the ground to an excited bound or autoionizing atomic state [22,24,25,27,28,34-36,59,106]. Utilization of quasi-resonant radiation substantially enriches the toolset of attosecond science, allowing for switching the pathways of multiphoton excitation and/or ionization of atoms by the LF field, and under certain conditions leading to quantum interference of these pathways [22,24,25,27,28,34-36,106]. Up to now, however, the experimental studies are mainly limited to investigation of helium atoms, possessing the highest ionization potential among the neutral atoms and the highest-frequency transitions between the bound states. This choice is primarily motivated

[3] Reprinted with permission from "Attosecond pulse formation via switching of resonant interaction by tunnel ionization" by V.A. Antonov, T.R. Akhmedzhanov, Y.V. Radeonychev and O. Kocharovskaya, 2015, Phys. Rev. A, vol. 91, pp. 023830, Copyright [2015] by American Physical Society.

by the aspiration to perform an intra-atomic excitation using high-order harmonics of laser radiation and attosecond pulses with sufficiently high carrier frequency generated in noble gases [52,54,56].

Recently, a method to produce extremely short pulses with relatively low carrier frequency in the vicinity of the resonances of hydrogen-like atoms was proposed [37,41,42] and discussed [38,39,107,108]. The pulses are produced due to *the resonant* interaction of an incident HF radiation with hydrogen-like atoms, dressed by a moderately strong LF laser field. While the resonant HF radiation excites atoms from the energy level n=1 to the energy level n=2 (where n is the principal quantum number), the LF field produces the *sub-LF-field-cycle* perturbation of the excited energy level. The perturbation constitutes (i) *time-dependent* splitting and shift of the excited energy levels via the Stark effect as well as (ii) *time-dependent* broadening of these levels via tunnel ionization from the corresponding excited states. The *sub-LF-field-cycle* variation of the instantaneous values of splitting and/or broadening of the excited energy levels, determined by the instantaneous strength of the LF field [25], leads to a multifrequency atomic response to the quasi-monochromatic incident HF radiation. As shown in references [37,39,41,42,107,108], under the appropriate conditions this corresponds to formation of extremely short few-femto- and attosecond pulses with carrier frequency inherently determined by the frequency of the resonant atomic transition. Since most of the spectral components of the produced pulses lay below the threshold of ionization and dissociation of various neutral atoms and molecules, such a source of the resonant attosecond pulses constitutes a unique tool for the nondestructive (nonionizing) study and control of ultrafast

dynamic of the bound atomic and molecular electrons. This essentially distinguishes the proposed technique from the commonly used approach to attosecond pulse formation via the high-order harmonic generation (HHG) of laser radiation in gases [52,54,56]. In the latter case, the pulses consist of high-order harmonics, corresponding to the plateau and/or cutoff regions of the generated spectrum, and possessing frequencies far above the ionization threshold of the generating atoms. Consequently, interaction of such pulses with atoms/ molecules, which ionization/dissociation potential is comparable to that of the generating medium, results primarily in photoionization or photodissociation, respectively. Another difference of the proposed technique for attosecond pulse formation from HHG in gases is the absence of attochirp [56]: the pulse formation does not imply adjustment of phases of the generated sidebands, since all of them are produced in-phase.

In the present chapter, we extend the method of extremely short pulse formation from resonant radiation to various non-hydrogenlike atoms and show the possibility to produce attosecond pulses in helium and neon. We derive an analytical solution uncovering the origin of attosecond pulse formation from the resonant HF radiation in the case of a relatively strong LF field [37,39,42,108]. In this case the probability of atomic ionization *from the excited state*, corresponding to the upper energy level of the resonant HF atomic transition, approaches unity over each half-cycle of the LF field. For hydrogen-like atoms this corresponds to amplitude of the LF field strength, E_C, exceeding $0.15\times Z^3/n^3 E_A$, where Z is the nucleus charge and $E_{\rm A}=m_e^2e^5/\hbar^4$ is the atomic unit of electric field (e and m_e are the charge and the mass of electron, respectively, $\hbar$ is the Planck's constant). Ionization from the ground atomic state remains unimportant as far as

$E_C < 0.05 \times Z^3 E_A$. The derived solution shows that the attosecond pulses are produced due to confinement of the resonant atomic response to the incident quasi-monochromatic HF radiation within the extremely short time-intervals in the vicinity of zero-crossings of the LF field. For the rest of the time the *resonant* interaction between the HF radiation and the atoms is effectively switched off (the resonance disappears) because of rapid ionization from the excited atomic state, produced by the LF field. Both analytically and numerically, we show that in this regime, the effect of extremely short pulse formation from the resonant radiation is insensitive to the particular dependences of (i) Stark shift / splitting of the excited atomic energy level as well as (ii) rate of quasistatic ionization from the corresponding excited state(s) on the LF field strength. Thus, the discussed mechanism can be used for attosecond pulse formation in a variety of atomic gases, possessing sufficiently high ionization potential. Extension of the proposed method to non-hydrogenlike media is important for an experimental realization, since both atomic hydrogen and hydrogen-like ions are unstable. Use of various media for attosecond pulse generation also substantially increases the practical value of the proposed technique, enabling formation of pulses at different carrier frequencies, suitable for ultrafast excitation of different atomic, molecular and solid-state systems.

The chapter is organized as follows: after the introduction, we describe the model and derive the analytical solution for a resonant HF radiation, propagating through an atomic gas dressed by an intense LF field. We compare the analytical results to the results of numerical solutions, obtained within the more general models [42,109] and discuss the possibilities to produce attosecond pulses from 58.4 nm vacuum-ultraviolet (VUV)

radiation in helium dressed by 3.9 μm laser field [110], as well as from 73.6 nm VUV radiation in neon dressed by 3.9 μm laser field and 1-fs pulses from 122 nm VUV radiation in atomic hydrogen dressed by a CO_2-laser field [111].

III.2 Analytical solution

Let us consider interaction of a HF radiation with an atomic gas. The incident HF radiation is monochromatic and propagates along the *z*-axis. At the entrance to the medium, *z*=0, it has the form

$$\vec{E}_{inc}(t) = \frac{1}{2}\vec{x}_0 E_0 \exp\{-i\,\omega t\} + \text{c.c.}, \qquad \text{(III.1)}$$

where E_0 is its amplitude, ω is the angular frequency, and c.c. stands for complex conjugation. The HF radiation (III.1) is chosen to be near-resonant to a transition $|1\rangle \leftrightarrow |2\rangle$ from the ground atomic state to one of the lowest excited states, $\omega \approx \omega_{21}^0$ (where ω_{21}^0 is the unperturbed frequency of the resonant transition).

The gas is simultaneously irradiated by a moderately strong linearly polarized LF laser field

$$\vec{E}_{LF}(\tau) = \frac{1}{2}\vec{x}_0 E_C \exp\left\{-i\left[\Omega\left(t - z/c\right) + \varphi_0\right]\right\} + \text{c.c.} \qquad \text{(III.2)}$$

Here E_C is the amplitude of the LF field, Ω is its angular frequency, φ_0 is its initial phase, and *c* is the speed of light in vacuum. The term low-frequency (LF) means that the frequency of the field is much smaller than the frequencies of all the transitions from both the ground and the resonantly excited by the HF radiation atomic states. Due to far-detuning from the relevant atomic resonances, the LF field (III.2) does not suffer from the

atomic dispersion at the considered propagation distances and traverses the medium without substantial modification along the direction of propagation of the HF radiation. Since both HF and LF fields are polarized in the same direction, $\vec{E}_{inc} \| \vec{E}_{LF} \| \vec{x}_0$, their polarizations are not changed during propagation through an isotropic gas, so that the vector notations will be omitted, for now on.

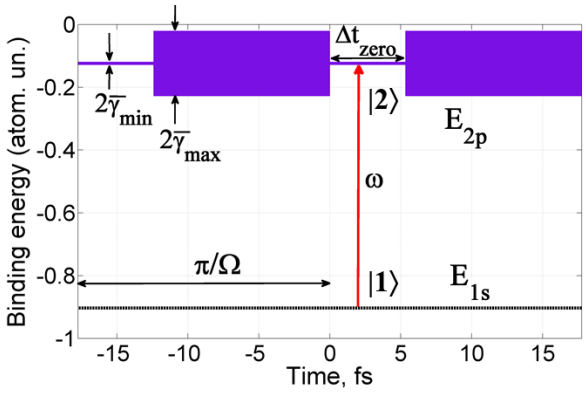

Figure 8. Sketch of the theoretical model used for derivation of the analytical solution. The incident HF radiation with frequency ω selects the lower, |1⟩, and upper, |2⟩, states of the resonant atomic transition, possessing the energy E_{1s} and E_{2p}, respectively. The LF field with frequency Ω rapidly ionizes atoms from the excited state |2⟩ leading to periodic broadening of the corresponding energy level twice within the LF field cycle. At the same time, the ground atomic state |1⟩ is unaffected by the LF field. The linewidth of the resonant transition |1⟩ ↔ |2⟩ takes the minimum value $2\bar{\gamma}_{\min}$ during the time-intervals Δt_{zero} near zero-crossings of the LF field and the maximum value $2\bar{\gamma}_{\max}$ during the time-intervals $\pi/\Omega - \Delta t_{\text{zero}}$ near the LF field crests.

The amplitude of the LF field is chosen to be under the threshold of atomic multiphoton excitation and/or ionization from the ground state |1⟩, however, the LF field is strong enough to almost completely ionize atoms from the excited state |2⟩ over *every* half-cycle, producing extreme broadening of the |1⟩↔|2⟩ transition line in the vicinity of its crests, Figure 8. The Keldysh parameter of the LF field for the excited state |2⟩ is much

smaller than unity, $\gamma_{Keldysh} << 1$, so that the excited-state-ionization takes place via tunneling mechanism. If the state $|2\rangle$ corresponds to an eigenstate in spherical coordinates, then according to [112], the ionization rate from it is given by

$$w_{ion}^{(2)}(\tau) = \frac{m_e e^4}{\hbar^3} C_{\kappa l}^2 \kappa^2 \left(2l+1\right) \frac{4^{n^*-|m|}\left(l+|m|\right)!}{|m|!\left(l-|m|\right)!} \times \\ \times \left|F_{LF}(\tau)\right|^{|m|+1-2n^*} \exp\left\{-\frac{2}{3\left|F_{LF}(\tau)\right|}\right\}, \qquad \text{(III.3)}$$

where $\tau \equiv t - z/c$ is the local time (in the reference frame, comoving with the LF wavefront), $\kappa = \sqrt{I_P^{(2)}/I_H}$, $I_P^{(2)}$ is the ionization potential from the excited atomic state $|2\rangle$, $I_H = \frac{m_e e^4}{2\hbar^2}$ is the ionization potential from the ground state of atomic hydrogen, m is the projection of the angular momentum l on the LF electric field, $n^* = Z/\kappa$ is the effective principal quantum number, Z is the atomic core charge, $C_{\kappa l}$ is the dimensionless asymptotic coefficient of the atom wave function, and $F_{LF}(\tau) \equiv \frac{E_{LF}(\tau)}{\kappa^3 E_A}$ is the reduced dimensionless LF field. The tunnel ionization rate from an eigenstate in parabolic coordinates differs from (III.3) only by the pre-exponential factor [37,42,113].

The LF field also produces instantaneous Stark shift of the energy level, corresponding to the excited atomic state $|2\rangle$, which energy E_2 takes the form

$$\mathrm{E}_2 = \mathrm{E}_2^{(0)} + \Delta\mathrm{E}_2(\tau), \qquad \text{(III.4)}$$

where $E_2^{(0)}$ is the unperturbed energy of the excited state $|2\rangle$, and ΔE_2 is the instantaneous shift of the energy level, induced by the LF field. In the lowest order of perturbation theory one has $\Delta E_2 \propto F_{LF}(\tau)$ for hydrogen-like atoms and $\Delta E_2 \propto F_{LF}^2(\tau)$ for non-hydrogen-like atoms.

Propagation of the HF radiation through the medium is described by the wave equation

$$\frac{\partial^2 E_{HF}}{\partial z^2} - \frac{1}{c^2}\frac{\partial^2 E_{HF}}{\partial t^2} = \frac{4\pi}{c^2}\frac{\partial^2 P}{\partial t^2}, \qquad \text{(III.5)}$$

where E_{HF} is the HF radiation strength and P is the *resonant* HF polarization of the gas. At the considered propagation distances, the nonresonant interaction of the HF radiation with atoms is unimportant and can be disregarded. Since the characteristic scales of spatial evolution of the HF radiation in any gas are much larger than the HF radiation wavelength, the substitution $t \to \tau \equiv t - z/c$ allows reducing wave equation (III.5) to

$$\frac{\partial E_{HF}}{\partial z} = -\frac{2\pi}{c}\frac{\partial P}{\partial \tau}. \qquad \text{(III.6)}$$

Equation (III.6) implies the slowly-evolving-wave approximation [114,115], $\left|\frac{\partial E_{HF}}{\partial z}\right| << \frac{1}{c}\left|\frac{\partial E_{HF}}{\partial \tau}\right|$. Within the additional approximation of slowly-varying-envelope,

$$E_{HF}(z,\tau) = \frac{1}{2}\tilde{E}_{HF}(z,\tau)\exp\{-i\,\omega\tau\} + \text{c.c.}, \qquad P(z,\tau) = \frac{1}{2}\tilde{P}(z,\tau)\exp\{-i\,\omega\tau\} + \text{c.c.},$$

$\left|\partial\tilde{E}_{HF}/\partial\tau\right| << \omega$, $\left|\partial\tilde{P}/\partial\tau\right| << \omega$, $\left|\partial\tilde{E}_{HF}/\partial z\right| << \omega/c$, $\left|\partial\tilde{P}/\partial z\right| << \omega/c$, equation (III.6) has the solution

$$\tilde{E}_{HF}(z,\tau) = \tilde{E}_{HF}(0,\tau) + \tilde{E}_{Scatt}(z,\tau), \quad \tilde{E}_{Scatt}(z,\tau) \equiv i\frac{2\pi\omega}{c}\int_0^z \tilde{P}(z',\tau)dz', \tag{III.7}$$

where $\tilde{E}_{Scatt}(z,\tau)$ is the slowly-varying envelope of HF radiation, resonantly scattered by the atoms, which is entirely determined by the slowly-varying envelope of the resonant polarization $\tilde{P}$.

The envelope of polarization $\tilde{P}$, in turn, is proportional to the envelope a_{21} of the atomic coherence $\rho_{21} = a_{21}\exp\{-i\omega\tau\}$ at the resonant transition $|1\rangle\leftrightarrow|2\rangle$:

$$\tilde{P}(z,\tau) = 2Nd_{12}a_{21}(z,\tau), \tag{III.8}$$

where N is the atomic density, and d_{12} is the dipole moment of the resonant transition. The value a_{21} satisfies an equation

$$\frac{da_{21}}{d\tau} + \left(i\left(\omega_{21}(\tau) - \omega\right) + \gamma_{21}(\tau)\right)a_{21} = \frac{i}{2\hbar}n_{12}d_{21}\tilde{E}_{HF}, \tag{III.9}$$

where $\omega_{21}(\tau)$ is the instantaneous frequency of the transition $|1\rangle\leftrightarrow|2\rangle$, $\gamma_{21}(\tau)$ is its instantaneous decoherence rate, $\tilde{E}_{HF}$ is the envelope of the HF radiation, n_{12} is population difference between the states $|1\rangle$ and $|2\rangle$, $n_{12} \equiv \rho_{11} - \rho_{22}$ (in the following we consider a relatively weak HF field, which does not change populations of the atomic states considerably during the interaction time, $n_{12} \cong 1$), and $d_{21} = d_{12}^*$.

In general, $\omega_{21}(\tau) = \omega_{21}^{(0)} + \Delta \mathrm{E}_2(\tau)/\hbar$ and $\gamma_{21}(\tau) = \gamma_{21}^{(0)} + w_{ion}^{(2)}(\tau)/2$, where $\omega_{21}^{(0)}$ and $\gamma_{21}^{(0)}$ are the unperturbed transition frequency and decoherence rate, correspondingly. However, $\Delta \mathrm{E}_2 \propto F_{LF}$ or F_{LF}^2, while $w_{ion}^{(2)} \propto \exp\left\{-\dfrac{2}{3|F_{LF}|}\right\}$. Hence, in the case of a strong LF field, $F_{LF}^{\max} \succ 0.1$, considered in this chapter, the peak value of ionization broadening of the resonant transition line considerably exceeds the depth of Stark sweeping of the resonant transition frequency, $\max\left\{w_{ion}^{(2)}\right\} >> \max\left\{\Delta \mathrm{E}_2/\hbar\right\}$. Therefore, in order to obtain an analytical solution one may neglect variation of frequency of the resonant transition as compared to variation of its linewidth, assuming $\omega_{21}(\tau) = \omega_{21}^{(0)}$. The opposite case of a relatively weak LF field, where $\max\left\{w_{ion}^{(2)}\right\} << \max\left\{\Delta \mathrm{E}_2/\hbar\right\}$, has been considered (for the hydrogen-like atoms) in our recent paper [38].

Taking into account the strongly nonlinear dependence of the tunnel ionization rate (III.3) on the LF field strength (III.2), we adapt a stepwise approximation for the local-time-dependence of decoherence rate of the resonant transition:

$$\gamma_{21}(\tau) = \begin{cases} \overline{\gamma}_{\min}, & 0 \le \tau < \Delta t_{\text{zero}}, \\ \overline{\gamma}_{\max}, & \Delta t_{\text{zero}} \le \tau < \pi/\Omega, \end{cases} \qquad \text{(III.10)}$$

$$\gamma_{21}(\tau + \pi/\Omega) = \gamma_{21}(\tau)\,.$$

The decoherence rate $\gamma_{21}(\tau)$ takes it minimum value $\overline{\gamma}_{\min}$ near zero-crossing of the LF field at $\tau = \Delta t_{\text{zero}}/2$ (corresponding to $\varphi_0 = [\pi - \Omega \Delta t_{\text{zero}}]/2$ in (III.2)), and maximum value $\overline{\gamma}_{\max}$ at the rest of time, Figure 8. Since the excited-state ionization rate

(III.3) is a periodic function of time, which period equals the half-cycle of the LF field, the decoherence rate (III.10) possesses the same periodicity.

According to the results of our numerical calculations [42] extremely short pulses can be produced from the quasi-monochromatic HF radiation in an infinitely thin medium, while an increase of the medium thickness leads only to an increase of the peak amplitude of the pulses (due to increased intensity of the generated sidebands) at the cost of slight increase of the pulse duration (because of phase mismatching of the sidebands). Therefore, similarly to [38], in order to derive an analytical solution we assume that the length of the medium L is small enough, such that the incident HF spectral component dominates over the generated sidebands. In this case, the resonant atomic response can be calculated accounting only for the scattering of the incident HF radiation, and neglecting rescattering of the generated sidebands. This corresponds to assumption $E_{HF}(z,\tau) \approx E_{inc}(\tau)$ in right hand of (III.9). Substitution of (III.1) into (III.9) and use of the approximations (III.10) and $\omega_{21}(\tau) = \omega_{21}^{(0)}$ lead to the steady-state solution

$$a_{21}(\tau) = \begin{cases} a_{21}^{(1)}(\tau), & 0 \le \tau < \Delta t_{\text{zero}}, \\ a_{21}^{(2)}(\tau), & \Delta t_{\text{zero}} \le \tau < \pi/\Omega, \end{cases} \tag{III.11}$$

where $a_{21}^{(1)}(0) = a_{21}^{(2)}(\pi/\Omega)$ and $a_{21}^{(2)}(\Delta t_{\text{zero}}) = a_{21}^{(1)}(\Delta t_{\text{zero}})$. The dependences $a_{21}^{(1)}(\tau)$ and $a_{21}^{(2)}(\tau)$ are given by

$$\begin{cases} a_{21}^{(1)}(\tau) = C_1 \exp\left\{\left(i\Delta\omega - \bar{\gamma}_{\min}\right)\tau\right\} + D_1, \\ a_{21}^{(2)}(\tau) = C_2 \exp\left\{\left(i\Delta\omega - \bar{\gamma}_{\max}\right)\left(\tau - \Delta t_{\text{zero}}\right)\right\} + D_2, \end{cases} \tag{III.12}$$

where $\Delta\omega \equiv \omega - \omega_{21}^{(0)}$ and

$$\begin{cases} D_1 = i\dfrac{n_{12}d_{21}E_0}{2\hbar\left(\bar{\gamma}_{\min} - i\Delta\omega\right)}, \\ D_2 = i\dfrac{n_{12}d_{21}E_0}{2\hbar\left(\bar{\gamma}_{\max} - i\Delta\omega\right)}, \end{cases} \tag{III.13}$$

$$\begin{cases} C_1 = \left(D_2 - D_1\right)\dfrac{\exp\left\{\left(i\Delta\omega - \bar{\gamma}_{\max}\right)\left(\pi/\Omega - \Delta t_{\text{zero}}\right)\right\} - 1}{\exp\left\{\left(i\Delta\omega - \bar{\gamma}_{\max}\right)\pi/\Omega\right\}\exp\left\{\left(\bar{\gamma}_{\max} - \bar{\gamma}_{\min}\right)\Delta t_{\text{zero}}\right\} - 1}, \\ C_2 = \left(D_1 - D_2\right)\dfrac{\exp\left\{\left(i\Delta\omega - \bar{\gamma}_{\min}\right)\Delta t_{\text{zero}}\right\} - 1}{\exp\left\{\left(i\Delta\omega - \bar{\gamma}_{\max}\right)\pi/\Omega\right\}\exp\left\{\left(\bar{\gamma}_{\max} - \bar{\gamma}_{\min}\right)\Delta t_{\text{zero}}\right\} - 1}. \end{cases} \tag{III.14}$$

According to (III.7) and (III.8), the envelope of the resonantly scattered HF radiation has the form

$$\tilde{E}_{Scatt}(\tau) = \begin{cases} \tilde{E}^{(1)}_{Scatt}(\tau), & 0 \le \tau < \Delta t_{\text{zero}}, \\ \tilde{E}^{(2)}_{Scatt}(\tau), & \Delta t_{\text{zero}} \le \tau < \pi/\Omega, \end{cases} \tag{III.15}$$

$$\tilde{E}_{Scatt}(\tau + \pi/\Omega) = \tilde{E}_{Scatt}(\tau),$$

where $\tilde{E}^{(1)}_{Scatt}(\tau) = i\mathrm{A} \times a^{(1)}_{21}(\tau)$ and $\tilde{E}^{(2)}_{Scatt}(\tau) = i\mathrm{A} \times a^{(2)}_{21}(\tau)$; $\mathrm{A} \equiv 4\pi N d_{12}\dfrac{\omega}{c}L$.

Equations (III.15), (III.11)-(III.14) acquire especially clear form in the case of almost complete ionization from the excited state |2⟩ in the vicinity of crests of the LF field, $\exp\left\{-\bar{\gamma}_{\max}\left(\pi/\Omega - \Delta t_{\text{zero}}\right)\right\} << 1$, and relatively small instantaneous ionization rate near the LF field zero-crossings, $\exp\left\{-\bar{\gamma}_{\min}\Delta t_{\text{zero}}\right\} \approx 1 - \bar{\gamma}_{\min}\Delta t_{\text{zero}}$, which is realized in a sufficiently strong LF field. Assuming that detuning of the incident HF radiation from the resonance is substantively smaller than the doubled LF field frequency, $\exp\left\{i\Delta\omega\tau\right\} \approx 1 + i\Delta\omega\tau$, one obtains

$$\begin{cases} \tilde{E}^{(1)}_{Scatt}(\tau) = -\chi E_0 \tau, \quad 0 \le \tau < \Delta t_{\text{zero}}, \\ \tilde{E}^{(2)}_{Scatt}(\tau) = -\chi E_0 \Delta t_{\text{zero}} \exp\left\{-\bar{\gamma}_{\max}\left(\tau - \Delta t_{\text{zero}}\right)\right\}, \quad \Delta t_{\text{zero}} \le \tau < \pi/\Omega. \end{cases} \tag{III.16}$$

where $\chi \equiv \dfrac{2\pi N n_{12} \left|d_{21}\right|^2 \omega}{\hbar c} L$. As follows from (III.16), the scattered HF radiation has a form of a pulse train with sub-LF-field-cycle duration $\tau_{pulse} = \dfrac{\sqrt{2}-1}{\sqrt{2}} \Delta t_{\text{zero}} + \dfrac{\ln 2}{2\bar{\gamma}_{\max}}$ $\approx 0.3\Delta t_{\text{zero}} + \dfrac{0.35}{\bar{\gamma}_{\max}}$ (the duration of pulses is defined as the full width at half-maximum of the scattered intensity $I_{Scatt} \propto \tilde{E}^2_{Scatt}(\tau)$).

The Fourier transform of the scattered radiation (III.15) has the form

$$\tilde{E}_{Scatt}(\tau) = i\mathrm{A} \cdot \sum_{n=-\infty}^{\infty} \alpha_{2n} \exp\left\{-i2n\Omega\tau\right\}. \tag{III.17}$$

In the particular case (III.16) the coefficients α_{2n} are determined by the following expressions:

$$\alpha_{2n} = i\frac{\chi E_0}{\mathrm{A}} \frac{\Omega}{\pi} \left[\frac{\exp\left\{i2n\Omega\Delta t_{\text{zero}}\right\} - 1}{4n^2\Omega^2} + \frac{\bar{\gamma}_{\max} \Delta t_{\text{zero}} \exp\left\{i2n\Omega\Delta t_{\text{zero}}\right\}}{2n\Omega\left(2n\Omega + i\bar{\gamma}_{\max}\right)} \right], \quad n \ne 0. \tag{III.18}$$

The direct component of the slowly-varying amplitude of the scattered field $\tilde{E}_{Scatt}(\tau)$ has the form

$$\alpha_0 = i\frac{\chi E_0}{\mathrm{A}} \frac{\Omega}{\pi} \left[\frac{\Delta t^2_{zero}}{2} + \frac{\Delta t_{\text{zero}}}{\bar{\gamma}_{\max}} \right]. \tag{III.19}$$

In general case (III.15) the coefficients α_{2n} can be expressed as

$$\alpha_{2n} = \frac{\Omega}{\pi}\Bigg[C_1 \frac{\exp\left\{\left[i\left(2n\Omega + \Delta\omega\right) - \bar{\gamma}_{\min}\right]\Delta t_{\text{zero}}\right\} - 1}{i\left(2n\Omega + \Delta\omega\right) - \bar{\gamma}_{\min}} + C_2 \frac{\exp\left\{\left[i\Delta\omega - \bar{\gamma}_{\max}\right]\left[\pi/\Omega - \Delta t_{\text{zero}}\right]\right\} - \exp\left\{i2n\Omega\Delta t_{\text{zero}}\right\}}{i\left(2n\Omega + \Delta\omega\right) - \bar{\gamma}_{\max}} + \left(D_1 - D_2\right)\frac{\exp\left\{i2n\Omega\Delta t_{\text{zero}}\right\} - 1}{i2n\Omega}\Bigg], \tag{III.20}$$

$$\alpha_0 = \frac{\Omega}{\pi}\Bigg[C_1 \frac{\exp\left\{\left(i\Delta\omega - \bar{\gamma}_{\min}\right)\Delta t_{\text{zero}}\right\} - 1}{i\Delta\omega - \bar{\gamma}_{\min}} + D_1\Delta t_{\text{zero}} + C_2 \frac{\exp\left\{\left(i\Delta\omega - \bar{\gamma}_{\max}\right)\left(\pi/\Omega - \Delta t_{\text{zero}}\right)\right\} - 1}{i\Delta\omega - \bar{\gamma}_{\max}} + D_2\left(\pi/\Omega - \Delta t_{\text{zero}}\right)\Bigg]. \tag{III.21}$$

where C_i, D_j are defined by equations (III.13), (III.14). The derived solution (III.7), (III.15)-(III.21) is valid for arbitrary atomic system. The quantitative features of field-atom interaction specific for a given medium and LF field are taken into account via parameters $\bar{\gamma}_{\min}$, $\bar{\gamma}_{\max}$, and Δt_{zero}. In the following, we compare the derived analytical solution to the results of numerical calculations within the more general models [42,109], taking into account the ground and two excited energy levels, which instantaneous positions and widths are modulated by the LF field through the nonlinear (taking into account the linear, quadratic and cubic constituents) Stark effect and the tunnel ionization, respectively. The numerical calculations are performed without the slowly-varying amplitude and rotating-wave approximations. The model [109] is designed specifically for non-hydrogen-like medium. Contrary to the models, used in papers [37,39,42,108], it takes into account not only the *adiabatic* influence of a LF field on the atomic system

through the sub-LF-field-cycle shift and/or broadening of the energy levels, but also *non-adiabatic* transitions between the nondegenerate excited energy levels, induced by the LF field.

III.3 Possibilities for experimental implementation in helium, neon and atomic hydrogen

Let us apply the above model to study the possibility to produce few-cycle attosecond pulses from 58.4 nm VUV radiation due to the resonant interaction with 1s↔2p transition of helium dressed by 3.9 μm infra-red (IR) laser field from OPCPA source [110]. The incident VUV radiation can be generated in different ways. Firstly, it can be produced via frequency tripling of 175 nm radiation in a gas. The 175 nm radiation, in turn, can be generated via frequency doubling of 350 nm radiation in a nonlinear crystal with sufficiently wide transparency range, such as lithium triborate (LBO). The latter radiation can be produced by OPA/OPO or via frequency tripling of either Nd: YLF or Nd: YAG laser field. Secondly, the incident VUV radiation can be obtained via the resonantly enhanced HHG of Ti:Sa laser field in InP plasma plume [96,97]. In both cases the efficiency of conversion of the radiation energy from visible/near-infrared to VUV spectral range normally exceeds the achieved conversion efficiency of attosecond pulse formation via HHG., This is because of (i)the absence of a tiny factor, determined by the probability of recombination of the detached electron [116], inherent to HHG process, and (ii) the possibility to resonantly enhance the atomic susceptibility. Under the action of the laser field with an intensity $I_{IR}=1.5\times10^{13}$ W/cm^2 the resonant response of helium atoms to the incident VUV radiation and, correspondingly, the resonantly scattered radiation, are

confined to the sub-IR-field-cycle time intervals near zero-crossings of the IR field, Figure 9. This can be understood referring to the dependence of the optical depth of a medium, *G*, on the linewidth of the resonant transition, γ: *G*~1/γ [117]. Since in the vicinity of the IR field crests excited-state-ionization greatly (by orders of magnitude) broadens the resonant transition line, it leads to the proportional decrease of the optical depth, making the medium transparent for the resonant VUV radiation. On the contrary, in the vicinity of zero-crossings of the IR field (during the time intervals Δt_{zero}) the ionization broadening is small, providing conditions for the resonant absorption and scattering of the incident VUV radiation. The Fourier transform of the atomic response is plotted in Figure 10. It corresponds to a broad comb of the equidistant spectral components, separated by the doubled frequency of the IR field. The generated sidebands are almost in-phase to each other and in-anti-phase to the incident VUV radiation, corresponding to burning of the extremely short dips in the time-dependence of the output VUV intensity because of the resonant absorption of the VUV radiation in the vicinity of zero-crossings of the IR field, Figure 11. In an optically thin medium the output intensity satisfies the relation

$$I_{HF}(z,\tau) = \frac{c}{8\pi}\left|\tilde{E}_{HF}\right|^2 \approx \frac{c}{8\pi}E_0^2\left(1+2\tilde{E}_{Scatt}(z,\tau)/E_0\right). \qquad \text{(III.22)}$$

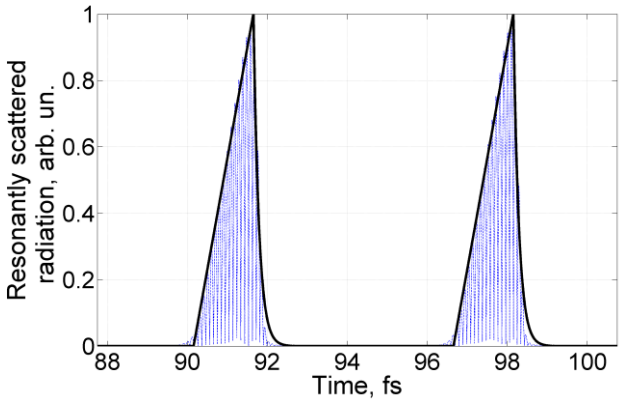

Figure 9. Time-dependence of radiation, resonantly scattered by the atoms of helium under the simultaneous action of the incident 58.4 nm VUV radiation, exciting 1s $\leftrightarrow$ 2p atomic transition, and 3.9 μm IR radiation with intensity $I_{IR}=1.5\times10^{13}$ W/cm^2, rapidly ionizing atoms from the 2p state twice within the IR field cycle. The resonant scattering is confined to the time intervals Δt_{zero} near zero-crossings of the IR field. For the rest of time the resonant scattering is suppressed due to the huge broadening of the resonant transition line, see Figure 8. The black solid line corresponds to the radiation envelope, calculated analytically (III.15), (III.16). The rapidly oscillating blue dashed line corresponds to absolute value of the radiation strength, calculated numerically within the three-level model [38], taking into account the nonadiabatic coupling between 2p and 2s states of helium, as well as instantaneous quadratic Stark shift of the corresponding energy levels and tunnel ionization from them.

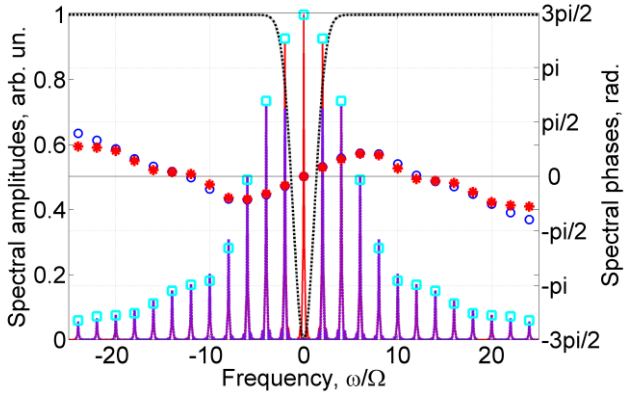

Figure 10. Fourier transform of the slowly-varying envelope of the resonantly scattered radiation plotted in Figure 9. The result of analytical calculation for the spectral amplitudes of the scattered radiation using equations (III.18) and (III.19) is shown by cyan squares. Amplitudes of the spectral components calculated numerically within the three-level model [38] (see caption to Figure 9) before and after spectral filtering (see the text) are shown by red solid and bold lavender dashed line, respectively (this lines almost overlap except for the three central spectral components). Transmission of the spectral filter, which is zero at the resonance frequency (zero frequency of the envelope) and unity far away from it, is shown by black dashed line. The result of analytical calculation for the spectral phases of the scattered radiation using equations (III.18) and (III.19) is shown by red stars. The numerically calculated [38] phases of the spectral components at the multiples of the doubled IR field frequency, $\pm 2\Omega$, $\pm 4\Omega$, ... are marked by blue cycles.

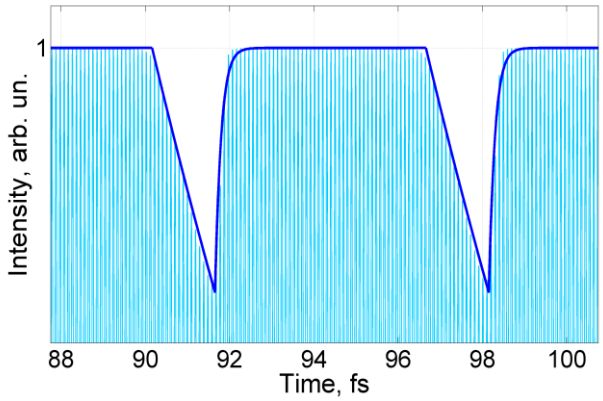

Figure 11. Intensity of the output VUV radiation, propagated through an optically thin medium of helium, simultaneously irradiated by the resonant 58.4 nm VUV radiation and the strong 3.9 μm IR field (see caption to Figure 9). The output radiation results from coherent summation of the resonantly scattered radiation (Figure 9) with the incident one. The blue solid line represents the result of analytical calculation for the envelope of the output VUV intensity. The rapidly oscillating dashed cyan curve corresponds to the square of the normalized VUV radiation strength, calculated numerically within the model [38]. It worth noting, that the presented calculations imply approximation of an infinitely thin medium, so that the depth of intensity dips in Figure 11 is much smaller than unity.

Naturally, the shape of the absorption dips in Figure 11 almost coincides with the inversed shape of extremely short bursts of resonantly scattered radiation, plotted in Figure 9. As is well known, the resonant absorption itself occurs due to the destructive interference of the incident and resonantly scattered radiation (which in turn is due to $\pi/2$ phase shift of the resonant component of polarization). Thus, elimination of the resonant component in the spectrum of the output VUV radiation (frequency of the resonant component coincides with the frequency of the incident VUV radiation) and slight attenuation of the nearest sidebands by a narrowband spectral filter results in the production of the attosecond pulses shown in Figure 12. The pulses arise at the positions of the intensity dips, i.e. where the resonant absorption and scattering take place. As seen

from Figure 9 and Figure 12, the produced pulses are shorter than the bursts of the resonantly scattered radiation. This is due to the facts, that (i) while Figure 9 shows the radiation strength, Figure 12 illustrates the time-dependence of the radiation intensity (squaring of the pulse envelope reduces the pulse duration), and (ii) suppression of the resonant component of the output VUV spectrum and attenuation of the most intense sidebands lead to effective broadening of the output spectrum and, hence, shortening of the produced pulses. The duration of pulses shown in Figure 12 equals 420 as, corresponding to 2.15 cycles of the VUV carrier, the pulse repetition period is determined by the half-cycle of the IR field and equals 6.5 fs. The produced attosecond pulses are nearly bandwidth-limited without external adjustment of phases of the generated sidebands. The values of the parameters $\Delta t_{\text{zero}} = 0.23\pi/\Omega$, $\bar{\gamma}_{\min} = 0.1\times\Omega$, $\bar{\gamma}_{\max} = 15\times\Omega$, used for the analytical calculations in Figure 9, Figure 10, Figure 11 and Figure 12, were chosen in order to support the best agreement between the analytical and numerical solutions. Although in this chapter we consider analytically the limit of small optical depth of the medium, the numerical analysis [39] for the larger values of the optical depth shows that efficiency of transformation of the incident VUV radiation into the attosecond pulses can reach ~ 50%, while efficiency of transformation of the total (IR + VUV) radiation can reach ~ 5%.

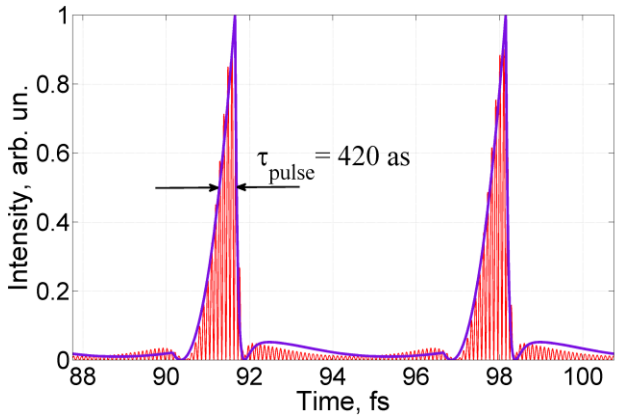

Figure 12. Intensity of the attosecond pulses produced from the output VUV radiation (see Figure 11) via suppression of the resonant components of its spectrum according to Figure 10. The lavender solid line represents the result of analytical calculation for the envelope of the pulses. The rapidly oscillating dashed red curve corresponds to the square of the normalized VUV radiation strength, calculated numerically within the model [38]. The pulse duration is τ_{pulse}=420 as, the pulse repetition period equals half-cycle of the IR field, T=6.5 fs.

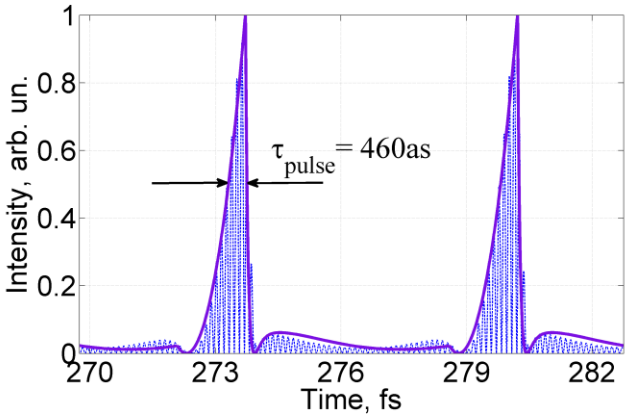

Figure 13. Time-dependence of intensity of the attosecond pulse train, produced from 73.6 nm VUV radiation in neon, dressed by 3.9 μm IR field with intensity I_{IR}=5×10^{13} W/cm^2, via the resonant interaction with $2s^22p^6 \leftrightarrow 2s^22p^5(^2P^0_{1/2})3s$ atomic transition and suppression of the resonant component of the output VUV spectrum. The solid lavender curve represents the analytical solution for the envelope of the pulses. The rapidly oscillating blue curve corresponds to the square of the normalized VUV radiation strength, calculated numerically within the eight-level model [109], which takes into account transitions between the ground atomic state $2s^22p^6$ and the excited states $2s^22p^53s$ and $2s^22p^53p$, coupled to each other by the VUV radiation and the IR field. The latter also induces time-dependent ionization from all the excited atomic states. The pulse duration is τ_{pulse}=460 as, the pulse repetition period equals half-cycle of the IR field, T=6.5 fs.

The pulses of comparable duration, 460 as, shown in Figure 13, can be produced from 73.6 nm VUV radiation via the resonant interaction with atoms of neon, dressed by 3.9 μm IR laser field. The incident VUV radiation is resonant to the transition from the ground atomic state, $2s^2 2p^6$, to one of the lowest excited states, $2s^2 2p^5$ ($^2P^0_{1/2}$)3s. The numerical model, used for calculations, also takes into account the $2s^2 2p^5$ ($^2P^0_{3/2}$)3s state and all the $2s^2 2p^5 3p$ states of neon. The transitions from the ground state to the excited $2s^2 2p^5 3s$ states are induced by the VUV radiation, while the transitions between $2s^2 2p^5 3s$ and $2s^2 2p^5 3p$ states are driven by the IR field. Simultaneously, the IR field induces rapid ionization from all the excited atomic states, which is taken into account via the time-dependent ionization rates (III.3). The intensity of the IR field, required for ionization switching of the resonant interaction in neon and generation of attosecond pulses, shown in Figure 13, equals $I_{IR}=5\times10^{13}$ W/cm^2. The higher IR field intensity compared to the case of helium is primarily caused by the larger value of ionization potential from the resonant excited state of neon (which equals 4.71 eV vs. 3.37 eV in helium). In order to achieve the same value of reduced dimensionless laser field, which determines the ionization rate (III.3), $F_{LF} \propto 1/\kappa^3$ ($\kappa \propto \sqrt{I_P^{(2)}}$ and $I_P^{(2)}$ is the ionization potential from the chosen excited atomic state), the laser intensity in neon should be increased approximately 2.7 times in comparison to that in helium. The pulses, shown in Figure 13, comprise 1.85 cycles of the VUV carrier and are nearly bandwidth-limited. The values of the parameters Δt_{zero}, $\bar{\gamma}_{\min}$, $\bar{\gamma}_{\max}$, used for the analytical calculation in Figure 13, are $\Delta t_{\text{zero}} = 0.25\pi/\Omega$, $\bar{\gamma}_{\min} = 0.1\times\Omega$, $\bar{\gamma}_{\max} = 15\times\Omega$.

In order to show that the effect of extremely short pulse formation from an incident VUV radiation via ionization switching of its resonant interaction with an atomic gas is insensitive to the choice of a specific medium we consider the pulse formation in atomic hydrogen. In Figure 14 we plot the time-dependence of the VUV intensity resulted from the resonant interaction of 122 nm VUV radiation with 1s↔2p transition of atomic hydrogen dressed by 10.65 μm CO_2-laser field with intensity $I_{IR}=2.2\times10^{13}$ W/cm^2 [111] and subsequent suppression of the resonant component of the output VUV spectrum. In such a case, the output radiation represents a train of pulses with duration 1.1 fs and repetition period 17.8 fs. The analytical solution in Figure 14 corresponds to the parameters values $\Delta t_{zero} = 0.21\pi/\Omega$, $\bar{\gamma}_{min} = 0.1\times\Omega$, $\bar{\gamma}_{max} = 10\times\Omega$. From Figure 12 and Figure 14 it follows that the ratio between duration of pulses, produced in atomic hydrogen and helium, 1.1 fs / 0.42 fs ≈ 2.6, almost coincides with the ratio between the wavelengths of respective IR fields, used for interruption of the resonant interaction, 10.65 μm / 3.9 μm ≈ 2.7. This can be understood within the applied approximation (III.10), taking into account that the dependencies of ionization rates from the 2p states of helium and atomic hydrogen on the IR field strength are quite close to each other (the corresponding ionization potentials are 3.37 eV for helium and 3.40 eV for atomic hydrogen). In the quasistatic approximation, the instantaneous excited-state-ionization rate (III.3) is determined solely by the IR field strength, while variation of frequency (wavelength) of the IR field results in stretching / shrinking of the time scale (see Figure 8). Therefore, since the pulse duration is proportional to the length of time-interval of the resonant

interaction in the vicinity of zero-crossings of the IR field, $\tau_{pulse} \propto \Delta t_{\text{zero}}$, it is proportional to the IR wavelength, $\Delta t_{\text{zero}} \propto \Omega^{-1} \propto \lambda_{IR}$.

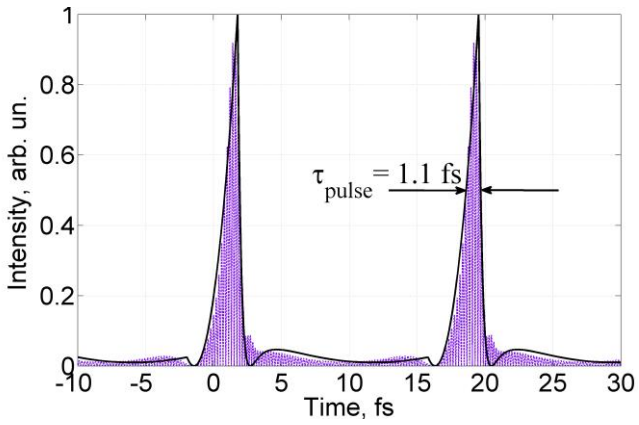

Figure 14. Intensity of the ultrashort pulses, produced from 122 nm VUV radiation due to the resonant interaction with 1s ↔ 2p transition of atomic hydrogen, dressed by 10.65 μm CO_2-laser field with intensity $I_{CO2}=2.2\times10^{13}$ W/cm^2, via suppression of the resonant component of the output VUV spectrum. The solid black curve represents the analytical solution for the envelope of the pulses. The rapidly oscillating lavender curve corresponds to the square of the normalized VUV radiation strength, calculated numerically within the three-level model [16], which takes into account both tunnel ionization from the excited atomic states $|2\rangle=(|2s\rangle+|2p\rangle)/\sqrt{2}$ and $|3\rangle=(|2s\rangle-|2p\rangle)/\sqrt{2}$, and Stark shift of the corresponding energy levels. The pulse duration is τ_{pulse}=1.1 fs, the pulse repetition period equals half-cycle of the CO_2-laser field, T=17.8 fs.

As follows from Figure 9, Figure 10, Figure 11, Figure 12, Figure 13 and Figure 14, regardless of the different dependencies of the instantaneous Stark shifts and excited-state-ionization rates on the IR field strength for helium, neon, and atomic hydrogen, the derived analytical solution even in its simplest form (III.7), (III.15)-(III.19) is in excellent agreement with the results of numerical calculations performed within the more general models [42,109] without the slowly-varying amplitude and the rotating-wave approximations, taking into account time-dependencies of the instantaneous Stark shifts and ionization rates from two excited energy levels [42], nonadiabatic coupling of them

[109], as well as complicated energy level structure in the case of neon. This agreement originates from the fact that the main effect of the IR field in the considered regime, - the periodic switching off the resonant interaction between the VUV radiation and the atoms near crests of the IR field strength and resumption of the resonant interaction near the IR field zero-crossings, is quite correctly described within the two-level model and stepwise approximation (III.10) for the time-dependence of the excited-state tunnel ionization rate.

III.4 Conclusion

In conclusion, in this chapter we extended the method of extremely short pulse formation from the resonant radiation, originally proposed in [42], to non-hydrogenlike media, particularly, to noble gases. We derived the analytical solution for the envelope of extremely short atto- and femtosecond pulses produced from the resonant VUV radiation in an atomic gas, dressed by an IR laser field [37,39,42,108]. The IR field is chosen to be strong enough to almost completely ionize atoms from the upper state of the resonant VUV transition during each IR half-cycle but does not essentially perturb the ground state during the interaction time. The derived solution reveals the origin of pulse formation, which is the interruption of the resonant interaction between the VUV radiation and the atoms near the crests of the IR field strength and resumption of the resonant interaction within extremely short time-intervals in the vicinity of zero-crossings of the IR field. Comparison of the derived analytical solution to the results of numerical calculations within the more general models [42,109] shows excellent agreement both for helium and atomic hydrogen. In such a way, the effect of extremely short pulse formation due to ionization switching of the resonant interaction is shown to be insensitive to the specific

properties of an atom (such as dependence of Stark shift and excited-state ionization rate on the IR field strength), and can be realized under conditions of tunnel ionization in arbitrary atomic gas, possessing spectrally isolated VUV transition from the ground to a bound excited state and a sufficiently high ionization potential from this excited state. Since the carrier frequency of the pulses lies below the ionization potential of neutral atoms and can be varied via the choice of generating atoms and a particular transition, the proposed technique for extremely short pulse formation constitutes a promising tool for nondestructive steering of ultrafast dynamics of the bound electrons inside atoms, molecules, and solids. The discussed approach can be straightforwardly applied for the shortening of pulses of existing extreme-ultraviolet and soft-x-ray lasers [43] towards the attosecond duration. It is worthwhile to mention, that although the present paper is devoted to an analytical description of the attosecond pulse train formation, as it was shown in our previous work [37], the same mechanism of interruption of the resonant interaction via tunnel ionization allows formation of a single attosecond pulse by means of techniques similar to those used for creation of isolated attosecond pulses via high harmonic generation, namely, by using a short (as compared to the period of the IR field) incident VUV radiation pulse, IR radiation pulse with a steep front edge, or fast polarization switch of the IR field.

CHAPTER IV

FORMATION OF A SINGLE ATTOSECOND PULSE VIA SWITCHING OF RESONANT INTERACTION BY TUNNEL IONIZATION[4]

IV.1 Introduction

In the recent decades there was a growing interest in investigation of the processes in atoms and molecules unfolding on the sub-femtosecond time scales. Ultrashort laser pulses represent one of the key tools being used in such studies. The most used method of producing such pulses is high order harmonics generation in gases (HHG). It allows to form pulses up to 67 as long [84], containing harmonics with frequencies up to thousands of electronvolts. However, typical efficiency of HHG is relatively low ($10^{-5} - 10^{-6}$) and formation of ultrashort pulses requires external correction of phases of generated harmonics. Additionally, a carrier frequency of generated pulses is usually higher than ionization potential of most atoms and molecules, which makes investigation of intra-atomic or intra-molecular processes more complicated and leads to photoionization.

Recently, a new method for generating of trains of attosecond pulses with a carrier frequency in the vicinity of atomic resonances was suggested [37,40,42]. Quasi-monochromatic extreme ultraviolet (XUV) laser field propagates through the medium of quasi-resonant atoms that are simultaneously interacting with moderately strong infrared linearly polarized (IR) laser field. IR field ionizes all the excited states of atoms, while

[4] Reprinted with permission from "Attosecond pulse formation via switching of resonant interaction by tunnel ionization" by T.R. Akhmedzhanov, V.A. Antonov, Y.V. Radeonychev and O. Kocharovskaya, 2015, *Proc. SPIE* 9589, X-Ray Lasers and Coherent X-Ray Sources: Development and Applications XI, 95890W, Copyright [2015] by SPIE.

ionization rate from the ground state is negligible. Ionization from excited states is adiabatic and follows instantaneous strength of IR field: ionization rate is extremely big around crests of IR field and negligible around its zeroes. Since effective optical density of a medium is inversely proportional to an ionization rate, there is strong resonant interaction between the medium and the XUV field around zeroes of an IR field, while around crests of an IR field the medium is effectively transparent for an XUV field. Thus, interaction of an XUV field and atoms is periodically switched on and off every half of period of an IR field, which can lead to formation of the trains of attosecond pulses.

In this chapter, we discuss possibility to form a single attosecond pulse using the ionization switching mechanism in He atoms. Formation of a train of attosecond of attosecond pulses manifests multifrequency response of atoms to XUV field. In order to form a single pulse, one needs to restrict such a response to an ultrashort period of time. This can be done using IR pulse with steep front edge [37]. In this approach XUV field resonantly excites resonance coherence which is then ionized by the coming IR field in less than its period. Thus, multifrequency response of atoms is effectively limited to an ultrashort period of time.

The rest of the chapter is structured as follows: in section IV.2 we briefly discuss a simple analytical model of an ionization switching mechanism of the attosecond pulses trains formation and present results of numerical calculation. In section IV.3 a formation of a single attosecond pulse on the steep front edge of IR pulse in the medium of He atoms is numerically investigated. Conclusion of the chapter is provided in section IV.4.

IV.2 Analytical model of pulse formation

In this section, we derive analytical solution describing pulse formation following [40]. Consider propagation of monochromatic XUV field

$$\vec{E}_{XUV} = \frac{1}{2}\vec{x}_0\tilde{E}(z,t)\exp(-i\omega(t - z/c)) + \text{c.c.}. \qquad \text{(IV.1)}$$

along z axis through the atomic medium. Here $\vec{x}_0$ is polarization vector, ω is carrier frequency of XUV field and $\tilde{E}(z,t)$ is its slowly varying envelope. The XUV field is quasi-resonant to transition from the ground atomic state $|1\rangle$ to some excited state $|2\rangle$: $\omega \approx \omega_{21}$. An atomic medium is simultaneously irradiated by a moderately strong low frequency IR field:

$$\vec{E}_{IR} = \vec{x}_0 E_{IR}\cos(\Omega(t - z/V_{IR}))\,. \qquad \text{(IV.2)}$$

where E_{IR} is an amplitude of the IR field, Ω is its frequency and $V_{IR} \approx c$ is its phase velocity. The IR field is off-resonant for any populated atomic transition and is assumed to propagate through the medium without any distortion. In the following we assume the IR field is strong enough to rapidly ionize the excited states of the medium, but not too strong, so that it cannot affect ground state. Since all the fields are linearly polarized in the same direction, they will not change their polarization during propagation and we can drop vector notation.

Propagation of the XUV field through the atomic medium is described by

$$\frac{\partial^2 E_{XUV}}{\partial z^2} - \frac{1}{c}\frac{\partial^2 E_{XUV}}{\partial t^2} = \frac{4\pi}{c^2}\frac{\partial^2 P}{\partial t^2}. \qquad \text{(IV.3)}$$

where P is a high frequency polarization of the medium. Switching to local time $\tau = t - z/c$, within slowly varying envelope approximation ($E_{XUV}(z,\tau) = \frac{1}{2}\tilde{E}_{XUV}(z,\tau)\exp(-i\omega\tau) + c.c.$, $P(z,\tau) = \frac{1}{2}\tilde{P}(z,\tau)\exp(-i\omega\tau) + c.c.$, $\left|\partial\tilde{E}_{XUV}(z,\tau)/\partial z\right| \ll \left|\tilde{E}_{XUV}\omega/c\right|$, $\left|\partial\tilde{E}_{XUV}(z,\tau)/\partial\tau\right| \ll \left|\tilde{E}_{XUV}\omega\right|$, $\left|\partial\tilde{P}(z,\tau)/\partial z\right| \ll \left|\tilde{P}\omega/c\right|$, $\left|\partial\tilde{P}(z,\tau)/\partial\tau\right| \ll \left|\tilde{P}\omega\right|$), reduces this equation is to:

$$\frac{\partial\tilde{E}}{\partial z} = i\frac{2\pi\omega}{c}\tilde{P}. \qquad \text{(IV.4)}$$

In the optically thin medium, the solution of the above equation is found to be:

$$\tilde{E}_{XUV}(z,\tau) = \tilde{E}_{XUV}(0,\tau) + \tilde{E}_{Scatt}(z,\tau) = \tilde{E}_{XUV}(0,\tau) + i\frac{2\pi\omega}{c}\int_0^z \tilde{P}(z',\tau)dz' \qquad \text{(IV.5)}$$

,

where $\tilde{E}_{Scatt}(z,\tau) = i\frac{2\pi\omega}{c}\int_0^z \tilde{P}(z',\tau)dz'$ is a high frequency field scattered by the atoms. In its turn, the slowly varying polarization $\tilde{P}$ is defined by the slowly varying coherence $\tilde{\rho}_{21}$: $\tilde{P} = 2Nd_{12}\tilde{\rho}_{21}$. An atomic coherence is governed by the equation

$$\frac{\partial\tilde{\rho}_{21}}{\partial t} + \left(i(\omega_{21}(\tau) - \omega) + \gamma_{21}(\tau)\right)\tilde{\rho}_{21} = \frac{i}{2\hbar}n_{12}d_{21}\tilde{E}, \qquad \text{(IV.6)}$$

where $\omega_{21}(\tau) = \bar{\omega}_{21} + \Delta\omega_{21}(\tau)$ is a transition frequency and $\gamma_{21}(\tau)$ is a decay rate. Both the transition frequency and decay rate are time dependent due to a presence of the IR field.

Transition frequency $\omega_{21}(\tau)$ contains time-averaged constant frequency $\bar{\omega}_{21}$ (which includes unperturbed transition frequency and constant part of Stark shift) and time-dependent part of Stark shift $\Delta\omega_{21}(\tau)$. Decay rate $\gamma_{21}(\tau) = \gamma_{21}{}^{0} + w_{ion}^{(2)}(\tau)/2$ includes unperturbed decoherence rate $\gamma_{21}{}^{0}$ and time-dependent part $w_{ion}^{(2)}(\tau)/2$, where $w_{ion}^{(2)}(\tau)$ is tunnel ionization rate. In the following we will assume that ionization of the excited states of atom is quasi-static in its nature, which means it follows instantaneous strength of IR field. This case corresponds to the small value of the Keldysh parameter $\gamma_{Keldysh} \ll 1$.

In the case when the major mechanism of excited state ionization is tunneling, ionization probability $w_{ion}^{(2)}(\tau)$ is given by [112]:

$$w_{ion}^{(2)}(\tau) = \frac{m_e e^4}{\hbar^3} C_{\kappa l}^2 \kappa^2 (2l+1) \frac{4^{n^*-|m|}(l+|m|)!}{|m|!(l-|m|)!} \times \\ \times |F_{IR}(\tau)|^{|m|+1-2n^*} \exp\left\{-\frac{2}{3|F_{IR}(\tau)|}\right\} \quad . \qquad \text{(IV.7)}$$

where $\kappa = \sqrt{I_P^{(2)}/I_H}$, $I_P^{(2)}$ is the ionization potential from the excited atomic state $|2\rangle$, $I_H = \frac{m_e e^4}{2\hbar^2}$ is the ionization potential from the ground state of an atomic hydrogen, m is the projection of the angular momentum l on the IR electric field, $n^* = Z/\kappa$ is the effective principal quantum number, Z is the atomic core charge, $C_{\kappa l}$ is the dimensionless asymptotic coefficient of the atom wave function, and $F_{IR}(\tau) \equiv \frac{E_{IR}(\tau)}{\kappa^3 E_A}$ is the reduced dimensionless IR field (E_A is atomic unit of field).

Tunneling ionization rate has a sharp dependence on instantaneous strength of the IR field: it is extremely big around its crests and negligible around its zeroes. Since an effective optical depth of medium is inversely proportional to decay rate $\gamma_{21}(\tau) = \gamma_{21}{}^{0}$, medium becomes almost transparent for XUV field twice during a period of the IR field (around its crests). Thus ionization switches a resonant interaction between the XUV field and medium twice during its period. It can be used for formation of the ultrashort pulses: due to ionization switching, scattered field will be a train of ultrashort pulses. Thus, if at the exit of the medium incident XUV field frequency is filtered out, the *output field* will also have a form of a train of ultrashort pulses.

Such sharp dependence of an ionization rate on the field strength can be effectively modelled by stepwise function with a repetition period equal to a half of the IR field period:

$$\gamma_{21}(\tau) = \begin{cases} \bar{\gamma}_{\min}, & 0 \le \tau < \Delta t_{\text{zero}}, \\ \bar{\gamma}_{\max}, & \Delta t_{\text{zero}} \le \tau < \pi/\Omega, \end{cases} \qquad \text{(IV.8)}$$
$$\gamma_{21}(\tau + \pi/\Omega) = \gamma_{21}(\tau)$$

where $\bar{\gamma}_{\min}$ is the minimum value of decoherence rate around zeroes of IR field and $\bar{\gamma}_{\max}$ is the big decoherence rate, corresponding to the rest of a half of the period. This simplified description of ionization of the excited state allows to solve the set of the wave and density matrix equations analytically (for strong enough IR field considered in this chapter, Stark effect can be neglected [38]). As it was shown in [40], the analytical steady state solution for a scattered field is given by:

$$\tilde{E}_{Scatt}(\tau)=\begin{cases}\tilde{E}^{(1)}_{Scatt}(\tau), & 0\le\tau<\Delta t_{\text{zero}},\\ \tilde{E}^{(2)}_{Scatt}(\tau), & \Delta t_{\text{zero}}\le\tau<\pi/\Omega,.\end{cases}$$
$$\tilde{E}_{Scatt}(\tau+\pi/\Omega)=\tilde{E}_{Scatt}(\tau) \qquad \text{(IV.9)}$$

where $\tilde{E}^{(1)}_{Scatt}(\tau)=i\mathrm{A}\times a^{(1)}_{21}(\tau)$ and $\tilde{E}^{(2)}_{Scatt}(\tau)=i\mathrm{A}\times a^{(2)}_{21}(\tau)$; $\mathrm{A}\equiv 4\pi N d_{12}\dfrac{\omega}{c}L$ and

$$a_{21}(\tau)=\begin{cases}a^{(1)}_{21}(\tau), & 0\le\tau<\Delta t_{\text{zero}},\\ a^{(2)}_{21}(\tau), & \Delta t_{\text{zero}}\le\tau<\pi/\Omega,\end{cases}. \qquad \text{(IV.10)}$$

where $a^{(1)}_{21}(0)=a^{(2)}_{21}(\pi/\Omega)$ and $a^{(2)}_{21}(\Delta t_{\text{zero}})=a^{(1)}_{21}(\Delta t_{\text{zero}})$. The dependences $a^{(1)}_{21}(\tau)$ and $a^{(2)}_{21}(\tau)$ are given by

$$\begin{cases}a^{(1)}_{21}(\tau)=C_1\exp\left\{\left(i\Delta\omega-\bar{\gamma}_{\min}\right)\tau\right\}+D_1,\\ a^{(2)}_{21}(\tau)=C_2\exp\left\{\left(i\Delta\omega-\bar{\gamma}_{\max}\right)\left(\tau-\Delta t_{\text{zero}}\right)\right\}+D_2,\end{cases} \qquad \text{(IV.11)}$$

where $\Delta\omega\equiv\omega-\omega^{(0)}_{21}$ and

$$\begin{cases}D_1=i\dfrac{n_{12}d_{21}E_0}{2\hbar\left(\bar{\gamma}_{\min}-i\Delta\omega\right)},\\ D_2=i\dfrac{n_{12}d_{21}E_0}{2\hbar\left(\bar{\gamma}_{\max}-i\Delta\omega\right)},\end{cases} \qquad \text{(IV.12)}$$

$$\begin{cases}C_1=\left(D_2-D_1\right)\dfrac{\exp\left\{\left(i\Delta\omega-\bar{\gamma}_{\max}\right)\left(\pi/\Omega-\Delta t_{\text{zero}}\right)\right\}-1}{\exp\left\{\left(i\Delta\omega-\bar{\gamma}_{\max}\right)\pi/\Omega\right\}\exp\left\{\left(\bar{\gamma}_{\max}-\bar{\gamma}_{\min}\right)\Delta t_{\text{zero}}\right\}-1},\\ C_2=\left(D_1-D_2\right)\dfrac{\exp\left\{\left(i\Delta\omega-\bar{\gamma}_{\min}\right)\Delta t_{\text{zero}}\right\}-1}{\exp\left\{\left(i\Delta\omega-\bar{\gamma}_{\max}\right)\pi/\Omega\right\}\exp\left\{\left(\bar{\gamma}_{\max}-\bar{\gamma}_{\min}\right)\Delta t_{\text{zero}}\right\}-1}.\end{cases} \qquad \text{(IV.13)}$$

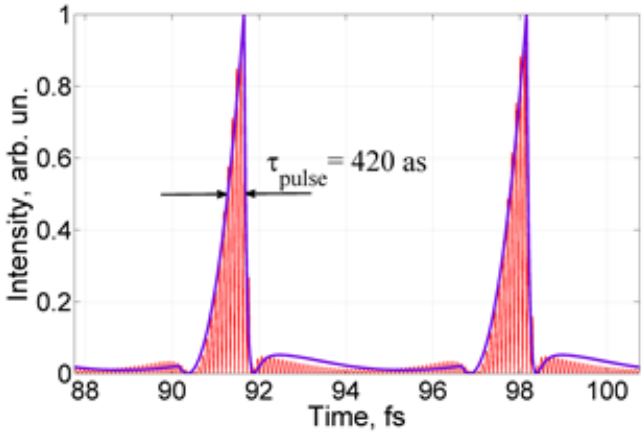

Figure 15. Intensity of a train of ultrashort pulses formed from output XUV radiation via spectral filtering of its resonant component. The lavender line corresponds to analytically calculated envelope of the pulses. The red oscillating curve corresponds to the results of numerical calculation (see text for details). Figure reprinted with permission from [40].

After filtering of an incident XUV field frequency the scattered field can have a form of the attosecond pulses train [40]. In order to verify the derived solution, we compare it with a numerical calculation for He atoms. It models interaction of a weak quasi-resonant XUV field with the three-level He (1s, 2s and 2p states) simultaneously interacting with the IR field. Ionization of excited state is described by (IV.7). Other excited states are taken into account via AC Stark shift. We find XUV field, scattered by atom and filter out incident XUV field frequency. We consider the following parameters: incident XUV field has wavelength 58.4 nm (resonant to unperturbed 1s-2p transition), IR field with wavelength 3.9 μm has intensity $I_{IR}=1.5\times10^{13}$ W/cm^2. The intensity of filtered output field is shown in Figure 15 by red oscillating line. Analytical solution with fitted parameters $\Delta t_{zero}=0.23\pi/\Omega$, $\bar{\gamma}_{min}=0.1\times\Omega$, $\bar{\gamma}_{max}=15\times\Omega$ is shown by lavender line. As

it can be seen from the Figure 15, an agreement between simple analytical model and numerical solution is excellent.

IV.3 Formation of a single attosecond pulse from the resonant XUV radiation on a steep front edge of a strong IR field

As it was shown in [40], ionization switching of resonant interaction leads to multi-frequency atomic response and, thus, formation of a train of attosecond pulses in the output XUV field (after filtering its resonant component). However, for many applications [54], ability to form a *single* attosecond pulses would be beneficial. In order to achieve single pulse formation, multifrequency response of atoms needs to be confined within an extremely short period of time.

One of the ways to achieve it is to use a strong IR pulse with steep front edge [37]. In this method, quasi-monochromatic quasi-resonant incident XUV field enters medium before an IR pulse and excites resonant polarization of the medium. At some moment, a strong IR field pulse enters medium ionizing most of the excited atoms and cancelling resonant interaction between atoms and an XUV field. If front edge of IR pulse is steep enough, excited atoms would be ionized within half-cycle of an IR field. It means that transient multifrequency response of atoms would be confined within extremely short period of time and single attosecond pulse can be formed.

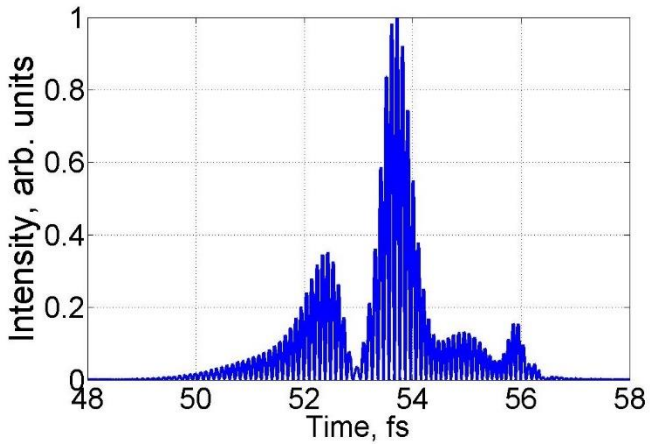

Figure 16. Intensity of the single ultrashort pulse produced from the output XUV radiation (after filtering incident XUV field frequency). The pulse length is about 640 as.

Formation of a single attosecond pulse in the medium of hydrogen-like ions was discussed in [37]. Here the possibility to form a single attosecond pulse in a thin layer of He atoms by the same method is shown. Time dependent Schrodinger equation (TDSE) for single He atom simultaneously interacting with the XUV and IR field pulses is numerically solved. We use a pseudospectral time-dependent method [93] and a model potential [94] for He atom. The XUV field scattered by atom is defined by high frequency part of the excited dipole moment (we filter out low-frequency oscillations caused by the IR field).

We consider the IR field with a carrier wavelength 2000 nm, 6^{th} power super-Gaussian envelope with FWHM about 22 fs, peak intensity $I_{IR}=1.0\times10^{14}$ W/cm^2 and the weak incident XUV field with a carrier wavelength 58.4 nm (resonant to transition from He ground state $1s^2$ to the excited state 1s2p). The attosecond pulse which will be formed at the exit of a thin medium is shown in Figure 16 (incident XUV frequency is filtered). As it can be seen, a single pulse with time duration of ~640 as is formed.

IV.4 Conclusion

We have investigated attosecond pulse formation via switching of resonant interaction by tunnel ionization. Quasi-static ionization from the resonantly populated state by an IR field leads to a periodic switching of resonant interaction between XUV radiation and atoms. This ionization switching allows producing of trains of extremely short pulses from the XUV radiation. Use of an IR field pulse with steep front edge allows confining multifrequency atomic response almost within a half-cycle of an IR field and producing of a single attosecond pulse. Results of numerical calculations show the possibility to form a single pulse with time duration of several hundred of attoseconds.

CHAPTER V

ULTIMATE CAPABILITIES FOR FEW-CYCLE PULSE FORMATION VIA RESONANT INTERACTION OF XUV RADIATION WITH IR-FIELD-DRESSED ATOMS[5]

V.1 Introduction

Starting from the turn of the millennium [83,118], attosecond physics has become a fascinating branch of modern science, opening the possibility for real-time imaging and steering of the electronic motion in atoms, molecules, and solids on its intrinsic timescale [56-59,119-121], conceptually similar to the femtosecond optical control of chemical reactions [122].

During the last years, a remarkable progress has been achieved in understanding and manipulating the sub-laser-cycle dynamics of the bound and autoionizing atomic states induced by an intense laser field combined with attosecond pulses/pulse trains of the extreme ultraviolet (XUV) radiation produced via high-harmonic generation (HHG) of a replica of the laser field [22,24,25,27,28,34-36,57,59,90,119,120,123]. In these studies, the laser field is not strong enough to ionize or excite atoms from their ground state, but it strongly perturbs the excited states resonantly populated by high-harmonic radiation. This perturbation has been visualized directly via the attosecond transient absorption technique [24,25,119]. Due to mutual coherence of the fundamental laser field

[5] Reprinted with permission from "Ultimate capabilities for few-cycle pulse formation via resonant interaction of XUV radiation with IR-field-dressed atoms" by T. R. Akhmedzhanov, M.Yu. Emelin, V. A. Antonov, Y. V. Radeonychev, M.Yu. Ryabikin, and Olga Kocharovskaya, 2017, accepted to Phys. Rev. A, Copyright [2017] by American Physical Society.

and its high-order harmonics, the pathways of atomic excitation and ionization through absorption of a higher harmonic photon or a lower harmonic photon along with a few photons of the laser field (or, explicitly, the pathways of atomic excitation by different harmonics into the same Floquet state) interfere, leading to beatings of the atomic ionization yield versus the sub-laser-cycle time delay between the harmonic signal and the laser field [22,24,25,28,34,35,123] and allowing for the complete transparency of the medium for the resonant XUV radiation [22,90]. However, the possibilities for such investigations and control over the ultrafast intra-atomic dynamics are limited by the nature of HHG process in gases, which is commonly used for the attosecond pulse formation and dictates the relatively high carrier frequency and low efficiency of generation of the XUV pulses [56,59,83].

Although in recent years both HHG and laser technologies have been considerably advanced, resulting, in particular, in the generation of high-energy (~ 1μJ) isolated attosecond pulses [124], the photon energy of these pulses remains above the ionization potential of both the generating medium and majority of neutral media, which prevents from using them for nonionizing manipulation of ultrafast intra-atomic and intra-molecular processes and impedes investigation of such processes without photoionization (to the best of our knowledge, studies of bound-state attosecond electron dynamics have been performed only in He and Ne, the atoms with highest ionization potentials). At the same time, the below-threshold harmonics can be produced with generation efficiency up to 1% (which is much higher than that of the above-threshold harmonics used in [124]) under the resonance conditions [125]. However, although the below-threshold harmonics

are generated in a comb [126], they are not phase-matched with each other and do not constitute attosecond pulses in time domain. Furthermore, the use of resonantly enhanced HHG and plasma-based x-ray lasers allow for producing XUV and soft x-ray field with high power, exceeding the power of nonresonant high harmonics at the same wavelength. In particular, the transitions from autoionizing states to the ground state of multielectron atoms (ions) allow to increase the intensity of the resonant (above-threshold) harmonic compared to nonresonant ones by two orders of magnitude and achieve 10^{-4} efficiency of a single harmonic generation [96,97,127], whereas transient inversion on high-frequency transitions of multiply charged ions in laser-produced plasmas provides an opportunity to generate picosecond pulses of XUV and soft x-ray field with energy up to several mJ [44-47]. However, these sources produce a quasi-monochromatic radiation, which is not suitable for the time-domain studies of the ultrafast femto- and attosecond processes.

Recently, a method has been proposed, which may allow for the conversion of XUV and soft x-ray radiation from these high-energy sources into the attosecond pulses. This method uses the resonant interaction of an incident XUV radiation with an atomic gas dressed by a moderately strong infrared (IR) laser field [41,42] and is based on sub-laser-cycle splitting (due to the linear Stark effect [25,128]) and/or broadening (due to ionization [112,129]) of the excited energy levels, selected and populated by the XUV radiation, under the action of the IR field. The magnitudes of the splitting and broadening of the atomic energy levels oscillate in time and space along with oscillation of the laser-field strength, leading to the multifrequency resonant response of the IR-field-dressed atoms to the (quasi-monochromatic) incident XUV radiation. Under the optimal

conditions, both Stark splitting of the resonant excited atomic energy level in a hydrogen-like medium [38,41] and rapid quasistatic ionization from the resonant excited state in arbitrary atomic gas [37,40,42] allow for the formation of nearly bandwidth-limited few-femto- or attosecond pulses without external adjustment of phases of the generated sidebands (in contrast with the attosecond pulse formation through HHG, which implies the attochirp compensation [130]). The possibilities to produce both the (quasi-) periodic pulse trains [38,40-42] and the isolated attosecond pulses [37] were shown. The efficiency of energy conversion of the XUV field into a pulse train can exceed 75 % [38] in the case of pulse formation based on the linear Stark effect and reach 10 % in the ionization-switching regime [39]. The discussed approach allows for the formation of attosecond pulses with the carrier frequency below the ionization potential of neutral atoms / molecules and solids (corresponding to the wavelength range of 50 to 200 nm), providing an opportunity for the nondestructive sub-femtosecond control of the bound electron dynamics [57,59,119-121]. Proximity of the carrier frequency of the pulses to various resonances in neutral and ionized media holds the promise to use the resonant enhancement of the nonlinear susceptibilities for the implementation of the attosecond pump - attosecond probe experiments [124,131]. Furthermore, the possibility to transform high energy picosecond pulses of x-ray plasma lasers [44-47,63,78,87] into the trains or isolated attosecond pulses, opens the door for numerous applications in dynamical, high temporal and high spatial resolution element-specific imaging in biochemistry and material science [80,81].

The previously obtained results were restricted to three- or two-level models, implying adiabatic approximation for atomic perturbation by the IR field and the resonant approximation for interaction of XUV radiation with atoms. The influence of the IR field on the atomic system was taken into account through space-time variation of instantaneous position and width of the resonant excited atomic energy levels, while interaction of the XUV radiation with atoms, although described dynamically, was considered in few-level models. Although this approach is correct in the limit of a low frequency and low intensity of the IR field and allows for the analytical solutions, as well as numerical treatment of the propagation problems, it does not allow for determining the ultimate capabilities and the limits of applicability of the method.

In the present chapter, we address these questions taking into account all the multiphoton processes in the considered system on the basis of numerical solution of the full three-dimensional time-dependent Schrödinger equation (TDSE) in the single-active-electron approximation. We find the maximal intensity and the minimal wavelength of the laser field suitable for few-femto- and attosecond pulse formation from an incident XUV radiation via modulation of the resonant atomic response, as well as the minimal duration of the produced pulses. The mechanisms of pulse formation due to the linear Stark effect [38,41] and the excited-state ionization [37,40,42] are considered for the hydrogen and helium atoms, respectively. The results of numerical calculations are compared to the analytical solutions obtained in [38,40]. In order to analyze the differences between these quasistatic analytical solutions [38,40] and the results of *ab initio* TDSE calculations, we develop a generalized analytical theory, which takes into account a sub-IR-field-cycle

space-time variation of the quadratic Stark effect and the excited-state ionization rates. The developed theory allows for distinguishing the differences between the simplified analytical solutions [38,40] and the *ab initio* calculations, which are caused by the interplay between the Stark effect and quasistatic ionization, from those originating from the nonadiabatic processes. Moreover, the generalized theory allows for tracing a transition between the two regimes of pulse formation (based on the linear Stark effect and excited-state ionization) with increasing intensity of the IR field. The performed TDSE calculations are free of most of the assumptions made in theoretical works (restricting the number of levels, neglecting the interaction with a continuum or using the quasi-static approximation for ionization rates, neglecting higher-order Stark effect, etc.) and, thus, provide a direct bridge to an experimental implementation of suggested mechanisms.

The chapter is organized as follows. In Section V.2, we analyze the possibilities for ultrashort pulse formation from XUV radiation via Stark splitting of the resonant excited energy level of the atomic hydrogen by a moderately strong IR field of various intensities and wavelengths. In Section V.3, we consider the ionization-switching mechanism of few-cycle attosecond pulse formation from the resonant XUV radiation in helium under the action of a strong IR field. The chapter is finalized by a conclusion.

V.2 Few-femtosecond pulse formation via linear stark effect in atomic hydrogen

Let us consider the propagation of XUV radiation through an optically thin medium of an atomic gas. At the entrance to the medium, x=0, the radiation is monochromatic and its electric field has the form

$$\vec{E}_{inc}(t) = \frac{1}{2}\vec{z}_0 E_0 \exp\{-i\omega_0 t\} + \text{c.c.}, \qquad \text{(V.1)}$$

where E_0 is the incident field amplitude, ω_0 is its angular frequency, and **c.c.** stands for the complex conjugation. The radiation (V.1) is chosen to be near-resonant to the transition $|1\rangle \leftrightarrow |2\rangle$ between the ground state and an excited atomic bound state, $\omega_0 \approx \omega_{21}^0$ (where ω_{21}^0 is the frequency of the unperturbed resonant transition).

The medium is simultaneously irradiated by a moderately strong IR laser field

$$\vec{E}_{IR}(x,t) = \frac{1}{2}\vec{z}_0 E_C \exp\{-i\Omega(t - x/c) + \varphi_0\} + \text{c.c.}, \qquad \text{(V.2)}$$

where E_C is the amplitude of the IR field, Ω is its angular frequency, φ_0 is its initial phase ($\varphi_0 = 0$, unless specified otherwise), and c is the speed of light in vacuum. Both the IR field and the XUV radiation propagate along the same direction and are identically polarized. Since in an isotropic gas the polarizations of the fields are not changed, the vector notations will be omitted for now on. Since the medium considered in the chapter is optically thin, due to far detuning from the relevant atomic resonances and tiny population of the excited states, the IR field (V.2) does not suffer from atomic dispersion and traverses the medium without appreciable distortions.

Propagation of the XUV radiation through the medium is described by the wave equation

$$\frac{\partial^2 E_{XUV}}{\partial x^2} - \frac{1}{c^2}\frac{\partial^2 E_{XUV}}{\partial t^2} = \frac{4\pi}{c^2}\frac{\partial^2 P_{XUV}}{\partial t^2}, \qquad \text{(V.3)}$$

where E_{XUV} is the XUV radiation strength, $E_{XUV}(x=0,t)=E_{inc}(t)$, and P_{XUV} is the high-frequency polarization of the medium.

Since the characteristic scales of a spatial evolution of XUV radiation in a gas are much larger than its wavelengths, the substitution $t \to \tau \equiv t - x/c$ (within the slowly-evolving wave approximation [114,115]) allows for reducing the wave equation (V.3) to

$$\frac{\partial E_{XUV}}{\partial x} = -\frac{2\pi}{c}\frac{\partial P_{XUV}}{\partial \tau}. \qquad \text{(V.4)}$$

Finally, in an optically thin medium (when rescattered field remains much weaker than the incident one) the output radiation transmitted through the medium of thickness L has the form

$$E_{XUV}(L,\tau) = E_{inc}(\tau) + E_{Scatt}(L,\tau), \quad E_{Scatt}(L,\tau) = \frac{2\pi L}{c}\frac{dP_{XUV}(\tau)}{d\tau}, \qquad \text{(V.5)}$$

where $E_{Scatt}(L,\tau)$ is the resonantly scattered XUV radiation determined by the incident fields (V.1), (V.2).

In a gas, $P_{XUV}(\tau) = Nd_{XUV}(\tau)$, where N is the concentration of atoms and $d_{XUV}(\tau)$ is the high-frequency part of the dipole moment of an individual atom, $d(\tau) = e\langle z(\tau)\rangle$ (where e is the electron charge and $\langle z(\tau)\rangle$ is the expectation value of the active atomic electron displacement along the polarization direction of the field).

In order to get an *ab initio* solution for $d(\tau)$, we numerically solve the three-dimensional TDSE for an atom simultaneously irradiated by the XUV and IR fields (V.1) and (V.2):

$$i\hbar\frac{\partial}{\partial t}\psi = \left(H_0 + V\right)\psi\,, \tag{V.6}$$

where ψ is the wavefunction of the active electron, $H_0 = -\frac{\hbar^2}{2m}\Delta + U(\vec{r})$ is the unperturbed atomic Hamiltonian (in the case of atomic hydrogen, $U(\vec{r}) = -e^2/r$ corresponds to the pure Coulomb potential), and $V = e\vec{E}_{IR}(t)\cdot\vec{r} + e\vec{E}_{XUV}(t)\cdot\vec{r}$ is the Hamiltonian of atom-field interaction. The solution is obtained using the generalized pseudospectral method [93]. The high-frequency component of the dipole moment $d_{XUV}(\tau)$ is calculated by filtering out the low-frequency components of the total dipole moment, $d(\tau)$, at the frequencies of low-order harmonics of the IR field and below. An additional filtering is applied for the spectral components with photon energies exceeding the atomic ionization potential, which accounts for a strong photoabsorption of XUV radiation just above the ionization potential.

In the following, the results of TDSE calculations are compared to the analytical solution [38] derived for atomic hydrogen exposed to XUV radiation, which is resonant to the transition n=1 ↔ n=2 (where n is the principal quantum number). The analytical solution takes into account the sub-laser-cycle splitting of the excited energy level n=2 due to the linear Stark effect produced by the IR field, but neglects time dependencies of the shift and broadening of the excited energy level due to the quadratic Stark effect and the excited-state ionization, respectively.

In order to analyze the discrepancies between the simplified modeling and TDSE solution, a generalized analytical solution is derived, which takes into account the interplay between the Stark effect and excited-state ionization, as well as the quadratic correction to the alternating-current (AC) linear Stark effect in atomic hydrogen. The analytical solution implies the approximation of slowly-varying amplitudes: $F(\tau) = \frac{1}{2}\tilde{F}(\tau)\exp\{-i\omega_0\tau\} + \text{c.c.}$, $\left|\frac{d\tilde{F}}{d\tau}\right| << \omega_0\left|\tilde{F}\right|$, where $F(\tau) = \{E_{XUV}(L,\tau), E_{Scatt}(L,\tau), P_{XUV}(\tau)\}$. Within such an approximation, Eq. (V.5) takes the form

$$\tilde{E}_{XUV}(L,\tau) = E_0 + \tilde{E}_{Scatt}(L,\tau), \quad \tilde{E}_{Scatt}(L,\tau) = i\frac{2\pi\omega L}{c}\tilde{P}_{XUV}(\tau). \tag{V.7}$$

The analytical solution for atomic hydrogen is derived within the three-level model, which includes the ground energy level n=1 and the two sublevels of the first excited energy level n=2 selected and populated by the resonant XUV radiation (V.1). The corresponding atomic states are $|1\rangle=|100\rangle$, $|2\rangle=(|200\rangle+|210\rangle)/\sqrt{2}$, and $|3\rangle=(|200\rangle-|210\rangle)/\sqrt{2}$ (numerals $|nlm\rangle$ label principal, orbital, and magnetic quantum numbers, respectively). In the three-level approximation, the nonresonant interaction of XUV radiation with the medium is neglected, while the slowly-varying amplitude of the resonant polarization is given by

$$\tilde{P}_{XUV}(\tau) = 2Nd_{tr}\left(a_{21}(\tau) - a_{31}(\tau)\right), \tag{V.8}$$

where N is the concentration of atoms, $d_{tr} = 2^7 er_B/3^5$ is the dipole moment of the resonant transitions (e is the charge of the electron, r_B is the Bohr radius), and a_{21}, a_{31} are the

slowly-varying amplitudes of the atomic coherencies ρ_{21}, ρ_{31} at the transitions $|1\rangle \leftrightarrow |2\rangle$ and $|1\rangle \leftrightarrow |3\rangle$, respectively. The coherency amplitudes satisfy the equations

$$\begin{cases} \dfrac{da_{21}}{d\tau} + \Big(i\big(\omega_{21}(\tau) - \omega_0\big) + \gamma_{21}(\tau)\Big)a_{21} = i\dfrac{d_{tr}E_0}{2\hbar}, \\ \dfrac{da_{31}}{d\tau} + \Big(i\big(\omega_{31}(\tau) - \omega_0\big) + \gamma_{31}(\tau)\Big)a_{31} = -i\dfrac{d_{tr}E_0}{2\hbar}, \end{cases} \tag{V.9}$$

where $\omega_{21}(\tau)$, $\omega_{31}(\tau)$ and $\gamma_{21}(\tau)$, $\gamma_{31}(\tau)$ are the instantaneous frequencies and decoherence rates of the transitions $|1\rangle \leftrightarrow |2\rangle$ and $|1\rangle \leftrightarrow |3\rangle$, respectively, which vary in space and time due to the sub-laser-cycle shift and broadening of the energy levels $|2\rangle$ and $|3\rangle$ introduced by the IR field; $\omega_{s1}(\tau) = \omega_{s1}^{(0)} + \Delta\mathrm{E}_s(\tau)/\hbar$ and $\gamma_{s1}(\tau) = \gamma_{s1}^{(0)} + w_{ion}^{(s)}(\tau)/2$, where $\omega_{s1}^{(0)}$ and $\gamma_{s1}^{(0)}$ are the unperturbed frequency and decoherence rate of the transition $|1\rangle \leftrightarrow |s\rangle$, while $\Delta\mathrm{E}_s(\tau)$ and $w_{ion}^{(s)}(\tau)$ are the instantaneous shift of / ionization rate from the excited state $|s\rangle$; $\hbar$ is the Planck's constant. The perturbation of the ground state $|1\rangle$ by the laser field of intensity relevant to this study is negligible.

In order to find the generalized analytical solution, we use the biharmonic approximation for the dependencies $\omega_{s1}(\tau)$ and $\gamma_{s1}(\tau)$:

$$\omega_{s1}(\tau) = \bar{\omega}_{tr} \mp \Delta_{\omega}^{(1)}\cos(\Omega\tau) - \Delta_{\omega}^{(2)}\cos(2\Omega\tau), \tag{V.10a}$$

$$\gamma_{s1}(\tau) = \bar{\gamma}_{tr} \pm \Delta_{\gamma}^{(1)}\cos(\Omega\tau) + \Delta_{\gamma}^{(2)}\cos(2\Omega\tau), \tag{V.10b}$$

where the upper and lower signs correspond to s=2 and s=3, respectively. The values $\bar{\omega}_{tr}$ and $\bar{\gamma}_{tr}$ characterize the time-averaged position and width of the atomic resonances in the presence of IR field; $\Delta_{\omega}^{(1)}$ and $\Delta_{\omega}^{(2)}$ are amplitudes of the sweeping of the transition

frequencies due to the linear and the quadratic Stark effect, respectively, while $\Delta_\gamma^{(1)}$ and $\Delta_\gamma^{(2)}$ are variations of ionization rates from the excited states $|2\rangle$ and $|3\rangle$ at the fundamental and the doubled frequency of the laser field (V.2). The values $\Delta_\omega^{(1)}$ and $\Delta_\gamma^{(1)}$ are nonzero due to an asymmetry of the states $|2\rangle$ and $|3\rangle$ of atomic hydrogen in parabolic coordinates.

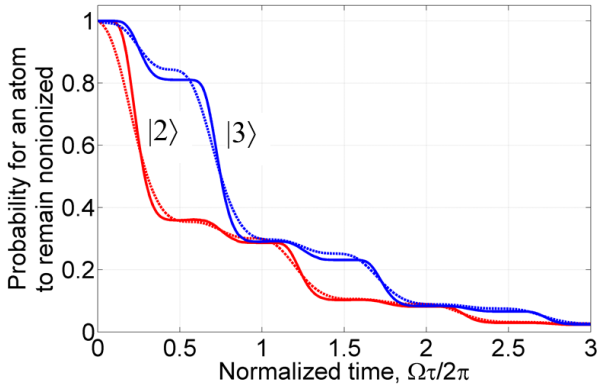

Figure 17. Time dependencies of a probability for a hydrogen atom initially excited into the state $|2\rangle$ or $|3\rangle$ to remain nonionized by the monochromatic IR field of intensity $I_{IR} = 2.5\times10^{12}$ W/cm^2 and wavelength $\lambda_{IR} = 8$ μm. The lower red curves correspond to the state $|2\rangle$, while the upper blue curves characterize the state $|3\rangle$. The solid curves are the results of *ab initio* solution of the TDSE, whereas the dashed curves represent the approximation (V.10 b).

The parameters $\overline{\gamma}_{tr}$, $\Delta_\gamma^{(1)}$, and $\Delta_\gamma^{(2)}$ of the decoherence rate for each combination of intensity and wavelength of the IR field were determined via *ab initio* solution of an independent auxiliary problem. For this purpose, TDSE was solved for an atom initially put into the resonant excited state and subjected to the IR field of required intensity and wavelength. Then, the norm of electron wavefunction in the vicinity of atomic core (inside a sphere with radius R=25 atomic units) was calculated numerically. As a result, the

probability for an atom to remain nonionized by the IR field was found as a function of time. An example of such a calculation is shown in Figure 17. The parameters $\overline{\gamma}_{tr}$, $\Delta_{\gamma}^{(1)}$, and $\Delta_{\gamma}^{(2)}$ were then found via fitting the obtained time dependence by $\exp\left\{\int_0^{\tau}\gamma_{s1}(\tau')d\tau'\right\}$, where $\gamma_{s1}(\tau')$ is given by Eq. (V.10 b). The amplitude of the linear Stark effect, $\Delta_{\omega}^{(1)}$, is calculated via the perturbation theory: $\Delta_{\omega}^{(1)}=\frac{3\hbar}{m_e e}E_C$ (m_e is the electron mass); the time-averaged transition frequency is $\bar{\omega}_{tr}=\omega_{21}^{(0)}-\Delta_{\omega}^{(2)}$; finally, the amplitude of the quadratic Stark shift, $\Delta_{\omega}^{(2)}$, is chosen to provide the best agreement between the generalized analytical solution and the results of TDSE calculations for the output XUV radiation. In the limit of low-frequency and low-intensity modulating IR field, the values of $\Delta_{\omega}^{(2)}$ determined in this way are comparable to those predicted by the perturbation theory. Thus, for 10.65 μm IR field with intensity 1.4×10^{12} W/cm^2, we get $\Delta_{\omega}^{(2)}=0.46\times\Omega$, while the static perturbation theory gives $\Delta_{\omega}^{(2)}=0.52\times\Omega$. In the case of stronger and higher-frequency IR fields, the perturbation theory overestimates the quadratic Stark shift.

The steady-state solution of Eqs. (V.7)-(V.10) reads

$$\tilde{E}_{Scatt}(L,\tau) = -E_0 L \frac{2\pi N d_{tr}^2 \omega_0}{\hbar c} \times \exp\left\{\left(iP_\omega^{(2)} - P_\gamma^{(2)}\right)\sin\left(2\Omega\tau\right)\right\} \times$$
$$\sum_{n,l,m,k=-\infty}^{\infty} (i)^{m+k} J_n\left(P_\omega^{(1)}\right) J_l\left(P_\omega^{(2)}\right) I_m\left(P_\gamma^{(1)}\right) I_k\left(P_\gamma^{(2)}\right) \times \exp\left\{-i2(l+k)\Omega\tau\right\} \times$$
$$\left[\frac{\exp\left\{\left(iP_\omega^{(1)} - P_\gamma^{(1)}\right)\sin\left(\Omega\tau\right) - i(n+m)\Omega\tau\right\}}{i\left(\bar{\omega}_{tr} - \omega - \left[(n+m)+2(l+k)\right]\Omega\right) + \bar{\gamma}_{tr}}\right.$$
$$\left. + \frac{\exp\left\{-\left(iP_\omega^{(1)} - P_\gamma^{(1)}\right)\sin\left(\Omega\tau\right) + i(n+m)\Omega\tau\right\}}{i\left(\bar{\omega}_{tr} - \omega + \left[(n+m)-2(l+k)\right]\Omega\right) + \bar{\gamma}_{tr}}\right], \qquad \text{(V.11)}$$

where $J_k(x)$ and $I_k(x)$ are the Bessel function of the first kind and the modified Bessel function of order *k*, respectively, and $P_\omega^{(1)} \equiv \frac{\Delta_\omega^{(1)}}{\Omega}$, $P_\gamma^{(1)} \equiv \frac{\Delta_\gamma^{(1)}}{\Omega}$, $P_\omega^{(2)} \equiv \frac{\Delta_\omega^{(2)}}{2\Omega}$, $P_\gamma^{(2)} \equiv \frac{\Delta_\gamma^{(2)}}{2\Omega}$ are the modulation indices.

The Fourier decomposition of the resonantly scattered radiation (V.11) has a form

$$\tilde{E}_{Scatt}(L,\tau) = -E_0 L \frac{2\pi N d_{tr}^2 \omega_0}{\hbar c} \times$$
$$\sum_{\substack{n,l,m,k,\\ g,s,p,f=-\infty}}^{\infty} (i)^{m+k+s+f} J_n\left(P_\omega^{(1)}\right) J_l\left(P_\omega^{(2)}\right) J_p\left(P_\omega^{(2)}\right) \times$$
$$I_m\left(P_\gamma^{(1)}\right) I_s\left(P_\gamma^{(1)}\right) I_k\left(P_\gamma^{(2)}\right) I_f\left(P_\gamma^{(2)}\right) \times \qquad \text{(V.12)}$$
$$\left[\frac{J_{(n+m)+2(l+k)-2(p+f)-(g+s)}\left(P_\omega^{(1)}\right)}{i\left(\bar{\omega}_{tr} - \omega - \left[(n+m)+2(l+k)\right]\Omega\right) + \bar{\gamma}_{tr}} + \right.$$
$$\left. \frac{J_{(n+m)-2(l+k)+2(p+f)+(g-s)}\left(P_\omega^{(1)}\right)}{i\left(\bar{\omega}_{tr} - \omega + \left[(n+m)-2(l+k)\right]\Omega\right) + \bar{\gamma}_{tr}}\right] \times \exp\left\{-ig\Omega\tau\right\}.$$

As mentioned above, along with the generalized solution (V.7), (V.11), (V.12), the results of TDSE calculations are compared to the simplified analytics derived previously

[38] within the approximations $P_{\omega}^{(2)} = P_{\gamma}^{(1)} = P_{\gamma}^{(2)} = 0$, $\bar{\gamma}_{tr} << \Omega$, and $\omega_0 = \bar{\omega}_{tr} + m_* \Omega$, where $m_* = 0, \pm 1, \pm 2, \ldots$:

$$\tilde{E}_{Scatt}(L,\tau) = -E_0 L J_{m_*}(P_{\omega}^{(1)}) \frac{4\pi N d_{tr}^2 \omega_0}{\hbar c \bar{\gamma}_{tr}} \exp\{i m_* \Omega t\} \times$$

$$\begin{cases} \sum_{n=-\infty}^{+\infty} J_{2n}(P_{\omega}^{(1)}) \exp\{-i 2n\Omega t\}, & m_* = 2k, \\ \sum_{n=-\infty}^{+\infty} J_{2n+1}(P_{\omega}^{(1)}) \exp\{-i(2n+1)\Omega t\}, & m_* = 2k+1. \end{cases} \qquad \text{(V.13)}$$

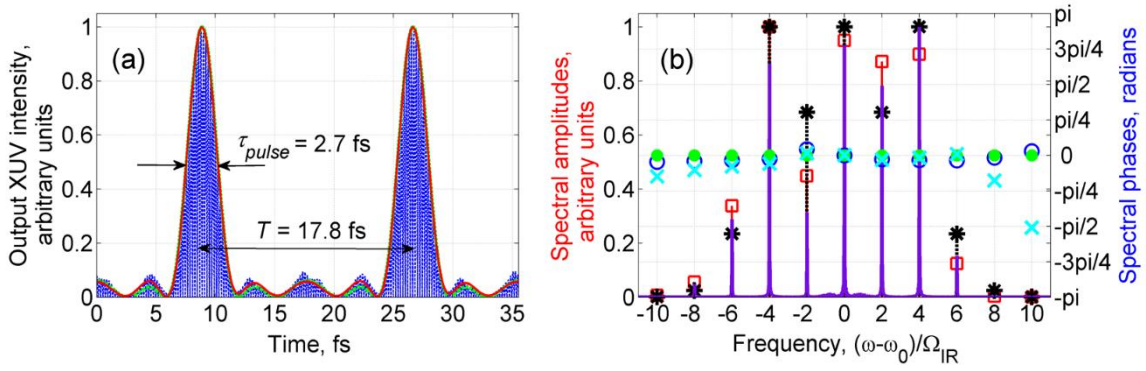

Figure 18**.** (a) Time dependence of intensity $I \sim \left|\tilde{E}_{XUV}\right|^2$ of XUV radiation at the exit of an optically thin medium of atomic hydrogen simultaneously irradiated by the CO_2-laser field with intensity $I_{IR} = 1.4\times10^{12}$ W/cm^2 and wavelength $\lambda_{IR} = 10.65$ μm and the XUV radiation with intensity $I_{XUV} = 2.2\times10^{8}$ W/cm^2 and wavelength $\lambda_{XUV} = 122.2$ nm. The dimensionless parameters in analytical solution are $P_{\omega}^{(1)} = 4.45$, $P_{\omega}^{(2)} = 0.23$, $P_{\gamma}^{(1)} = 0.05$, $P_{\gamma}^{(2)} = 0.015$, and $\bar{\gamma}_{tr} = 0.04\Omega$. The bold red curve and the dashed green curve correspond to the analytical solutions (V.11) and (V.13), respectively. The rapidly oscillating blue curve shows the numerical solution of the TDSE for the squared value of the XUV field strength, $\left|E_{XUV}\right|^2$. (b) Fourier transform of the output XUV radiation corresponding to the time dependence in (a). The results provided by the generalized analytical solution (V.12) for the amplitudes and phases of the spectral components are shown by red squares and blue circles, while the predictions of the simplified analytical theory (V.13) for the spectral amplitudes and phases are plotted by black asterisks and filled green circles. The dashed lavender curve and cyan crosses show *ab initio* solution of the TDSE for the amplitudes and phases of spectral components at the combinational frequencies, $\omega = \omega_0 + n\Omega$, $n = 0, \pm1, \pm2, \ldots$, respectively. The resonant spectral component, $\omega = \omega_0$, of the output XUV radiation is attenuated to the level of the generated sidebands.

Due to its simplicity, the analytical solution (V.13) allows to determine the optimal conditions for ultrashort pulse formation via the linear Stark effect in atomic hydrogen. As shown in [38], the output XUV radiation represents a train of bandwidth-limited pulses if (i) the incident radiation is tuned to the time-averaged position of the atomic resonance, $\omega_0 = \bar{\omega}_{tr}$, (ii) the modulation index $P_{\omega}^{(1)}$ satisfies the inequality $\nu_0^{(1)} < P_{\omega}^{(1)} < \nu_2^{(1)}$, where $\nu_0^{(1)} \cong 2.40$ is the first root of equation $J_0(\nu) = 0$ and $\nu_2^{(1)} \cong 5.14$ is the first root of

equation $J_2(\nu)=0$, and (iii) the resonant component of the output XUV radiation is attenuated to the level of the generated sidebands. In Figure 18, Figure 19, Figure 20 and Figure 21 we compare the results of both the generalized, (V.11), (V.12), and the simplified, (V.13), analytical solutions to the *ab initio* solutions of the TDSE under these optimal conditions for different combinations of intensity, I_{IR}, and wavelength, λ_{IR}, of the IR field (V.2).

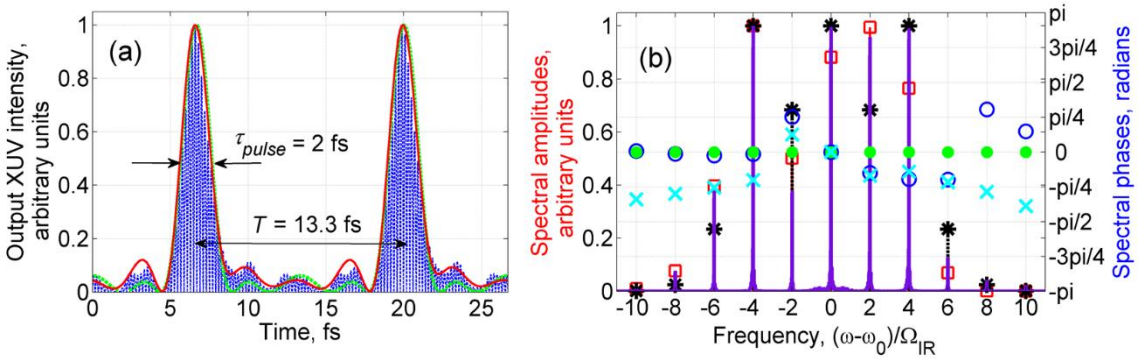

Figure 19. (a) Same as Figure 18 (a), but for IR field with intensity $I_{IR} = 2.5\times10^{12}$ W/cm^2 and wavelength $\lambda_{IR} = 8$ μm, and XUV radiation with intensity $I_{XUV} = 1.6\times10^{9}$ W/cm^2 and wavelength $\lambda_{XUV} = 122.6$ nm. The dimensionless parameters in analytical solutions are $P_{\omega}^{(1)}=4.45$, $P_{\omega}^{(2)}=0.32$, $P_{\gamma}^{(1)}=0.21$, $P_{\gamma}^{(2)}=0.074$, and $\overline{\gamma}_{tr}=0.19\Omega$. (b) Fourier transform of the output XUV radiation corresponding to the time dependence in (a). Designations are the same as in Figure 18 (b).

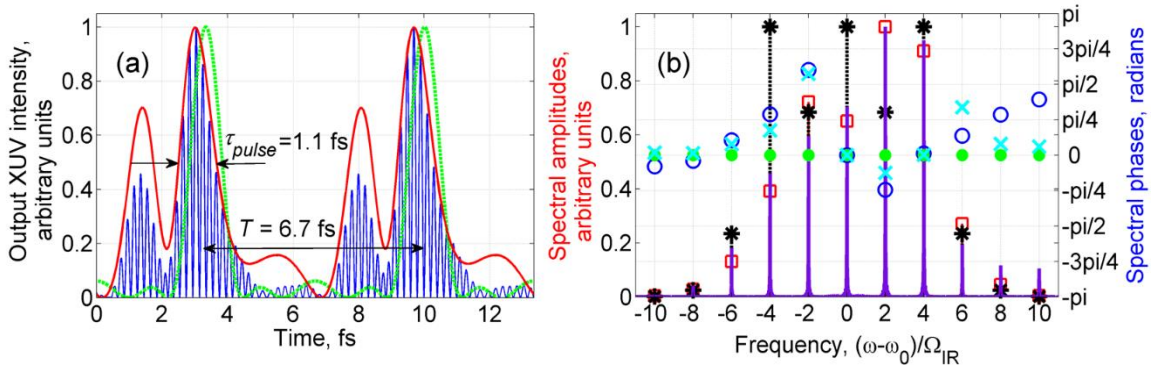

Figure 20. (a) Same as Figure 18 (a), but for IR field with intensity $I_{IR} = 10^{13}$ W/cm^2 and wavelength $\lambda_{IR} = 4$ μm, and XUV radiation with intensity $I_{XUV} = 10^9$ W/cm^2 and wavelength $\lambda_{XUV} = 124.6$ nm. The dimensionless parameters in analytical solutions are $P_{\omega}^{(1)} = 4.45$, $P_{\omega}^{(2)} = 0.23$, $P_{\gamma}^{(1)} = 0.8$, $P_{\gamma}^{(2)} = 0.6$, and $\overline{\gamma}_{tr} = 1.3\Omega$. (b) Fourier transform of the output XUV radiation corresponding to the time dependence in (a). Designations are the same as in Figure 18 (b).

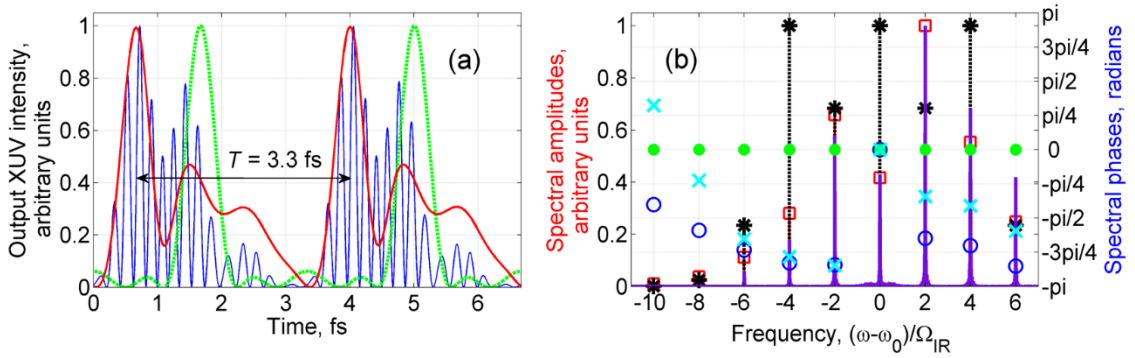

Figure 21. (a) Same as Figure 18 (a), but for IR field with intensity $I_{IR} = 4\times10^{13}$ W/cm^2 and wavelength $\lambda_{IR} = 2$ μm, and XUV radiation with intensity $I_{XUV} = 4\times10^9$ W/cm^2 and wavelength $\lambda_{XUV} = 133.4$ nm. The dimensionless parameters in analytical solutions are $P_{\omega}^{(1)} = 4.45$, $P_{\omega}^{(2)} = 0.5$, $P_{\gamma}^{(1)} = 1.9$, $P_{\gamma}^{(2)} = 1.8$, and $\overline{\gamma}_{tr} = 3.8\Omega$. (b) Fourier transform of the output XUV radiation corresponding to the time dependence in (a). Designations are the same as in Figure 18 (b).

The analytically calculated envelope (V.7), (V.11) of the output XUV radiation is slightly shifted along the time axis in order to provide the best fit to the numerical results. This shift originates from inertia of electronic response to the IR field. The timing of pulses predicted by the analytical solution is fully determined by time dependencies of

frequencies and decoherence rates of the resonant transitions $|1\rangle \leftrightarrow |2\rangle$ and $|1\rangle \leftrightarrow |3\rangle$. Equations (V.10 a) and (V.10 b) assume that both the frequencies and the decoherence rates reach their maximum values at maxima of absolute value of the IR field strength. This is correct for the linear Stark shifts but not exactly correct for the decoherence rates. The resonant interaction between the atoms and the XUV field decreases with decrease of an overlap between the wavefunctions of the atomic ground state and of the ionized electron. Therefore, the peak of decoherence rate is slightly delayed with respect to the peak of the excited-state ionization rate (and the peak of IR field strength) by a time interval needed for the electron to move away from the nucleus by a distance equal to the average radius of its wavefunction (which can be estimated on the basis of initial wavefunction of the resonant excited state). In such a case, if there were no Stark effect, the results of *ab initio* solution for the time dependence of the output XUV intensity would be delayed with respect to the analytical solution by this time interval, which is not taken into account by Eq. (V.10 b) but naturally arises in numerical TDSE solution. However, as far as the IR field intensity is below the threshold of rapid excited-state ionization, the pulse shape is predominantly determined by the linear Stark effect, which is instantaneous. For this reason, in the case of low-intensity IR fields, the temporal shift, τ_0, between the analytical and numerical solutions for the output XUV intensity which maximizes their overlap, is very small ($\sim 10^{-3}$ of the IR field cycle). With increasing intensity and frequency of the IR field, the value of τ_0 increases to $\sim 10^{-2}$ of the IR field cycle. In the TDSE calculations, we assume the IR field in the form $E_{IR}(\tau) = E_C(\tau)\sin(\Omega\tau)$, with the slowly-varying amplitude $E_C(\tau) = \sin^2(\Omega\tau/40)$ for $0 \le \tau \le 20\pi/\Omega$ and $E_C(\tau) = 1$ for

$20\pi/\Omega < \tau \le 230\pi/\Omega$. The XUV radiation has the form $E_{XUV}(\tau) = E_{XUV}(\tau)\sin\left(\omega_0(\tau-\tau_0)\right)$, where $\tau_0 = 30\pi/\Omega$ and $E_{XUV}(\tau) \equiv 0$ for $0 \le \tau \le 30\pi/\Omega$, $E_{XUV}(\tau) = \sin^2\left(\Omega\left(\tau-\tau_0\right)/20\right)$ for $30\pi/\Omega < \tau \le 40\pi/\Omega$, $E_{XUV}(\tau) = 1$ for $40\pi/\Omega < \tau \le 220\pi/\Omega$, and $E_{XUV}(\tau) = \cos^2\left(\Omega\left(\tau-220\pi/\Omega\right)/20\right)$ for $220\pi/\Omega < \tau \le 230\pi/\Omega$. For each combination of intensity and wavelength of the IR field, the wavelength of XUV radiation, λ_{XUV}, is adjusted to the Stark-shifted position of the atomic resonance.

In Figure 18, we present the results for atomic hydrogen irradiated by the CO_2-laser field with intensity $I_{IR} = 1.4\times10^{12}$ W/cm^2 and wavelength $\lambda_{IR} = 10.65$ μm, corresponding to the modulation index value $P_{\omega}^{(1)} = 4.45$. These are exactly the same parameters as in the original paper [38]. The medium is simultaneously irradiated by the XUV radiation with wavelength $\lambda_{XUV} = 122.2$ nm and intensity $I_{XUV} = 2.2\times10^8$ W/cm^2, resonantly exciting the atomic transition n=1↔n=2. As seen from this figure (whose panels (a) and (b) are remarkably similar to Figure 3 and Figure 4 of [38]), the *ab initio* TDSE solution fully confirms the possibility of pulse train formation. The pulses produced in this case are bandwidth-limited and have the duration τ_{pulse}=2.7 fs and repetition period T=17.8 fs. The analytical solutions (V.11), (V.12), and (V.13) are in excellent agreement with each other and with the *ab initio* TDSE solution both in time and frequency domain representations, see panels (a) and (b) of Figure 18, respectively. This is what we should actually expect, since for such parameters of the IR field the applicability conditions of

Eq. (V.13) are well satisfied: (i) the spectral lines of the resonant transitions are narrow with respect to the laser frequency due to the very low excited-state ionization rates, (ii) the sub-laser-cycle oscillations of the quadratic Stark shift and the ionization rates are not important, since their amplitudes are small compared to both the laser frequency and the amplitude of linear Stark splitting, and (iii) for the considered values of frequency and intensity of the IR field, the nonadiabatic effects are negligible.

The duration of the bandwidth-limited pulses is inversely proportional to their bandwidth. Therefore, according to (V.13), for a fixed value of modulation index $P_{\omega}^{(1)}$ the pulse duration (as well as the repetition period) is inversely proportional to the frequency of the IR field and proportional to its wavelength, $\tau_{\text{pulse}} \sim \Omega^{-1} \sim \lambda_{IR}$. Let us further examine the possibilities to shorten the pulses via the reduction of the wavelength of the IR field. In the following, we consider the cases of λ_{IR} = 8 μm, 4 μm, and 2 μm. In order to keep the modulation index constant, $P_{\omega}^{(1)} = 4.45$, the intensity of the IR field is chosen to increase inversely proportional to the square of its wavelength, $I_{IR} \sim \lambda_{IR}^{-2}$. Figure 19 and Figure 20 correspond to the IR field with wavelength λ_{IR} = 8 μm and 4 μm and intensity $I_{IR} = 2.5\times10^{12}$ W/cm^2 and 10^{13} W/cm^2, respectively. Due to increasing time-averaged quadratic Stark shift of the excited energy levels $|2\rangle$ and $|3\rangle$, the wavelength of the resonant XUV radiation grows with increasing intensity of the IR field. For instance, we have λ_{XUV} = 122.6 nm for 8 μm IR field and λ_{XUV} = 124.6 nm for 4 μm IR field. The intensity of XUV radiation is $I_{XUV} = 1.6\times10^{9}$ W/cm^2 and 10^{9} W/cm^2, respectively (it should be much lower than the intensity of the modulating field and much higher than the intensity of its high-order harmonics). In both cases, a train of pulses is produced at the exit of the

medium. It is worth noting that we regard the parameter values as suitable for the pulse formation if the peak intensity of spikes in between the pulses does not exceed half peak intensity of the pulses. Certainly, the "suitability" criterion can be defined in different ways depending on the application of the pulses which one keeps in mind. In the case of 8 μm IR field, Figure 19, the duration of pulses equals τ_{pulse}=2 fs, the repetition period is T=13.3 fs, while for 4 μm IR field, Figure 20, the pulse duration and repetition period are τ_{pulse}=1.1 fs (which corresponds to 2.6 cycles of the carrier) and T=6.7 fs, respectively. Accordingly, the *ab initio* calculation results show the possibility of producing nearly 1 fs few-cycle pulses via the linear Stark effect in atomic hydrogen (reducing the ultimate pulse duration by a factor of more than two compared to the results of [38]) using IR fields with wavelength ≥ 4 μm. It is noteworthy that at the cost of reducing the ratio of pulse repetition period to the pulse duration, one is able to use a shorter wavelength IR field of intensity $I_{IR} \le 10^{13}$ W/cm^2, corresponding to $P_{\omega}^{(1)} > 2.4$, for the pulse formation. Experimentally, such an IR field can be produced by an OPCPA laser system [110], while the resonant XUV radiation can be generated via nonlinear up-conversion of a visible laser field [132,133]. Further reduction of the pulse duration can be achieved via the linear Stark effect in hydrogen-like ions [38,41]. As follows from similarity between the hydrogen-like ions, using the ions with nucleus charge $-eZ$, reducing the wavelengths of both the XUV radiation and the IR field by a factor of Z^2, and increasing the intensity of the IR field by a factor of Z^6 with respect to the case of atomic hydrogen will result in the formation of pulses with Z^2 times shorter duration and repetition period. In particular, in

the case of Li^{2+} ions, $Z = 3$, exposed to the XUV radiation with wavelength λ_{XUV} = 13.84 nm and the IR field with wavelength λ_{IR} = 440 nm and intensity $I_{IR} = 7.3\times10^{15}$ W/cm^2, a train of pulses will be produced with the same shape as in Figure 20(a) but with the pulse duration τ_{pulse}=120 as and repetition period T=730 as.

With decreasing wavelength and increasing intensity of the IR field, the results of *ab initio* calculations for atomic hydrogen increasingly deviate from the predictions of the simplified analytical theory (V.13), see Figure 18, Figure 19 and Figure 20. However, these deviations are basically reproduced by the generalized analytical solution (V.11). Thus, they can be attributed to (i) ionization broadening of the resonant transition lines, as well as (ii) sub-laser-cycle oscillations of both the quadratic Stark shift of the excited energy levels and ionization rates from them. The generalized analytics shows that in the cases of 8 μm and 4 μm IR fields, the distortions of the pulse shape predominantly originate from the time-independent part of the excited-state ionization rate, causing broadening of the resonant transition lines and violation of the inequality $\bar{\gamma}_{tr} << \Omega$. In the case of shorter wavelength, λ_{IR} = 2 μm, and, respectively, higher intensity, $I_{IR} = 4\times10^{13}$ W/cm^2, of the IR field, which is addressed in Figure 21 (the corresponding wavelength of the resonant XUV radiation is λ_{XUV} = 133.4 nm; the XUV intensity is chosen to be $I_{XUV} = 4\times10^{9}$ W/cm^2), sub-laser-cycle oscillations of ionization rate become quite important. As shown in [40], rapid quasi-static ionization, which depopulates the resonant excited state within each half-cycle of the IR field, itself leads to the transformation of XUV radiation into few-cycle pulses due to the periodic switching of its resonant interaction with atoms on and off twice within the IR field cycle. The intensity

of the IR field assumed in Figure 21 is not yet enough for such an ionization switching to occur. However, the peak excited-state ionization rate already exceeds the amplitude of the linear Stark effect, so that the simplified analytical solution (V.13) is not yet applicable, and the two mechanisms of pulse formation compete with each other, leading to beatings in the time dependence of the output XUV intensity, see Figure 21 (a). At the same time, the generalized analytical solution (V.11), (V.12) remains valid in this case, being in a qualitative agreement with the results of *ab initio* solution both in time domain, Figure 21 (a), and frequency domain, Figure 21 (b).

In summary, the *ab initio* calculations show that intensities of the IR field suitable for the ultrashort / few-cycle pulse formation via the linear Stark effect are limited by the values at which atomic ionization from the resonant excited state becomes significant. Further increase of intensity of the IR field leads to the dominating effect of the excited-state ionization on the resonant atomic response and provides the conditions for the few-cycle pulse formation due to the ionization-switching mechanism [40]. As was previously shown, the ionization switching can be implemented in arbitrary atomic gas. In the following section, we consider this regime of pulse formation in a helium, which is more convenient for an experimental implementation compared to the atomic hydrogen.

V.3 Attosecond pulse formation via excited-state ionization in helium

In the case of helium, we use the unperturbed atomic Hamiltonian from [94], which provides a relatively good description of the lowest excited states of He in the single-active-electron approximation.

The incident XUV radiation is tuned in resonance with the unperturbed atomic transition $1s^2 \leftrightarrow 1s2p$. As shown in [40], this choice of frequency of the XUV radiation is optimal for attosecond pulse formation via ionization switching of its resonant interaction with the atoms: the interaction is switched on in the vicinity of zero-crossings of the IR field strength, when the atomic transition is nearly unperturbed, and switched off at the rest of time, when the transition line is strongly broadened due to rapid excited-state ionization. Similarly to the case of hydrogen, in order to analyze the results of *ab initio* calculations, we derive the generalized analytical theory taking into account space-time dependencies of both the Stark effect and excited-state ionization. However, in the case of helium, it is considerably simpler: since the energy level 1s2p is nondegenerate, the resonant atomic response is correctly described within the two-level approximation, in which the lower and upper energy levels correspond to the states $|1\rangle=1s^2$ and $|2\rangle=1s2p$, respectively. In such a case, the slowly-varying amplitude of the atomic polarization is given by

$$\tilde{P}(\tau) = 2Nd_{tr}a_{21}(\tau) \tag{V.14}$$

and the amplitude of the atomic coherence satisfies the equation

$$\frac{da_{21}}{d\tau} + \left(i\left(\omega_{21}(\tau) - \omega_0\right) + \gamma_{21}(\tau)\right)a_{21} = i\frac{d_{tr}E_0}{2\hbar}. \tag{V.15}$$

Since both $|1\rangle$ and $|2\rangle$ states possess a central symmetry, the simplest approximation for the time dependencies of the instantaneous frequency, $\omega_{21}(\tau)$, and decoherence rate, $\gamma_{21}(\tau)$, of the resonant transition is harmonic:

$$\omega_{21}(\tau) = \bar{\omega}_{tr} + \Delta_{\omega}^{(2)} \cos(2\Omega\tau), \tag{V.16a}$$

$$\gamma_{21}(\tau) = \bar{\gamma}_{tr} + \Delta_{\gamma}^{(2)} \cos(2\Omega\tau), \tag{V.16b}$$

where $\bar{\omega}_{tr} = \omega_{21}^{0} + \Delta_{\omega}^{(2)}$ and $\bar{\gamma}_{tr} = \gamma_{21}^{0} + \Delta_{\gamma}^{(2)}$. Similarly to the case of atomic hydrogen, for each combination of intensity and wavelength of the IR field, the values γ_{21}^{0} and $\Delta_{\gamma}^{(2)}$ are found via fitting to the results of the auxiliary TDSE calculation for the time dependence of the probability for an atom, which was initially excited into the state $|2\rangle$ and exposed to the IR field, to remain nonionized. The fitting gives $\gamma_{21}^{0} = 0$ in all the cases. The amplitude of the quadratic Stark effect, $\Delta_{\omega}^{(2)}$, is chosen to provide the best agreement between the time dependencies of the output XUV intensity calculated analytically and numerically. The obtained values of $\Delta_{\omega}^{(2)}$ are comparable to the values of $\Delta_{\gamma}^{(2)}$ and are much smaller than the those predicted by the perturbation theory, similarly to what has been obtained in the previous studies of Stark effect in strong fields [134,135].

The steady-state solution of Eqs. (V.7), (V.14)-(V.16) has the form

$$\begin{aligned} \tilde{E}_{Scatt}(L,\tau) = -E_0 L \frac{2\pi N d_{tr}^2 \omega_0}{\hbar c} \times \exp\left\{-\left(iP_{\omega}^{(2)} + P_{\gamma}^{(2)}\right)\sin\left(2\Omega\tau\right)\right\} \times \\ \sum_{k,m=-\infty}^{\infty} (i)^m J_{k+m}\left(P_{\omega}^{(2)}\right) I_m\left(P_{\gamma}^{(2)}\right) \times \frac{\exp\{i2k\Omega\tau\}}{i\left(\bar{\omega}_{tr} - \omega + 2k\Omega\right) + \bar{\gamma}_{tr}}, \end{aligned} \tag{V.17}$$

where $P_{\omega}^{(2)} \equiv \Delta_{\omega}^{(2)}/2\Omega$ and $P_{\gamma}^{(2)} \equiv \Delta_{\gamma}^{(2)}/2\Omega$.

The Fourier decomposition of (V.17) is

$$\tilde{E}_{Scatt}(L,\tau) = -E_0 L \frac{2\pi N d_{tr}^2 \omega_0}{\hbar c} \times$$
$$\sum_{k,n,l,m=-\infty}^{\infty} (i)^{l+m} J_{n+m-l-k}\left(P_\omega^{(2)}\right) J_n\left(P_\omega^{(2)}\right) I_l\left(P_\gamma^{(2)}\right) I_m\left(P_\gamma^{(2)}\right) \times \qquad \text{(V.18)}$$
$$\frac{\exp\{i2k\Omega\tau\}}{i\left(\bar{\omega}_{tr} - \omega + 2(n-l)\Omega\right) + \bar{\gamma}_{tr}}.$$

Along with the generalized analytical solution (V.17), (V.18), the results of TDSE calculations for helium are compared to the previously derived solution [40], which neglects the Stark effect by assuming $\omega_{21}(\tau) = \bar{\omega}_{tr}$ and assumes a stepwise temporal change of the excited-state ionization rate:

$$\gamma_{21}(\tau) = \begin{cases} \bar{\gamma}_{\min}, & 0 \le \tau < \Delta t_{\text{zero}}, \\ \bar{\gamma}_{\max}, & \Delta t_{\text{zero}} \le \tau < \pi/\Omega, \end{cases} \quad \gamma_{21}(\tau + \pi/\Omega) = \gamma_{21}(\tau). \qquad \text{(V.19)}$$

The decoherence rate (V.19) possesses a half-IR-field-cycle periodicity, taking the minimum value, $\bar{\gamma}_{\min}$, near a zero-crossing of the IR field at $\tau = \Delta t_{\text{zero}}/2$ (which corresponds to $\varphi_0 = \left[\pi - \Omega\Delta t_{\text{zero}}\right]/2$ in Eq. (V.2)) and the maximum value, $\bar{\gamma}_{\max}$, at the rest of time. In order to find the values $\bar{\gamma}_{\min}$, $\bar{\gamma}_{\max}$, and Δt_{zero} for each combination of intensity and wavelength of the IR field, we perform the following steps: first, we find the ratio $\bar{\gamma}_{\max}/\bar{\gamma}_{\min}$ using the nonadiabatic tunneling ionization rate [136] and calculate the time-averaged decoherence rate $\bar{\gamma}_{av} \equiv \frac{\Omega}{\pi}\left(\bar{\gamma}_{\min}\Delta t_{\text{zero}} + \bar{\gamma}_{\max}\left(\frac{\pi}{\Omega} - \Delta t_{\text{zero}}\right)\right)$. Then, we use the exponential function $\exp\left(-2\bar{\gamma}_{av}\tau\right)$ for fitting to the results of auxiliary TDSE calculation for the time dependence of the probability for an atom in the state $|2\rangle$ to remain nonionized under the action of the IR field. These steps allow us to represent $\bar{\gamma}_{\min}$ and $\bar{\gamma}_{\max}$ as

$\bar{\gamma}_{\min} = \bar{\gamma}_{\min}(\Delta t_{\text{zero}})$ and $\bar{\gamma}_{\max} = \bar{\gamma}_{\max}(\Delta t_{\text{zero}})$, respectively. Finally, we choose Δt_{zero} to provide best agreement between the analytical and numerical results for the time dependence of the output XUV intensity.

In such an approximation, the slowly-varying amplitude of the resonantly scattered XUV radiation takes the form

$$\tilde{E}_{Scatt}(\tau) = \begin{cases} \tilde{E}^{(1)}_{Scatt}(\tau), & 0 \le \tau < \Delta t_{\text{zero}}, \\ \tilde{E}^{(2)}_{Scatt}(\tau), & \Delta t_{\text{zero}} \le \tau < \pi/\Omega, \end{cases}, \qquad \tilde{E}_{Scatt}(\tau + \pi/\Omega) = \tilde{E}_{Scatt}(\tau) \tag{V.20}$$

where

$$\begin{cases} \tilde{E}^{(1)}_{Scatt}(\tau) = \tilde{C}_1 \exp\left\{\left(i\Delta\omega - \bar{\gamma}_{\min}\right)\tau\right\} + \tilde{D}_1, \\ \tilde{E}^{(2)}_{Scatt}(\tau) = \tilde{C}_2 \exp\left\{\left(i\Delta\omega - \bar{\gamma}_{\max}\right)\left(\tau - \Delta t_{\text{zero}}\right)\right\} + \tilde{D}_2. \end{cases} \tag{V.21}$$

The coefficients $\tilde{C}_1, \tilde{C}_2$, and $\tilde{D}_1, \tilde{D}_2$, in their turn, have the form

$$\begin{cases} \tilde{D}_1 = -E_0 L \dfrac{2\pi N d_{tr}^2 \omega}{\hbar c\left(\bar{\gamma}_{\min} - i\Delta\omega\right)}, \\ \tilde{D}_2 = -E_0 L \dfrac{2\pi N d_{tr}^2 \omega}{\hbar c\left(\bar{\gamma}_{\max} - i\Delta\omega\right)}, \end{cases} \tag{V.22}$$

$$\begin{cases} \tilde{C}_1 = \left(\tilde{D}_2 - \tilde{D}_1\right) \dfrac{\exp\left\{\left(i\Delta\omega - \bar{\gamma}_{\max}\right)\left(\pi/\Omega - \Delta t_{\text{zero}}\right)\right\} - 1}{\exp\left\{\left(i\Delta\omega - \bar{\gamma}_{\max}\right)\pi/\Omega\right\}\exp\left\{\left(\bar{\gamma}_{\max} - \bar{\gamma}_{\min}\right)\Delta t_{\text{zero}}\right\} - 1}, \\ \tilde{C}_2 = \left(\tilde{D}_1 - \tilde{D}_2\right) \dfrac{\exp\left\{\left(i\Delta\omega - \bar{\gamma}_{\min}\right)\Delta t_{\text{zero}}\right\} - 1}{\exp\left\{\left(i\Delta\omega - \bar{\gamma}_{\max}\right)\pi/\Omega\right\}\exp\left\{\left(\bar{\gamma}_{\max} - \bar{\gamma}_{\min}\right)\Delta t_{\text{zero}}\right\} - 1}. \end{cases} \tag{V.23}$$

An analytical expression for the Fourier transform of the solution (V.20)-(V.23) for the resonantly scattered radiation is given in [40].

In the regime of rapid excited-state ionization, which depopulates the resonant excited atomic state twice per IR-field cycle, the generated XUV sidebands are in antiphase with the incident XUV radiation and in phase with each other, which corresponds to confinement of the resonant absorption of the XUV radiation within extremely short time intervals near zero-crossings of the IR field [40]. In such a case, the resonantly scattered XUV radiation (V.17), or (V.20)-(V.23), itself represents a train of few-cycle pulses. Therefore, the generation of attosecond pulses at the output of the medium can be achieved via suppression of the central spectral component of XUV radiation (at the frequency of the incident field), for example, via its resonant absorption in an additional layer of helium, which is not modulated by the IR field.

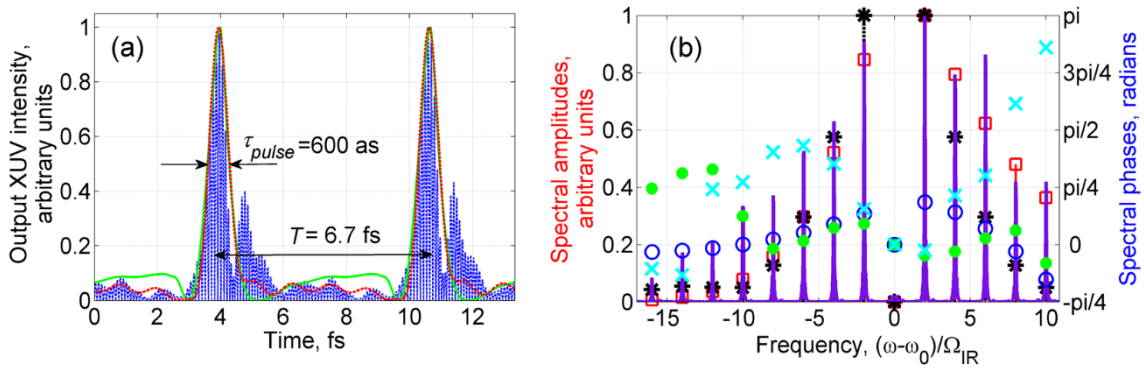

Figure 22. (a) Time dependence of intensity of XUV radiation at the exit of an optically thin medium of helium irradiated by the IR field with intensity $I_{IR} = 1.5\times10^{14}$ W/cm^2 and wavelength $\lambda_{IR} = 4$ μm, and the XUV radiation with intensity $I_{XUV} = 10^{11}$ W/cm^2 and wavelength $\lambda_{XUV} = 58.4$ nm. The incident spectral component of XUV radiation is suppressed. The dashed red curve and the solid green curve correspond to the harmonical and step-like analytical solutions (V.17) and (V.20)-(V.23), respectively. The dimensionless parameters in analytical calculations are $P_{\omega}^{(2)} = 15$, $P_{\gamma}^{(2)} = 11.5$, $\overline{\gamma}_{\min}/\Omega = 0.056$, $\overline{\gamma}_{\max}/\Omega = 2.7$, and $\Omega\Delta t_{\text{zero}} = 0.2\pi$. The rapidly oscillating blue curve is the numerical solution of the TDSE for the squared value of the XUV field strength, $|E_{XUV}|^2$. (b) Fourier transform of the output XUV radiation corresponding to the time dependence in (a). Red squares and blue circles are the amplitudes and phases of the spectral components calculated analytically via the harmonical analytical solution (V.18). The corresponding results of step-like analytical solution (V.20)-(V.23) are plotted by black asterisks and green filled circles. The dashed lavender curve and cyan crosses show the *ab initio* solution of the TDSE for the amplitudes and phases, respectively, of the spectral components at the combinational frequencies, $\omega = \omega_0 + n\Omega$, $n = 0, \pm1, \pm2, \ldots$ The upper frequency limit corresponds to the ionization potential of helium.

The results provided by both analytical solutions (V.17), (V.18) and (V.20)-(V.23) are compared in Figure 22, Figure 23, Figure 24, Figure 25 and Figure 26 to the *ab initio* TDSE calculations for the helium. Timing of the analytically calculated envelopes of the output XUV radiation is fitted to the numerical solutions within a few percent of the laser cycle. Similarly to the case of atomic hydrogen, this time shifting originates from inertia of atomic response to the IR field: the ionized electron continues participate in the intra-

atomic processes while its wavefunction overlaps with the atomic ground state. The TDSE calculations presented in this section imply the IR field in the form $E_{IR}(\tau) = E_C(\tau)\sin(\Omega\tau)$, with $E_C(\tau) = \sin^2(\Omega\tau/40)$ for $0 \le \tau \le 20\pi/\Omega$ and $E_C(\tau) = 1$ for $20\pi/\Omega < \tau \le 90\pi/\Omega$. The XUV radiation has the form $E_{XUV}(\tau) = E_{XUV}(\tau)\sin\left(\omega_0(\tau - \tau_0)\right)$, where $\tau_0 = 30\pi/\Omega$, $E_{XUV}(\tau) \equiv 0$ for $0 \le \tau \le 30\pi/\Omega$, $E_{XUV}(\tau) = \sin^2\left(\Omega(\tau - \tau_0)/20\right)$ for $30\pi/\Omega < \tau \le 40\pi/\Omega$, $E_{XUV}(\tau) = 1$ for $40\pi/\Omega < \tau \le 80\pi/\Omega$, and $E_{XUV}(\tau) = \cos^2\left(\Omega(\tau - 80\pi/\Omega)/20\right)$ for $80\pi/\Omega < \tau \le 90\pi/\Omega$. The wavelength and peak intensity of the incident XUV radiation are λ_{XUV} = 58.4 nm and $I_{XUV} = 10^{11}$ W/cm^2, respectively, for all the plots.

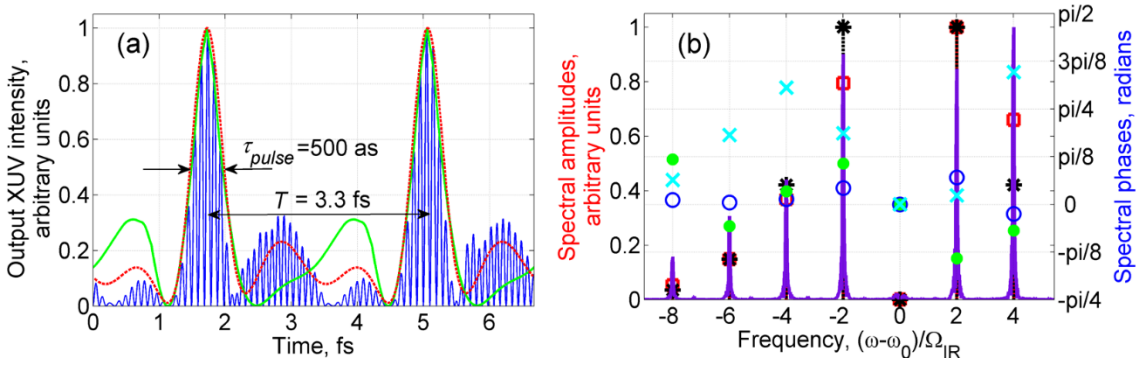

Figure 23. (a) Same as Figure 22 (a), but for IR field with wavelength λ_{IR} = 2 μm. The dimensionless parameters in analytical solutions are $P_\omega^{(2)} = 4.0$, $P_\gamma^{(2)} = 4.6$, $\bar{\gamma}_{\min}/\Omega = 0.14$, $\bar{\gamma}_{\max}/\Omega = 1.5$, and $\Omega\Delta t_{\text{zero}} = 0.25\pi$. (b) Fourier transform of the output XUV radiation corresponding to the time dependence in (a). Designations are the same as in Figure 22 (b).

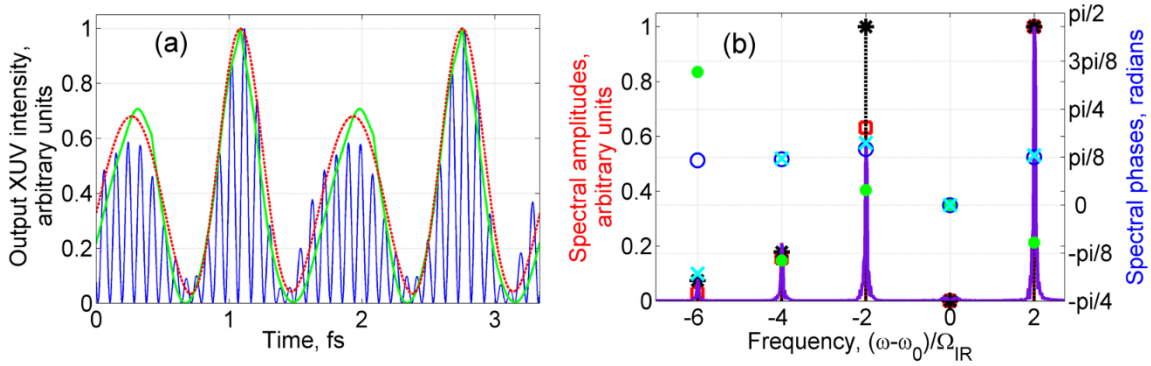

Figure 24. (a) Same as Figure 22 (a), but for IR field with wavelength λ_{IR} = 1 μm. The dimensionless parameters in analytical solutions are $P_{\omega}^{(2)} = 1.0$, $P_{\gamma}^{(2)} = 1.2$, $\bar{\gamma}_{\min}/\Omega = 0.22$, $\bar{\gamma}_{\max}/\Omega = 0.88$, and $\Omega\Delta t_{\text{zero}} = 0.4\pi$. (b) Fourier transform of the output XUV radiation corresponding to the time dependence in (a). Designations are the same as in Figure 22 (b).

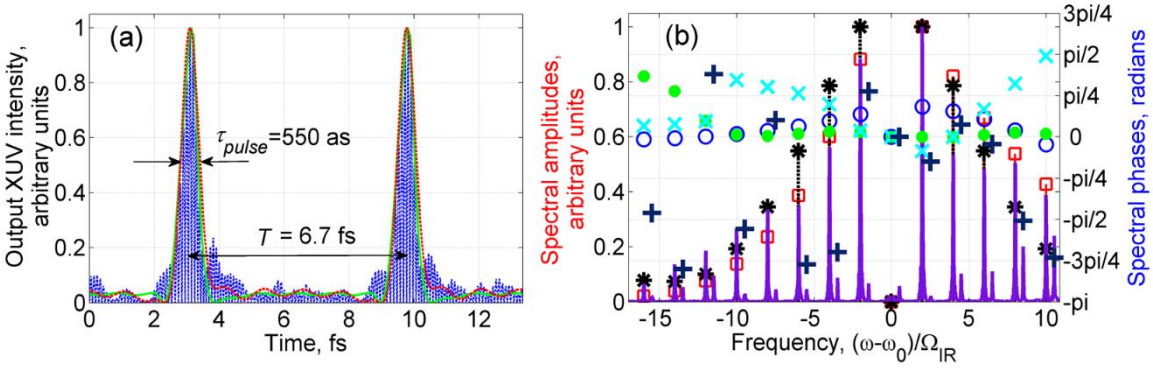

Figure 25. (a) Same as Figure 22 (a), but for IR field with intensity I_{IR} = 4×10^{14} W/cm^2. The dimensionless parameters in analytical solutions are $P_{\omega}^{(2)} = 25$, $P_{\gamma}^{(2)} = 20.7$, $\bar{\gamma}_{\min}/\Omega = 0.24$, $\bar{\gamma}_{\max}/\Omega = 6.2$, and $\Omega\Delta t_{\text{zero}} = 0.16\pi$. (b) Fourier transform of the output XUV radiation corresponding to the time dependence in (a). Designations are the same as in Figure 22 (b). (i) Cyan crosses and (ii) dark blue pluses show the results of TDSE solution for the phases of spectral components at (i) the combinational frequencies, $\omega = \omega_0 + n\Omega$, $n = 0, \pm 1, \pm 2, \ldots$, and (ii) the high-order harmonics of the IR field, $\omega = (2k+1)\Omega$, $k = 1, 2, \ldots$, respectively.

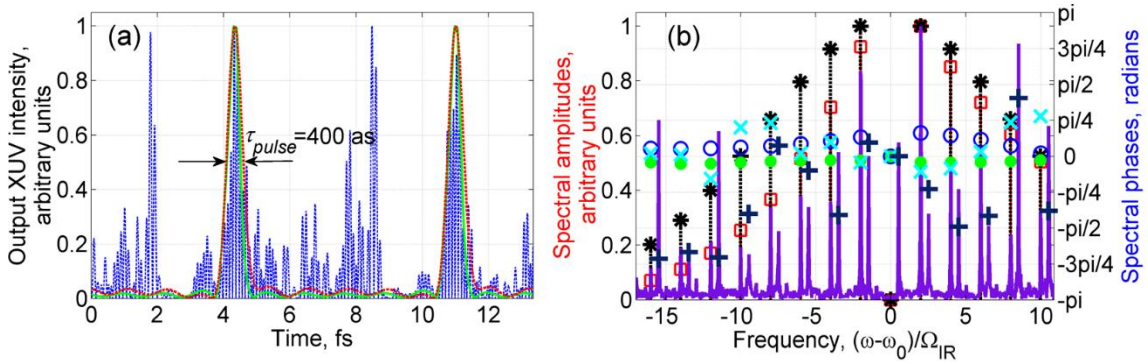

Figure 26. (a) Same as Figure 22 (a), but for IR field with intensity I_{IR} = 8×10^{14} W/cm^2. The dimensionless parameters in analytical solutions are $P_{\omega}^{(2)} = 50$, $P_{\gamma}^{(2)} = 51$, $\bar{\gamma}_{\min} = 0.66\Omega$, $\bar{\gamma}_{\max} = 11.2\Omega$, and $\Delta t_{\text{zero}} = 0.1\pi/\Omega$. (b) Fourier transform of the output XUV radiation corresponding to the time dependence in (a). Designations are the same as in Figure 25 (b).

Figure 22 represents the case of helium atoms simultaneously irradiated by the resonant XUV radiation and the IR field with wavelength λ_{IR} = 4 μm and intensity I_{IR} = 1.5×10^{14} W/cm^2. After suppression of the incident spectral component, the output XUV radiation corresponds to a train of pulses with duration τ_{pulse}=600 as and repetition period T=6.7 fs, see Figure 22 (a). Both analytical solutions (V.17) and (V.20)-(V.23) correctly describe the shape of the *main* pulse. However, the generalized analytics (V.17) better reproduces the pedestal. This is predominantly due to the fact that, for the assumed strength of the IR field, ionization from the resonant excited state is due to suppression of the atomic potential barrier rather than tunneling through it. In such a case, the harmonic approximation (V.16b) for the time dependence of the ionization rate is more suitable than the step-function model (V.19), which better works in the tunneling regime [137]. It is worth noting that accounting for the quadratic Stark effect in the analytical solution (V.17), (V.18) for the resonantly scattered XUV radiation in the presence of a rapidly ionizing IR field, as applied in the present Section, is not as critical as accounting for time-

dependent excited-state ionization in Section V.2. In the former case, there is only a slight improvement of the agreement with the TDSE calculations. Meanwhile, according to the *ab initio* calculations, the intensity of the IR field required for the pulse formation due to ionization switching of the resonant interaction is one order of magnitude higher than that estimated from the tunneling formula [40]. This follows from the fact that the tunneling models overestimate the ionization rate in the barrier-suppression regime [137,138]. As seen in Figure 22 (b), which plots the Fourier transform of the output XUV radiation, for the chosen parameters of the IR field, the generalized analytical solution (V.18) provides a good agreement with the numerical results both in time and frequency domain representations.

Let us further examine the possibilities to reduce the pulse duration via reducing the wavelength of the IR field (leading to shrinking of the overall time scale) or via increasing the intensity of the IR field (leading to the speed-up of the excited-state ionization). Figure 23 and Figure 24 represent the case of the helium atoms irradiated by the IR field with the same intensity as in Figure 22, $I_{IR} = 1.5\times10^{14}$ W/cm^2, but with shorter wavelengths. The atoms are simultaneously exposed to the resonant XUV radiation. Figure 23 corresponds to the IR field with wavelength $\lambda_{IR} = 2$ μm. In this case, the output XUV radiation has a form of a pulse train with pulse duration τ_{pulse}=500 as and repetition period T=3.3 fs. As seen from the comparison of Figure 23 and Figure 22, the twofold reduction of the wavelength of the IR field expectedly leads to a proportional reduction of the pulse repetition period. However, the duration of pulses is only slightly reduced. This is due to the fact that the pulse duration is determined by the ionization-limited lifetime of

the resonant excited state |2⟩, which approximately equals Δt_{zero} and is nearly the same for 2 μm and 4 μm IR fields of the same intensity. In Figure 24 we show the time dependence of the intensity and the spectrum of the output XUV radiation for the case of helium irradiated by the resonant XUV field and the IR field with wavelength λ_{IR} = 1 μm. The resonant component of the output XUV radiation is suppressed. For such a short wavelength of the IR field, the pulse formation does not occur, since the intensity of the IR field is not high enough to provide complete atomic ionization from the resonant excited state during half-cycle of the IR field (which is four times shorter compared to the half-cycle of the 4 μm IR field assumed in Figure 22). Correspondingly, ionization never switches off the resonant interaction between the XUV field and the atoms, and the necessary condition for pulse formation [40] is not met. As follows from Figure 23 and Figure 24, for all the considered wavelengths of the IR field, the analytical solutions (V.17), (V.18) and (V.20)-(V.23) are in a rather good agreement with the results of TDSE calculations. This is due to a quasistatic nature of excited-state ionization in the barrier-suppression regime [137]. However, the generalized solution (V.17), (V.18) better reproduces the results of *ab initio* calculations due to a proper description of time dependence of the excited-state ionization rate in the barrier-suppression regime and accounting for the sub-laser-cycle quadratic Stark effect.

Figure 25 and Figure 26 show the results of the study aimed to examine the possibilities to reduce the pulse duration via increasing the intensity of the IR field. The wavelength of the IR field is fixed to λ_{IR} = 4 μm. Figure 25 corresponds to the laser intensity $I_{IR} = 4\times10^{14}$ W/cm^2. As seen from the comparison of this figure with Figure 22,

the increase of the IR field intensity leads to a slight reduction of the pulse duration, from τ_{pulse}=600 as to τ_{pulse}=550 as, and suppression of the pulse pedestal. The reason of such a slow decrease of the pulse duration with increasing laser field intensity is that the duration of pulses is predominantly determined by the length of the time interval near zero-crossing of the IR field during which the ionization rate is negligible and the resonant interaction occurs rather than by the peak ionization rate. With increasing intensity of the IR field, this time interval is shortened quite slowly, therefore, the dependence of the pulse duration on the laser intensity is weak. In Figure 26 we show the time dependence of intensity and the spectrum of the output XUV radiation after suppression of its resonant component for the case of the IR field with wavelength λ_{IR} = 4 μm and intensity $I_{IR} = 8\times10^{14}$ W/cm^2. As follows from Figure 26 (a), the duration of pulses produced from the resonant radiation is reduced to τ_{pulse}=400 as. However, along with the pulses of resonantly scattered radiation, the other spikes appear due to HHG of the modulating IR field. Indeed, for the parameters of the XUV and IR fields related to this case, there are two distinct groups of spectral components of comparable amplitudes, see Figure 26 (b). The first group corresponds to the combinational frequencies of the XUV and IR fields, $\omega = \omega_0 + 2n\Omega$, $n = \pm1, \pm2, \ldots$, while the second group is the high-order harmonics of the IR field, $\omega = (2k+1)\Omega$, $k = \pm1, \pm2, \ldots$ Unless the depletion of the ground state is considerable, the HHG yield is proportional to the ground-state ionization rate and, thus, grows exponentially with increasing IR field strength. Even a small increase in laser intensity beyond the above-mentioned value will lead to domination of the high-harmonic signal over the resonantly scattered radiation. Thus, for the intensities of the incident XUV radiation discussed here,

the ultimate intensity of the IR field suitable for few-cycle pulse formation from XUV radiation via ionization switching of its resonant interaction with atoms is limited to the value at which ionization from the ground atomic state, leading to HHG of the IR field, becomes significant. At the same time, as follows from the results of calculations based on few-level and quasistatic approximations, the ionization-switching mechanism works even if the intensity of the incident XUV radiation reaches quarter intensity of the modulating IR field [39]. In such a case, HHG via atomic ionization from the ground state does not hamper sub-fs pulse formation from XUV radiation due to the ionization switching mechanism. Instead, ultimate capabilities for the pulse formation are limited by depletion of the atomic ground state through (i) direct ionization by the IR field and (ii) resonant excitation by the XUV radiation followed by excited-state ionization by the IR field.

In summary, based on the *ab initio* solution of the TDSE, we have shown the possibility to produce trains of ~500 as pulses from the XUV radiation with wavelength 58.4 nm via ionization switching of its resonant interaction with the helium atoms dressed by the IR field with wavelength 2-4 μm and intensity $1.5\text{-}4\times10^{14}$ W/cm^2. Experimentally, the IR field with these parameters can be generated by a parametric laser system [110], while the resonant XUV radiation can be produced, for example, via the resonantly enhanced HHG of Ti:Sa laser field in InP plasma plume [97,127]. As discussed in [37,40], few-cycle pulse formation via the ionization-switching mechanism can be implemented in arbitrary atomic gas. In particular, TDSE calculations show the possibility to produce pulses similar to those plotted in Figure 22, Figure 23, Figure 24, Figure 25 and Figure 26

from XUV radiation with wavelength 121.6 nm in atomic hydrogen dressed by the IR field with wavelength 4 μm and intensity of the order of 10^{14} W/cm^2. The pulses of shorter duration can be produced using ions with higher ionization potential from the ground state. It is worth noting that few-cycle pulses similar to those discussed above can be produced via ionization-switching mechanism in media with lower ionization potential also. In such a case, the carrier frequency of the pulses can be considerably lower, which would make them especially valuable for non-ionizing steering and probing transient physical, chemical, and biological intra-atomic and intra-molecular processes in various media.

V.4 Conclusion

In the present chapter, we have studied ultimate capabilities for few-cycle pulse formation from XUV radiation via the resonant interaction with IR-field-dressed atoms. This study was carried out on the basis of full time-dependent Schrödinger equation. Taking into account all the multiphoton processes in the considered systems in the single-active-electron approximation, we have confirmed the possibilities for few-femtosecond pulse formation via the linear Stark effect in atomic hydrogen, as well as attosecond pulse formation via quasistatic excited-state ionization in helium. We have found the ultimate limitations on the parameters (the minimum wavelength and the maximum intensity) of the IR field suitable for the few-cycle pulse formation, as well as characteristics of the produced pulses. Particularly, in the case of XUV pulse formation via the linear Stark effect in atomic hydrogen, the output pulses can be as short as 1 fs, which is two times shorter than predicted by the previous calculations based on the three-level approximation [38]; the laser intensity can be up to 10^{13} W/cm^2, while the laser wavelength can be as

short as 4 μm. The ionization switching of the resonant interaction in helium requires the laser intensity up to 4×10^{14} W/cm^2, whereas the laser wavelength can be as short as 2 μm; the duration of output pulses is ~ 500 as.

In order to analyze the results of *ab initio* calculations, we derived the generalized analytical solution, which takes into account the interplay between sub-IR-field-cycle variations of position and width of the resonant atomic energy levels due to the Stark effect and excited-state ionization, respectively. The derived analytical solution is in a good agreement with the results of TDSE calculations both in the case of atomic hydrogen in a relatively weak IR field and in the case of helium in a strong IR field. Thus, such a solution can be used for the analysis of the various resonant phenomena in a system of IR-field-dressed atoms. Based on a comparison of the numerical and analytical solutions, we revealed the limitations of the considered method for few-cycle pulse formation. In particular, the possibility of shortening the pulses produced via the linear Stark effect in atomic hydrogen by increasing the intensity of the IR field is limited by the growing role of exited-state ionization, which leads to a misalignment of phases of the generated sidebands. The ultimate intensity of the IR field suitable for attosecond pulse formation via rapid quasistatic ionization from the resonant excited state of helium is limited to a value at which atomic ionization from the ground state becomes significant, entailing HHG and blurring the produced pulses by the high-harmonic signal. To overcome both these limitations and produce shorter pulses, we proposed the use of the medium of hydrogen-like or helium-like ions with higher ionization potentials from both the ground and the excited states. We also pointed out the possibility to produce few-cycle pulses with

lower carrier frequency, in a close proximity to resonances of various atomic and molecular systems, using media with lower ionization potential. The chapter contains accurate estimation of wavelengths and intensities of XUV and IR fields suitable for experimental implementation of the method. The proposed method provides a unique tool for nonionizing steering of electronic processes inside atoms, molecules, and solids at the few-femtosecond and attosecond timescales, thus extending the capabilities of attosecond science. Furthermore, the method is very promising for transformation of the picosecond pulses produced by the x-ray plasma lasers into sub-femtosecond pulses, which could widely extend the applications of such lasers for element selective imaging of the fast dynamical processes in biochemistry and material sciences.

CHAPTER VI

COHERENT FORWARD SCATTERING OF GAMMA-RAY AND XUV RADIATION IN THE MEDIUM WITH THE MODULATED QUASI-RESONANT TRANSITION[6]

VI.1 Introduction

Propagation of a weak electromagnetic field in a quasi-resonant two-level medium experiencing piston-like vibrations has been widely studied both theoretically and experimentally in connection with the problem of coherent forward scattering of γ-radiation in a vibrating nuclear quasi-resonant absorber (see [139-143] and references therein). Many interesting effects have been experimentally demonstrated, including an observation of vibrational Stokes and anti-Stokes sidebands in the transmitted radiation [139,141], demonstration of strongly suppressed absorption of quasi-monochromatic incoming γ-radiation [141], demonstration of ultra-short pulses formation and of coherent control of the single γ-photon waveforms [142,143]. The possibility of acoustically induced transparency, namely, absorptionless propagation of two- or multi-component radiation with a specific ratio of their complex amplitudes, determined by the amplitude and phase of vibration, has been theoretically predicted [144]. The theoretical studies of the above effects were based on analytical and numerical solutions of the Maxwell-Bloch equations for the quasi-monochromatic γ-radiation propagating in a quasi-resonant two-

[6] Reprinted with permission from "Coherent forward scattering of gamma-ray and XUV radiation in the medium with the modulated quasi-resonant transition" by T.R. Akhmedzhanov, V.A. Antonov and O. Kocharovskaya, 2016, J. Phys. B: At. Mol. Opt. Phys., vol. 49**,** pp. 205602, Copyright [2016] by IOP Publishing.

level medium experiencing coherent harmonic vibrations under the condition that the absorber's thickness was much smaller than the acoustic wavelength.

In this chapter we establish a direct physical and mathematical analogy between these effects occurring in coherent forward scattering of γ-radiation in a vibrating nuclear absorber and similar effects taking place within the propagation of a weak XUV field through a quasi-resonant absorbing atomic medium in the presence of a moderately strong IR field. The experimentally demonstrated effects include modulation of both ionization yield [22,34,35] and absorption of the individual spectral components of XUV field as a function of the IR field delay [24,26,36], as well as suppression or enhancement of some spectral components of the incoming radiation [27,33]. The IR field in these experiments was not strong enough to ionize atoms from the ground state. However, it significantly perturbed atoms in the excited state allowing to control XUV absorption spectrum [26,145-148], and ionization yield from the resonantly populated excited state [35,36,149]. The XUV field was produced from the same IR field via high harmonic generation (HHG) in a different gas jet and typically contained several high order odd harmonics of the IR field below ionization potential, one of which was close to the resonance between the ground and some excited atomic states. The theoretically predicted (but not yet demonstrated) effects include generation of IR Stokes and anti-Stokes sidebands in the transmitted radiation and formation of extremely short pulses, as well as XUV transparency, namely, absorptionless propagation of two-component XUV field (with a specific ratio of component amplitudes determined by the amplitude of the IR field) through the quasi-resonant absorbing medium [22]. The theoretical studies were

mainly based on numerical simulations of the time-dependent Schrodinger equation (TDSE). The Floquet approach [88] provided an important insight into experimentally observed modulation effects [24,35,123] interpreting them as a result of interference of the resonant excitation paths, originating from the interaction of different spectral components of XUV radiation with the corresponding Fourier components of the same Floquet state.

In this chapter we show that both processes, under certain conditions, are described by the same set of Maxwell-Bloch equations for a two-level medium with modulated parameters of the resonant transition and find a rather general analytical solution of these equations, describing transformation of the electromagnetic field in such a modulated medium. It leads to a conclusion that the effects predicted and/or demonstrated in one of these physical systems can also be realized in another one. In particular, we show that acoustically induced transparency for γ-rays [144] and IR induced transparency for XUV field are two different manifestations of the same general phenomenon of modulation induced transparency (MIT), i.e. transparency caused by modulating the parameters of the resonant transition.

The outline of the chapter is as follows. In Sec. VI.2 we derive an analytical solution for a high-frequency (HF) quasi-resonant field propagating through an ensemble of two-level atoms, whose transition frequency and/or decoherence rate are periodically modulated in space and time. Modulation of the parameters of the resonant transition leads to the inelastic Raman type (Stokes and anti-Stokes) scattering of an incident field. In the case of two- or multi-component incident radiation an elastically scattered resonant

component of an incident field and the resonant contributions of the inelastically scattered components of an incident field interfere either constructively or destructively depending on the difference between a relative phase of the spectral components and the modulation phase. In general, it leads to enhancement/suppression of some incident spectral components and appearance of new spectral components at the exit of the medium, as well as variation of the total output intensity as a function of the modulation phase. With a proper phase relation and optimal ratio between the amplitudes of the incident spectral components (dependent on the modulation amplitude) a complete destructive interference is reached resulting in the modulation induced transparency (MIT), i.e., elimination of the medium's effect on propagation of quasi-resonant radiation. We show that under the phase matching condition the problem of interaction of the incident HF radiation with the modulated resonant transition can be reduced to the problem of interaction of some effective field with the non-modulated transition. In these terms, MIT appears when the resonant component of the (multi-frequency) incident effective field equals zero.

In Sec. VI.3 we consider the problem of coherent forward γ-ray scattering by the vibrating nuclear absorber and show that it is described by the same set of equations with modulation of the transition frequency, caused by the Doppler effect. The change of variables in this case corresponds to the change of reference frame from the laboratory one to the co-moving with the nuclei. We show how the full MIT could be achieved both in the case of quasi-monochromatic and bichromatic incident γ-ray radiation and discuss the experimental demonstration of partial MIT in the first case [141].

In Secs. VI.4 and VI.5 we consider atoms with a manifold of N and, as an example, of two non-degenerate excited energy levels, one of which is simultaneously coupled to the ground state by quasi-resonant XUV field and to the other excited states by the IR field. Using the Floquet approach we find that, under certain conditions, this rather complicated problem can also be reduced to the same problem of quasi-resonant XUV field interaction with the effective two-level atoms with modulated parameters of the resonant transition. In Section VI.6, we show that a very simple two-level model with modulated parameters of the resonant transition provides a rather good description of the results of the recent experiment [22], which was analyzed previously by a numerical simulation of TDSE. We also show that lowering the frequency of the IR field is favorable for MIT, and suggest possible experiments for demonstration of nearly perfect transparency. Finally, the comparison of MIT for the XUV field with other types of field induced transparency (transparency caused by Autler-Townes splitting and electromagnetically induced transparency (EIT)) is given and foreseen applications are discussed.

VI.2 Transformation of electromagnetic field during its propagation through two-level medium with modulated parameters of the resonant transition

Let us consider a linearly polarized quasi-monochromatic high-frequency (HF) radiation, propagating along *x*-axis in the quasi-resonant two-level medium,

$$\vec{E}(x,t) = \vec{z}_0 \frac{1}{2} \tilde{E}(x,t) \exp\left\{-\mathrm{i}\omega\left(t - x/c\right)\right\} + \text{c.c.}, \qquad \text{(VI.1)}$$

where $\vec{z}_0$ is the unit vector directed along the polarization of the field, $\tilde{E}(x,t)$ is a slowly varying complex amplitude of the field, $\left|\partial\tilde{E}/\partial t\right| \ll \omega\left|\tilde{E}\right|$, $\left|\partial\tilde{E}/\partial x\right| \ll \omega/c\left|\tilde{E}\right|$, ω is its carrier frequency, c is the speed of light in vacuum, and c.c. stands for complex conjugation). Let the transition frequency ω_{21} and the coherence decay rate γ_{21} depend on space coordinate, x, and time, t, as in the running waves (see Figure 27):

$$\begin{cases} \omega_{21}(x,t) = \bar{\omega}_{21} + \Delta\omega_{21}(t - x/V_M), \\ \gamma_{21}(x,t) = \bar{\gamma}_{21} + \Delta\gamma_{21}(t - x/V_M). \end{cases} \tag{VI.2}$$

The wave of modulation propagates along x-axis; V_M is the phase velocity of modulation; $\bar{\omega}_{21}, \bar{\gamma}_{21}$, and $\Delta\omega_{21}$, $\Delta\gamma_{21}$ are the constant and alternating components of the transition frequency and decoherence rate, respectively, $\int_{-\infty}^{+\infty} \Delta\omega_{21}(\tau')d\tau' = \int_{-\infty}^{+\infty} \Delta\gamma_{21}(\tau')d\tau' = 0$, $\frac{\partial\bar{\omega}_{21}}{\partial\tau} = \frac{\partial\bar{\gamma}_{21}}{\partial\tau} = 0$. A variable $\tau = t - x/V_M$ is the local time in the reference frame, co-moving along with the wave of modulation.

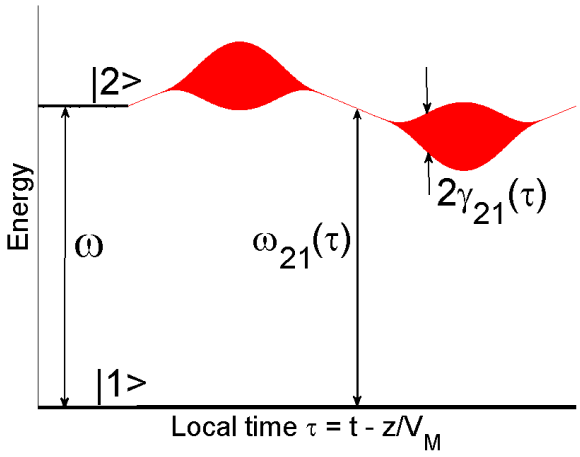

Figure 27. The bold black horizontal line, as well as the oscillating red line of variable thickness schematically show the instantaneous position and width of the energy levels, corresponding accordingly to the ground state, $|1\rangle$, and the excited state, $|2\rangle$, of an atom. The excited atomic state is selected and populated by the XUV radiation with frequency ω. Both the instantaneous energy and linewidth of the level $|2\rangle$ are periodically modulated in time and space according to Eq. (VI.2).

An excitation of two-level atoms by the XUV field is described by the density-matrix equation:

$$\frac{\partial \tilde{\rho}_{21}}{\partial t} + \left(\mathrm{i}(\omega_{21}(\tau) - \omega) + \gamma_{21}(\tau)\right)\tilde{\rho}_{21} = \frac{\mathrm{i}}{2\hbar} n_{12} d_{21} \tilde{E} \,. \qquad \text{(VI.3)}$$

It implies the rotating-wave approximation (RWA), assuming that the radiation field in Eq. (VI.1) is quasi-resonant to the atomic transition, $|\omega - \omega_{21}| \ll \omega$; $\tilde{\rho}_{21}$ is the slowly-varying amplitude of the atomic coherence $\rho_{21}(x,t) = \tilde{\rho}_{21}(x,t)\exp\{-\mathrm{i}\omega(t - x/c)\}$, $|\partial\tilde{\rho}_{21}/\partial t|$ $\ll \omega|\tilde{\rho}_{21}|, |\partial\tilde{\rho}_{21}/\partial x| \ll \omega/c|\tilde{\rho}_{21}|$; d_{21} is the electric dipole moment of the resonant transition, $\hbar$ is the Planck's constant, and $n_{12} \equiv \rho_{11} - \rho_{22}$ is the population difference between the lower, $|1\rangle$, and the upper, $|2\rangle$, atomic states. We consider a relatively weak XUV radiation (VI.1), which does not appreciably change populations of the atomic states during

interaction time, so that $n_{12} \approx n_{12}^0$, where n_{12}^0 is the unperturbed value of the population difference. Atomic transitions induced by the XUV field (VI.1) result in appearance of the resonant polarization of the medium $\vec{P}(x,t) = \vec{z}_0 \frac{1}{2} \tilde{P}(x,t) \exp\{-\mathrm{i}\omega(t - x/c)\} + \text{c.c.}$, $\left|\partial \tilde{P}/\partial t\right| \ll \omega\left|\tilde{P}\right|$, $\left|\partial \tilde{P}/\partial x\right| \ll \omega/c\left|\tilde{P}\right|$ with the slowly-varying amplitude

$$\tilde{P} = 2Nd_{12}\tilde{\rho}_{21}, \tag{VI.4}$$

where N is the concentration of atoms and $d_{12} = d_{21}^*$.The induced polarization, in its turn, leads to modification of the XUV field, which satisfies wave equation for the slowly-varying amplitude:

$$\frac{\partial \tilde{E}}{\partial x} + \frac{1}{c}\frac{\partial \tilde{E}}{\partial t} = \mathrm{i}\frac{2\pi\omega}{c}\tilde{P}. \tag{VI.5}$$

The Eqs. (VI.2)-(VI.5) along with the boundary condition for the quasi-resonant field (VI.1) make up a self-consistent system describing evolution of the field as well as the atomic coherence in the medium. In order to distinguish the effect of the modulation (VI.2) on the atomic coherence and the quasi-resonant field, let us introduce the following variable:

$$\tilde{\zeta}_{21}(x,t) = \tilde{\rho}_{21}(x,t)\exp\{\mathrm{i}\Phi(\tau) + \Psi(\tau)\}, \tag{VI.6}$$

where

$$\Phi(\tau) \equiv \int_{-\infty}^{\tau} \Delta\omega_{21}(\tau')d\tau' \text{ and } \Psi(\tau) \equiv \int_{-\infty}^{\tau} \Delta\gamma_{21}(\tau')d\tau'. \tag{VI.7}$$

Plugging Eqs. (VI.6), (VI.7) into Eqs. (VI.3), (VI.5) and using the substitution

$$\tilde{E}_{eff}(x,t) \equiv \tilde{E}(x,t)\exp\{\mathrm{i}\Phi(\tau)+\Psi(\tau)\} \tag{VI.8}$$

results in the following system of equations:

$$\begin{cases} \dfrac{\partial \tilde{E}_{eff}}{\partial x}+\dfrac{1}{c}\dfrac{\partial \tilde{E}_{eff}}{\partial t}+\left(1/V_M-1/c\right)\left(\mathrm{i}\Delta\omega_{21}(\tau)+\Delta\gamma_{21}(\tau)\right)\tilde{E}_{eff}=\mathrm{i}\dfrac{4\pi N d_{12}\omega}{c}\tilde{\zeta}_{21}, \\ \dfrac{\partial \tilde{\zeta}_{21}}{\partial t}+\left(\mathrm{i}\left(\bar{\omega}_{21}-\omega\right)+\bar{\gamma}_{21}\right)\tilde{\zeta}_{21}=\dfrac{\mathrm{i}}{2\hbar}n_{12}d_{21}\tilde{E}_{eff}. \end{cases} \tag{VI.9}$$

Let us further assume that

$$L\left(1/V_M-1/c\right)\times\max\left\{\left|\Delta\omega_{21}(\tau)\right|;\left|\Delta\gamma_{21}(\tau)\right|\right\}\ll 1, \tag{VI.10}$$

where L is the length of the medium. The last inequality implies that the phase difference between the XUV field and the wave of modulation, acquired within the medium as a result of difference between the phase velocities c and V_{M}, is negligible. In particular, this condition can be fulfilled if the modulation is produced by an electromagnetic wave, which phase velocity is close to the speed of light in vacuum, $V_M \approx c$, or, in case $V_M \ll c$, if the length of the medium is small enough to satisfy the inequality $\max\left\{\left|\Delta\omega_{21}(\tau)\right|;\left|\Delta\gamma_{21}(\tau)\right|\right\}\times L/V_M \ll 1$. If the condition (VI.10) is fulfilled, Eqs. (VI.9) take the form

$$\begin{cases} \dfrac{\partial \tilde{E}_{eff}}{\partial x}+\dfrac{1}{c}\dfrac{\partial \tilde{E}_{eff}}{\partial t}=\mathrm{i}\dfrac{4\pi N d_{12}\omega}{c}\tilde{\zeta}_{21}, \\ \dfrac{\partial \tilde{\zeta}_{21}}{\partial t}+\left(\mathrm{i}\left(\bar{\omega}_{21}-\omega\right)+\bar{\gamma}_{21}\right)\tilde{\zeta}_{21}=\dfrac{\mathrm{i}}{2\hbar}n_{12}d_{21}\tilde{E}_{eff}. \end{cases} \tag{VI.11}$$

As seen from comparison of Eqs. (VI.11) with Eqs. (VI.3)-(VI.5), the value $\tilde{E}_{eff}$ has a meaning of slowly-varying amplitude of an *effective* quasi-resonant field, while the value $\tilde{\zeta}_{21}$ has a meaning of slowly-varying amplitude of an *effective* coherence of the

unmodulated atoms. Thus, the original problem of propagation of the quasi-resonant radiation (VI.1) through the medium with space-time-dependent parameters (VI.2) is reduced to the problem of propagation of an effective field (VI.8) through the medium with constant parameters, which has the well-known solution [150]. Using this solution along with the substitution (VI.8) we obtain the analytical expressions for the electric field inside the medium both in terms of Fourier transform:

$$\begin{aligned}\tilde{E}(x,t) &= \frac{1}{2\pi}\exp\{-\mathrm{i}\Phi(\tau)-\Psi(\tau)\}\times \\ &\int_{-\infty}^{\infty}\left[\int_{-\infty}^{\infty}\tilde{E}(x=0,t')\exp\{\mathrm{i}\Phi(t')+\Psi(t')\}\exp\{\mathrm{i}\omega' t'\}\,dt'\right]\times \\ &\exp\left\{-\frac{2\pi N n_{12}|d_{12}|^2\omega x}{\hbar c\left[\mathrm{i}\left(\bar{\omega}_{21}-\omega-\omega'\right)+\bar{\gamma}_{21}\right]}\right\}\exp\{-\mathrm{i}\omega'\tau\}\,d\omega'\end{aligned} \qquad \text{(VI.12)}$$

and convolution of an incident field with the Green function:

$$\begin{aligned}\tilde{E}(x,t) &= \frac{1}{2\pi}\exp\{-\mathrm{i}\Phi(\tau)-\Psi(\tau)\}\times \\ &\int_{-\infty}^{\infty}\tilde{E}(x=0,t-t')\exp\{\mathrm{i}\Phi(t-t')+\Psi(t-t')\}R(x,t'-x/c)dt'\end{aligned}. \qquad \text{(VI.13)}$$

Here $R(x,t)$ is the Green function of absorber of thickness z [151]:

$$R(x,t)=\delta(t)-e^{\left(\mathrm{i}(\omega-\bar{\omega}_{21})-\bar{\gamma}_{21}\right)t}\Theta(t)\sqrt{\frac{b}{t}}J_1\left(2\sqrt{bt}\right), \qquad \text{(VI.14)}$$

where $\Theta(t)$ is Heaviside step function, $J_1(x)$ is Bessel function of the first kind of the first order and $b=\dfrac{2\pi\omega N n_{12}|d_{21}|^2}{\hbar c}x$.

This is worth to note that the expressions (VI.12)-(VI.14) describe a transformation of an arbitrary incident field in the quasi-resonant two-level medium with an arbitrary modulation of transition frequency and decay rate.

Let us further assume that the modulation (VI.2) is periodic with the period $T = 2\pi/\Omega$. In such a case, the function $\exp\{(\mathrm{i}\Phi(\tau) + \Psi(\tau))\}$ can be expanded in the Fourier series:

$$\exp\{(\mathrm{i}\Phi(\tau) + \Psi(\tau))\} = \sum_n a_n \exp(in\Omega\tau), \tag{VI.15}$$

where n is an integer, $-\infty < n < \infty$, and the amplitude of the effective field takes a form

$$\tilde{E}_{eff}(x,t) = \tilde{E}(x,t) \sum_{n=-\infty}^{+\infty} a_n \exp(\mathrm{i}n\Omega\tau). \tag{VI.16}$$

In this case the field inside the medium, according to Eqs. (VI.12) and (VI.13), is a periodic function of τ. In the case of the multifrequency incident field (VI.1) in a form of a spectral comb

$$\tilde{E}(x=0,t) = \sum_m \tilde{E}_m \exp\{-\mathrm{i}m\Omega t\} \tag{VI.17}$$

with one of the components resonant to the atomic transition (without loss of generality one can choose $\omega = \bar{\omega}_{21}$), and with a separation between the components, equal to the frequency of modulation, Ω, the incident effective field takes the form

$$\tilde{E}_{eff}(x=0,t) = \left(\sum_n \tilde{E}_n \exp(-\mathrm{i}n\Omega t)\right) \times \left(\sum_m a_m \exp(\mathrm{i}m\Omega t)\right). \tag{VI.18}$$

In such a case, the effective field contains both resonant, $E_{eff,res}$, and nonresonant, $E_{eff,non-res}$, components with the slowly-varying amplitudes

$$\tilde{E}_{eff,res}(x=0,t)=\sum_n \tilde{E}_n a_n,$$
$$\tilde{E}_{eff,non-res}(x=0,t)=\sum_n \tilde{E}_n\left[\left(\sum_m a_m \exp(\mathrm{i}(m-n)\Omega t)\right)-a_n\right]. \qquad \text{(VI.19)}$$

If the time-averaged decoherence rate of the atomic transition is small as compared to the frequency of modulation, $\overline{\gamma}_{21} \ll \Omega$, and the optical thickness of the medium is not too large (so that the off-resonant dispersion is negligible, namely $\frac{2\pi N n_{12}|d_{12}|^2 \omega L}{\hbar c \Omega} \ll 1$), the nonresonant part of the effective field propagates through the medium without modification, while the resonant part, $E_{eff,res}(x,t)$, is attenuated according to Beer's law: $\tilde{E}_{eff,res}(x,t)=\left(\sum_n \tilde{E}_n a_n\right)e^{-\alpha_B x/2}$, where $\alpha_B=\frac{4\pi\omega N n_{12}|d_{12}|^2}{\overline{\gamma}_{21}\hbar c}$ is the decrement of resonant absorption. As a result, the effective field in the medium equals to

$$\tilde{E}_{eff}(x,t)=\sum_n \tilde{E}_n\left(\sum_m a_m \exp\{\mathrm{i}(m-n)\Omega\tau\}\right)+\left(\sum_n \tilde{E}_n a_n\right)(e^{-\alpha_B x/2}-1). \qquad \text{(VI.20)}$$

As it follows from Eq. (VI.20), in an optically dense medium ($\alpha_B L/2 \gg 1$) for an arbitrary multicomponent field (VI.17), an output effective field tends to form the "transparent" mode, which is equal to the incident effective field minus its resonant component: $\tilde{E}_{eff} \to \sum_n \tilde{E}_n\left(\sum_m a_m \exp\{\mathrm{i}(m-n)\Omega\tau\}\right)-\left(\sum_n \tilde{E}_n a_n\right)$. Going back from the effective field given by Eq. (VI.20) to the actual XUV field, one obtains

$$\tilde{E}(x,t)=\sum_n \tilde{E}_n \exp\{-\mathrm{i}n\Omega\tau\}+\left(\sum_n \tilde{E}_n a_n\right)(e^{-\alpha_B x/2}-1)\exp\{-\mathrm{i}\Phi(\tau)-\Psi(\tau)\}. \qquad \text{(VI.21)}$$

As it is seen from Eq. (VI.21), when the following condition is fulfilled:

$$\sum_n \tilde{E}_n a_n = 0, \qquad \text{(VI.22)}$$

the field at the exit of the medium remains the same as an incident field, i.e. the quasi-resonant XUV radiation is not modified during its propagation through the medium at all. This phenomenon can be called Modulation Induced Transparency (MIT), since the transparency is induced by the modulation of parameters of the resonant transition. As it follows from Eq. (VI.19), the MIT condition in Eq. (VI.22) corresponds to zero amplitude of the resonant component of the effective field. It has a simple physical meaning. An effective field propagating in the effective "unmodulated" two-level medium does not interact with such medium when its net component, resonant to the atomic transition, is zero.

In the optically thin medium the output field is a superposition of an incident field and coherently forward scattered field, proportional to the resonant polarization:

$$\tilde{P} = \mathrm{i}\frac{N|d_{12}|^2 n_{12}}{\hbar\gamma}\left(\sum_{m=-\infty}^{+\infty}\tilde{E}_m a_m\right)\exp\{-\mathrm{i}\Phi(\tau)-\Psi(\tau)\}. \qquad \text{(VI.23)}$$

Different spectral components of an incident field contribute to an excitation of the resonant polarization due inelastic (Stokes and anti-Stokes) Raman scattering processes caused by modulation of the parameters of the resonant transition. The MIT condition (VI.22) corresponds to a destructive interference of these contributions, i.e. to zero net resonant polarization, leading to vanishing net coherently scattered field.

If only the transition frequency is modulated ($\Psi(\tau)=0$), the intensity of the n^{th} harmonic in the output field in Eq. (VI.21) is equal to:

$$\tilde{I}_n(x) = \frac{c}{8\pi}\begin{pmatrix} \left|\tilde{E}_n\right|^2 + \left|\sum_m \tilde{E}_m a_m\right|^2 |a_n|^2 \left(\exp(-\alpha x/2)-1\right)^2 + \\ 2\,\mathrm{Re}\left(a_n \tilde{E}_n \sum_m \tilde{E}_m{}^* a_m{}^* \left(\exp(-\alpha x/2)-1\right)\right) \end{pmatrix}, \qquad \text{(VI.24)}$$

while sum of intensities of all the spectral components of the output field (24) is

$$\tilde{I}(x) = \sum_n \tilde{I}_n(x) = \frac{c}{8\pi}\left(\sum_n \left|\tilde{E}_n\right|^2 - \left|\sum_m \tilde{E}_m a_m\right|^2 \left(1-\exp(-\alpha x)\right)\right). \qquad \text{(VI.25)}$$

According to Eq. (VI.24) an intensity of field components during the propagation would be decreasing or increasing depending on the phase relations between the elastically and inelastically scattered spectral components. As it can be seen from Eq. (VI.25), the total intensity of the field averaged over the period of modulation is decreasing as it propagates through the medium. For an infinitely long medium, the constant component of the output intensity would be $\sum_n |E_n|^2 - \left|\sum_m E_m a_m\right|^2$.

In the case of a monochromatic incident field, $\tilde{E}(x=0,t) = \tilde{E}_m$, detuned from the time-averaged position of the perturbed atomic resonance by the multiple frequency of modulation, $\omega = \bar{\omega}_{21} + m\Omega$, $m = 0, \pm 1, \pm 2, \ldots$, the MIT condition takes form $a_m = 0$ and is fully determined by the modulation parameters. It is worth to note that if a_m is not equal to zero, the incident field with frequency $\omega = \bar{\omega}_{21} + m\Omega$ experiences resonant absorption and resonant scattering (even when m is not zero) leading to generation of combinational spectral components at the frequencies $\omega = \bar{\omega}_{21} + n\Omega$, $n = 0, \pm 1, \pm 2, \ldots$ which, under the appropriate conditions, may form trains of ultrashort pulses.

In the case of two- (or multi-) component incident field, according to Eq. (VI.18), each spectral component of the field leads to the specific *effective* multicomponent incident field (Figure 28). As a result, the origin of MIT is remarkably different, as compared to the case of the monochromatic incident radiation (VI.1). The MIT results from a destructive interference between contributions from the different spectral components of the incident HF radiation to the resonant component of the total effective field. Namely, MIT is a result of a destructive interference of the resonant components of the effective fields produced by each from the spectral components of the incident radiation, as it is illustrated by Figure 28. It critically depends on the phase relations between the spectral components of the incident field and the modulation phase. This is worth to point out that each spectral component of the multicomponent incident field (VI.17), in general case, will be partially absorbed and partially transformed into sidebands if it is send through the medium alone. However, two (or more) components together with specific ratio of the amplitudes and specific phases, satisfying MIT condition (VI.22), propagate through the modulated medium without any modification.

In appendix A, we discuss the particular case of harmonically modulated transition frequency and modulation.

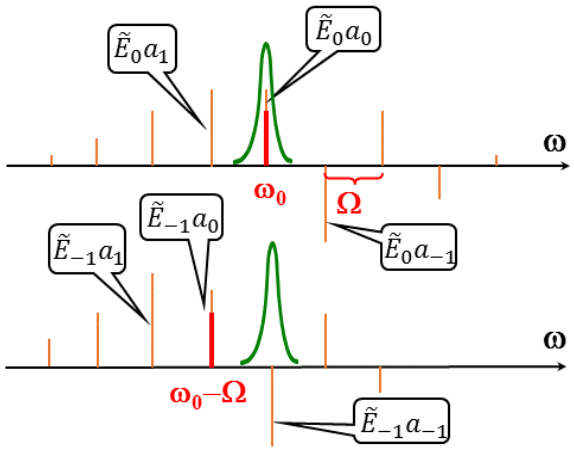

Figure 28. The amplitude spectra of constituents of the effective field (VI.18), corresponding to the different spectral components of the bichromatic incident quasi-resonant radiation (VI.1). The upper panel shows the spectrum of the effective field, corresponding to the resonant spectral component of the incident radiation. The lower panel shows the spectrum of the effective field, corresponding to the spectral component of the incident radiation, detuned from the resonance by the frequency of modulation, Ω. The bold green curve schematically shows the resonant absorption profile. The vertical lines correspond to the amplitudes of spectral components of the effective field, indicated in the inserts. The total amplitude spectrum of the effective field is given by the sum of the spectral combs, shown in upper and lower panels. The MIT condition (VI.22) corresponds to zero amplitude of the resonant component of the total effective field.

VI.3 Coherent forward scattering of gamma-ray radiation in the vibrating nuclear absorber

In particular, the set of Eqs. (VI.3)-(VI.5) and its solution (VI.12) describe the process of coherent forward scattering of γ-ray radiation in the vibrating nuclear absorber. In this case only frequency modulation is present. It is caused by Doppler frequency shift, $\omega_{21} = \omega_{21}^{\,0} + \frac{2\pi R}{\lambda}\Omega\cos(\Omega t)$, induced by an acoustic vibration: $z = R\sin(\Omega t)$, of a solid nuclear absorber along the direction of propagation of γ-radiation [142]. The typical case of harmonic vibrations was studied both experimentally and theoretically. Ultrasonic vibrations (at 10 MHz-10 GHz frequencies) allow one to achieve deep modulation of

frequencies of the Mössbauer γ-ray (10keV-100keV) nuclear transitions (as compared to the extremely narrow, 1 kHz-1 MHz, linewidths of these transitions, see [142] and references therein). Besides, due to the favorable combination of high nuclear density and narrow linewidths of the Mössbauer transitions, the condition (VI.10) can be easily satisfied for an optically dense medium.

The effective field (VI.8) has an obvious physical meaning. Namely, it corresponds to the γ-radiation "seen" by the nuclei in the reference frame, co-moving along with the vibrating absorber [144]. In this reference frame the transition frequency is independent of time and the resonant polarization can be excited only by the resonant component of the electromagnetic field. Thus, the MIT condition (VI.22), which requires the resonant component of the effective field to be zero, corresponds to elimination of the resonant interaction between an incident field and the nuclei in the absorber's reference frame. Since frequency modulation is caused by vibration, MIT in this case can be equivalently termed as acoustically induced transparency [144].

In the case of harmonic pure frequency modulation and quasi-monochromatic incident field in the form: $E(t,z)=\Theta(t)E_0\exp(-\gamma t-\mathrm{i}\omega(t-z/c))$ (inherent to the radioactive sources used in these experiments) detuned from the time-averaged position of the perturbed atomic resonance by the multiple frequency of modulation, $\omega=\bar{\omega}_{21}+m\Omega$, $m=0,\pm1,\pm2,\ldots$ and under condition of equal linewidths of the source and absorber (typical for Mossbauer experiments) the solution (VI.12) takes a form, coinciding with the previously obtained in [143]:

$$
\begin{aligned}
&I_{out}(\tau) = I_0\theta(\tau)e^{-\Gamma_s\tau}\left[1+2S_m(\tau)\cos\{\psi_m(\tau)\}+S_m^2(\tau)\right],\\
&S_m(\tau) = J_m(P_\omega)\left[J_0(2\sqrt{b\tau})-1\right], \qquad .\\
&\psi_m(\tau) = m\left(\Omega\tau+\vartheta_0\right)-P_\omega\sin\left(\Omega\tau+\vartheta_0\right).
\end{aligned}
\qquad \text{(VI.26)}
$$

According to the above equation, the transparency condition implies: $J_n(P_\omega)=0$. For $n=0$ it occurs when $P_\omega = 2.40, 5.52, ...$

Such values of the modulation index correspond to the absence of the scattered field in the laboratory frame, or to zero amplitude of a resonant incident field as "seen" by nuclei. It is worth to emphasize that strong suppression of the resonant absorption of 14,4 keV γ-radiation due to vibration with a particular vibration amplitude of a stainless steel foil (completely opaque in the absence of the vibration) was demonstrated in [141]. It corresponded to experimental demonstration of the partial MIT for the quasi-monochromatic incident field. In particular, the output field contained not only the resonant component, but also two Stokes and two anti-Stokes sidebands, which would not be present under condition of full MIT. The full MIT was not achieved because of variation of the vibration amplitude along the surface of the film.

As it was already pointed out above, in the case of two-component γ-ray field and harmonic frequency modulation, MIT condition (A.6) corresponds to destructive interference between contributions of two spectral components of an incident field into the resonant component of the field "seen" by vibrated nuclei (or to zero resonant polarization in the laboratory frame). This case was studied earlier in [144]. Two-component incident field, required for the experimental demonstration of this effect, can be produced using an additional combination of vibrated absorber with relatively small

modulation index, for example, $P_\omega = 1.3$, producing just three component field, and a resonantly tuned absorber, eliminating one of those components.

It is hardly possible to provide a deep acoustic modulation of the atomic transitions in the visible or XUV spectral ranges, possessing several orders of magnitude smaller frequencies (corresponding to the proportionally reduced Doppler shifts) and several orders of magnitude larger linewidths. Besides, in the case of acoustic modulation of an atomic transition frequency, it is impossible to satisfy the condition (VI.10) for a typical optically dense medium.

At the same time, as it was noticed in [38,40-42,144], deep modulation of both the frequency and the decoherence rate of a HF atomic transition, complying with the phase-matching condition (VI.10), can be produced by a low frequency electromagnetic field, propagating through the medium simultaneously with the HF radiation. As it will be proven in the following sections, interaction of an XUV radiation, quasi-resonant to an atomic transition $|1\rangle \leftrightarrow |2\rangle$, with atoms in the presence of a moderately strong IR field under certain condition, indeed, can be reduced to an interaction of the XUV field with the dressed two-level system with the modulated parameters of the two-level transition.

VI.4 Multi-level atoms coupled to IR field: Floquet formalism and an effective two-level model with modulated parameters of the resonant transition

In the following, we analyze propagation of a linearly polarized XUV radiation, resonantly coupled to an atomic transition from the ground state $|1\rangle$ to one of N excited bound states, namely, the state $|\alpha_0\rangle$. We consider an atomic gas in the presence of a linearly polarized IR field, propagating in the same direction as the XUV radiation and

coupling the state $|\alpha_0\rangle$ with other excited states. The XUV field is considered to be sufficiently weak and far detuned from any atomic transition, except the resonant one, so that its interaction with the nonresonant transitions is negligible. The IR field is moderately strong; it is not directly coupled to the XUV transition, but it couples the state $|\alpha_0\rangle$ to some other excited states of an atom. We will show that under certain conditions the considered problem can be reduced to the problem of interaction of the XUV radiation with an effective quasi-resonant two-level system with sub-IR-field-cycle spatiotemporal modulation of its properties. This spatiotemporal modulation is caused by the IR field and provides conditions for realization of MIT for the XUV radiation. In this section we consider a general case of a rather strong or close to some atomic resonances IR field. The case of rather weak IR field, when perturbation theory is applicable is discussed in Appendix B. Using the Floquet formalism [88], we formulate the conditions under which an interaction of the XUV field with the quasi-resonant atomic medium in the presence of rather strong IR field can be reduced to an interaction of the XUV field with the effective two-level atoms with the modulated parameters of the two-level transition.

Mixing of $|\alpha_0\rangle$ with the other $N-1$ excited states by the IR field leads to appearance of *N* Floquet states. Due to a periodicity of the Hamiltonian describing interaction of an atom with the IR field, $H_{atom-IR} = E_{IR}(\tau)\left(\sum_{\alpha,\beta} d_{\alpha,\beta}|\alpha\rangle\langle\beta| + c.c\right) = \tilde{E}_{IR}\cos(\omega_{IR}\tau + \varphi_M)\left(\sum_{\alpha} d_{\alpha,\beta}|\alpha\rangle\langle\beta| + c.c\right)$, the wave function of the IR-field-dressed atom can be represented in the Floquet basis as following:

$$\left|\psi\right\rangle = c_1\left|1\right\rangle + \sum_i c_{\lambda_i} \exp(-\mathrm{i}\lambda_i(\tau + \varphi_M / \omega_{IR}))\left|\Phi_{\lambda_i}(\tau)\right\rangle, \qquad \text{(VI.27)}$$

where energy of ground state is chosen to be zero. Here λ_i is the quasi-energy of the i^{th} Floquet state $\left|\Phi_{\lambda_i}\right\rangle$, which periodically depends on time and constitutes the Fourier series:

$$\left|\Phi_{\lambda_i}(\tau)\right\rangle = \sum_{m=-\infty}^{+\infty} \exp(-\mathrm{i}m(\omega_{IR}\tau + \varphi_M))\sum_\alpha a_m^{i;\alpha}\left|\alpha\right\rangle, \qquad \text{(VI.28)}$$

c_{λ_i} is amplitude of this Floquet state, and φ_M is the laser phase. The amplitudes $a_{i;\alpha}^m$ of Fourier components of Floquet states (VI.28) and their quasi-energies λ_i are determined by the intensity and the frequency of the IR field and can be found analytically in terms of the infinite continued fractions (see, e.g. [89]). The index α enumerates excited states of a bare atom (an atom in the absence of the IR field), e.g., 2s, 2p, 3d states, etc. It is worth to note that the quasi-energies λ_i are defined up to an addition of multiple of ω_{IR}, i.e. $\exp(-\mathrm{i}\lambda_i(\tau + \varphi_M / \omega_{IR}))\sum_{m=-\infty}^{+\infty} \exp(-\mathrm{i}m(\omega_{IR}\tau + \varphi_M))\sum_\alpha a_m^{i;\alpha}\left|\alpha\right\rangle$ is equivalent to $\exp(-\mathrm{i}(\lambda_i + n\omega_{IR})(\tau + \varphi_M / \omega_{IR}))\sum_{m=-\infty}^{+\infty} \exp(-\mathrm{i}m(\omega_{IR}\tau + \varphi_M))\sum_\alpha a_{m+n}^{i;\alpha}\left|\alpha\right\rangle$. In accordance with Eq. (VI.28), each Floquet state corresponds to an energy ladder (a set of the equidistant energy levels) with the frequency interval between the neighboring "steps" equal to the frequency of an IR field. However, due to the dipole transition selection rules (the central symmetry of atoms), for an even m, the amplitudes $a_m^{i;\alpha}$ are not zeroes only for atomic states α of the same parity: depending on the choice of the quasi-energy, it could be only the odd parity states (such as 2p, 3p, 3f, etc.) or only the even parity states (such as 2s, 2d,

3s, 3d, etc.). Vice versa, for an odd m, the amplitudes $a_m^{i;\alpha}$ would be not zeros only for even parity states (such as 2s, 2d, 3s, 3d, etc.) /odd parity atomic states (such as 2p, 3p, 3f, etc.) [24]. Therefore, the neighboring "steps", containing bare atomic states of the same parity, are separated by the double frequency of the IR field.

The coefficients c_{λ_i} in Eqn. (VI.27) are the amplitudes of excitation of the corresponding Floquet states under the action of the XUV field. If the XUV field is weak, they can be calculated in the first order of the perturbation theory as follows [24]:

$$c_{\lambda_i} = \frac{\mathrm{i}}{\hbar}\int_{-\infty}^{\tau} \exp(\mathrm{i}\lambda_i\tau')\left\langle \Phi_{\lambda_i}\left| H_{HF}(\tau')\right|1\right\rangle d\tau',\ c_1 \approx 1, \qquad \text{(VI.29)}$$

where $H_{HF} = \frac{1}{2}\exp(-\mathrm{i}\omega\tau)\tilde{E}_{XUV}(\tau)\sum_{\alpha} d_{\alpha 1}|\alpha\rangle\langle 1|$ is a Hamiltonian describing excitation of atom by the XUV field in rotating wave approximation (RWA) and XUV field is assumed to be of finite duration.

Each "step" in a given Floquet ladder consists of a different mixture of the bare states (the "even" steps consist of the odd parity states, while the "odd" states consists of the even parity states or vice versa). However, in the considered case, when a linear response of the medium to the XUV field is determined by transitions to a single bare state $|\alpha_0\rangle$, only a contribution of that $|\alpha_0\rangle$ in each Floquet "step" participates in this response. In this case $H_{HF} = \frac{1}{2}\exp(-\mathrm{i}\omega\tau)\tilde{E}_{XUV}(\tau)d_{\alpha_0 1}|\alpha_0\rangle\langle 1|$ and the high frequency polarization and the probability of atomic excitation from the ground state (which determines the ionization yield in the combined IR+XUV radiation), are given by

$$\tilde{P}(\tau)=\frac{\mathrm{i}N\left|d_{\alpha_0 1}\right|^2}{\hbar}\sum_i e^{-\mathrm{i}(\lambda_i-\omega)\tau}\left\langle\alpha_0\middle|\Phi_{\lambda_i}\right\rangle\int_{-\infty}^{\tau}\exp(\mathrm{i}(\lambda_i-\omega)\tau')\tilde{E}_{XUV}(\tau')\left\langle\Phi_{\lambda_i}\middle|\alpha_0\right\rangle d\tau', \qquad \text{(VI.30)}$$

$$P_{excitation}=\sum_i\left|\frac{\mathrm{i}d_{\alpha_0 1}}{2\hbar}\int_{-\infty}^{\tau}\exp(\mathrm{i}(\lambda_i-\omega)\tau')\tilde{E}_{XUV}(\tau')\left\langle\Phi_{\lambda_i}\middle|\alpha_0\right\rangle d\tau'\right|^2, \qquad \text{(VI.31)}$$

accordingly, where $\left\langle\alpha_0\middle|\Phi_{\lambda_i}\right\rangle=\sum_m\exp(-\mathrm{i}m(\omega_{IR}\tau+\varphi_M))a_m^{i;\alpha_0}$. Combining equation for the resonant polarization (VI.30) with the wave equation for the XUV field envelope (VI.5), one can analyze the dynamics of the field during its propagation through the dressed medium.

Let us consider the situation, when the XUV field is tuned into resonance with only one (i^{th}) Floquet state involving a large admixture of the state $|\alpha_0\rangle$ and Floquet states are separated by the frequency interval, substantially exceeding their spectral widths. In this case, the XUV field excites only the i^{th} state and the slowly varying polarization is given by:

$$\begin{aligned}\tilde{P}(\tau)=&\frac{\mathrm{i}N\left|d_{\alpha_0 1}\right|^2}{\hbar}e^{-\mathrm{i}(\lambda_i-\omega)\tau}\sum_m\exp(-\mathrm{i}m(\omega_{IR}\tau+\varphi_M))a_m^{i;\alpha_0}\times\\&\int_{-\infty}^{\tau}\exp(\mathrm{i}(\lambda_i-\omega)\tau')\tilde{E}_{XUV}(\tau')\sum_m\exp(\mathrm{i}m(\omega_{IR}\tau'+\varphi_M))\left(a_m^{i;\alpha_0}\right)^*d\tau'\end{aligned}. \qquad \text{(VI.32)}$$

We would like to point out that the same polarization would be excited if we consider propagation of the same XUV field through the two-level medium described by Eqs. (VI.3)-(VI.5)) with the ground state $|1\rangle$ and the excited state $|\alpha_0\rangle$ with dipole moment $\tilde{d}_{\alpha_0 1}=d_{\alpha_0 1}\sum_n\left(a_{2n}^{i,\alpha_0}\right)^*\exp\left(2\mathrm{i}n(\omega_{IR}\tau+\varphi_M)\right)$ (and correspondingly $\tilde{d}_{1\alpha_0}=\tilde{d}_{\alpha_0 1}{}^*$) and constant

transition frequency $\bar{\omega}_{21} = \lambda_i$. Thus, interaction of the XUV field with the medium of IR-dressed atoms is equivalent to interaction of this field with two-level medium with space-time modulated dipole moment. Generally, both phase and absolute moment of dipole moment are modulated: $\tilde{d}_{\alpha_0 1} = d_{\alpha_0 1} \times \sum_n \left(a_{2n}^{i,\alpha_0} \right)^* \exp\left(2in\left(\omega_{IR}\tau + \varphi_M\right)\right) = A(\tau)\exp\{i\Phi(\tau)\}$, where $A(\tau)$ and $\Phi(\tau)$ are real valued functions. Equivalently, interaction of the XUV field with the Floquet state may be treated as interaction of the XUV field with two-level atom possessing modulated transition frequency $\omega_{21}(\tau) = \lambda_i + \Delta\omega_{21}(\tau)$ (where $\Phi(\tau) \equiv \int_{-\infty}^{\tau} \Delta\omega_{21}(\tau')d\tau'$) and space-time dependent dipole moment amplitude are given by $\tilde{d}_{21}(\tau) = A(\tau)$ (but not time modulated frequency and decay rate and constant dipole moment). From this point of view, it is meaningful to choose the quasi-energy λ_i in such way that $|\Delta\omega_{21}(\tau)|$ is as small as possible, so that tuning of the XUV field carrier frequency close to λ_i corresponds to closest tuning to atomic resonance. In the case when only phase modulation of dipole moment is important (like in the adiabatic limit of sufficiently low frequency of an IR field), an interaction of XUV field with the medium of the IR-dressed atoms is equivalent to interaction of this field with two-level medium with space-time modulated transition frequency $\omega_{21}(\tau) = \lambda_i + \Delta\omega_{21}(\tau)$ and constant dipole moment $\tilde{d}_{21} = \bar{A}$.

Let us consider the incident XUV field in the form of a spectral comb with a finite duration of its constituents, $E_{HF} = \frac{1}{2}\sum_n \tilde{E}_{2n}(\tau)\exp(-i(\omega + 2n\omega_{IR})\tau) + \text{c.c.}$ with carrier frequency ω close to resonance with λ_i. We assume that a characteristic duration of each

XUV spectral component is much larger than the IR-field-cycle, $\tau_{XUV,env} \gg 1/\omega_{IR}$, so that the spectral components are well separated from each other. In this case, we find from Eqs. (VI.30) and (VI.31) the atomic polarization and the excitation probability are

$$\tilde{P}(\tau) = \frac{\mathrm{i}N\left|d_{\alpha_0 1}\right|^2}{\hbar} e^{-\mathrm{i}(\lambda_i-\omega)\tau}\left(\sum_{2m} a_{2m}^{i,\alpha_0}\exp(-2\mathrm{i}m(\omega_{IR}\tau+\varphi_M))\right)\times \int_{-\infty}^{\tau}\exp(\mathrm{i}(\lambda_i-\omega)\tau')\sum_n \tilde{E}_{-2n}(\tau')\exp(-2\mathrm{i}n\varphi_M)\left(a_{-2n}^{i,\alpha_0}\right)^* d\tau', \quad \text{(VI.33)}$$

$$P_{excitation} = \left|\int_{-\infty}^{\tau}\frac{d_{\alpha_0 1}}{2\hbar}\exp(\mathrm{i}(\lambda_i-\omega)\tau')\sum_n \tilde{E}_{-2n}(\tau')\exp(-\mathrm{i}2n\varphi_M)\left(a_{-2n}^{i,\alpha_0}\right)^* d\tau'\right|^2. \quad \text{(VI.34)}$$

In this case both the absorption of the XUV field and the atomic ionization yield in the combined XUV+IR field (which is proportional to the excitation probability in the case of resonantly enhanced ionization) are defined by an interference term $\sum_n \tilde{E}_{-2n}\exp(-2\mathrm{i}n\varphi_M)\left(a_{-2n}^{i,\alpha_0}\right)^*$, see Eqs. (VI.33), (VI.34). Thus, such interference may be equivalently treated either as an interference of atomic excitation paths by the different spectral components of the field via the corresponding steps of the same Floquet ladder [35,123] or as an interference between contributions from the different spectral components of the incident XUV field into the resonant polarization due to elastic and inelastic (Raman Stokes- anti-Stokes) scattering processes caused by modulation of the parameters of the effective dressed transition. It critically depends on the relative phases of resonant polarization components, produced by the different spectral components of the incident XUV radiation. In its turn, those phases are determined by the phase of the IR field, φ_M, which can be changed by delaying the IR field with respect to the XUV

radiation, $\varphi_M \sim \omega_{IR}\tau_{delay}$. Depending on this delay, the interference is either constructive or destructive resulting in modulation of the absorption and the ionization yield. With the proper choice of the relative amplitudes of the incident XUV spectral components, satisfying the condition $\sum_n \tilde{E}_{-2n} \exp(-2in\varphi_M)\left(a_{-2n}^{i,\alpha_0}\right)^* = 0$ one gets the total destructive interference, i.e. the perfect MIT.

VI.5 The three-level atoms coupled to IR field: Floquet formalism and an effective two-level model with modulated parameters of the resonant transition

In this section, we illustrate the general result of Section VI.4 with a particular case, when IR field couples only two excited states of the bare atom. It happens, if the IR field is close to resonance with the transition between these states and is not too strong. In this case, one can restrict the model to the three levels, namely, the ground, $|1\rangle$, and the excited, $|2\rangle$ and $|3\rangle$, energy levels. Without loss of generality, we assume that XUV field couples ground state $|1\rangle$ and excited state $|3\rangle$. The high frequency polarization and the probability of atomic excitation from the ground state (which determines the ionization yield in the combined IR+XUV radiation) could be found in a way similar to the one described in the previous section. The details of the derivation are provided in Appendix C.

Similar to the analysis of the previous section, if the bichromatic (or the multicomponent) XUV field is tuned into resonance with only one of the Floquet states, and the Floquet states are separated by the frequency interval, substantially exceeding their spectral width, then the excitation of the IR-dressed atoms by the XUV field is reduced to

the excitation of a single two-level system formed by the ground state and the corresponding dressed space-time modulated excited atomic state (see Figure 29). In this case both the absorption of the XUV field and the atomic ionization yield in the combined XUV+IR field are defined by an interference term $\sum_n \tilde{E}_{-2n} \exp(-2in\varphi_M)\left(a_{-2n}^{i,3}\right)^*$, see Eqs. (C.6), (C.7). Total destructive interference, i.e. the perfect MIT, corresponds to $\sum_n \tilde{E}_{-2n} \exp(-2in\varphi_M)\left(a_{-2n}^{i,3}\right)^* = 0$.

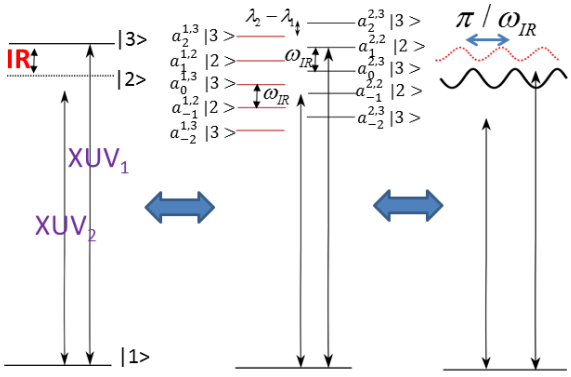

Figure 29. Interaction of the combined quasi-resonant XUV and intense IR radiation with an atomic system is equivalent to interaction of solely the XUV radiation with the Floquet states, produced from the excited atomic states by the IR field. Coupling of two bare excited states by the IR field results in a formation of two multifrequency dressed Floquet states, each corresponding to the energy ladder, i.e. a set of equidistant energy levels. The steps of ladders containing the same state ($|2\rangle$ or $|3\rangle$) are separated by the doubled photon energy of the IR field. Accordingly, an excitation of each Floquet state by the XUV field is equivalent to an excitation of a two-level system (involving the ground state $|1\rangle$ and the corresponding quasi-energy state) with a periodically space-time-dependent both transition frequency and a magnitude of dipole moment.

Let us consider a possible experimental realization of the MIT for the XUV radiation, resonant to the $1s^2 \leftrightarrow$ 1s2p transition of helium (with the wavelength 58.4 nm)

dressed by the IR field with the wavelength $\lambda_{IR} = 2.01\mu m$ and intensity $I = 4\times10^{12}$ W/cm^2. Note that the intensity of the IR field is an order of magnitude larger than in the case, discussed in Appendix B, so that the perturbation theory is no longer applicable for description of its influence on the atoms. However, since (i) the IR field is very far-detuned from all the transitions between the resonantly populated 1s2p state and the other excited states of He, except for the 1s2s ↔ 1s2p transition, and (ii) the Rabi frequency of the IR field is substantially smaller than the frequencies of all the transitions from the 1s2p state, one can neglect all the atomic states, except the $1s^2$, 1s2s and 1s2p, when investigating the MIT. Choosing the XUV radiation consisting of the 33rd and 35th harmonics of the IR field (35th harmonic is resonant to one of the two Floquet states), one obtains the transparency condition $\left|\tilde{E}_{35} / \tilde{E}_{33}\right| = 1.0 / 2.3$, which follows from the ratio of amplitudes of the adjacent steps $\left|a_0^{j,\alpha_0} / a_{-2}^{j,\alpha_0}\right| = 2.3 / 1.0$ of the resonant Floquet ladder.

VI.6 Comparison with experimental results

In this section, we discuss the recent experiment [22] devoted to the sub-laser-cycle modulation of the atomic ionization probability by a moderately strong IR laser field, combined with its high-order harmonics. We show that the observed modulation of the ionization yield corresponds to the partial MIT and discuss the possibilities to achieve a complete transparency of an atomic gas for resonant XUV radiation, corresponding to suppression of atomic ionization by the combined IR+XUV field. In that experiment, the helium atoms were simultaneously irradiated by a moderately strong Ti:Sa IR laser field with the wavelength in the range 750-785 nm and intensity 4×10^{12} W/cm^2 as well as by

its 11-th and 13-th harmonics with low intensity. The laser field strength was considerably below the threshold of atomic ionization or multiphoton excitation from the ground state, $1s^2$, however, it was sufficient for ionization from every excited state of helium. The 13-th harmonic resonantly promoted atoms from the ground state to the 1s2p excited state, while the frequency of the 11-th harmonic was below the frequencies of all the transitions from the ground state of helium. The intensity of the harmonics was insufficient for a multiphoton excitation. It was shown that probability of atomic ionization by the IR field, combined simultaneously with both the 11-th and 13-th harmonics can be appreciably smaller, than the probability of ionization by the laser field, combined with each harmonic separately. It was also shown, that the probability of atomic ionization oscillates with twice the laser frequency as the harmonics are delayed with respect to the oscillation of the IR field. Finally, it was pointed out, that a vanishing ionization yield can be achieved in the case of a specific delay under the specific ratio of amplitudes of the resonant and off-resonant harmonics [22]. These results were interpreted as a consequence of interference of the two multiphoton ionization paths: (i) the 13-th harmonic plus three photons of the laser field, and (ii) the 11-th harmonic plus five photons of the laser field. (Since the ionization was experimentally proven to be resonantly enhanced, the suppression of the ionization yield was caused by suppression of the atomic excitation to an intermediate 2p state and equivalently could be viewed as a result of interference of the two excitation paths: through absorption of the 13-th harmonic and trough absorption of the 11-th harmonic and two photons of the laser field.) This interpretation has a simple physical meaning, but it does not explain directly why the optimal conditions for

transparency imply tuning the 13-th harmonic to the resonance with a dressed (Floquet) state and satisfying Eq. (VI.22). These optimal conditions straightforwardly follow from the Floquet formalism [88], but the last one lacks simple physically intuitive picture. Viewing the observed effect as a partial MIT allows for both understanding of the optimal conditions for transparency and getting of its physically intuitive picture, as it is shown below.

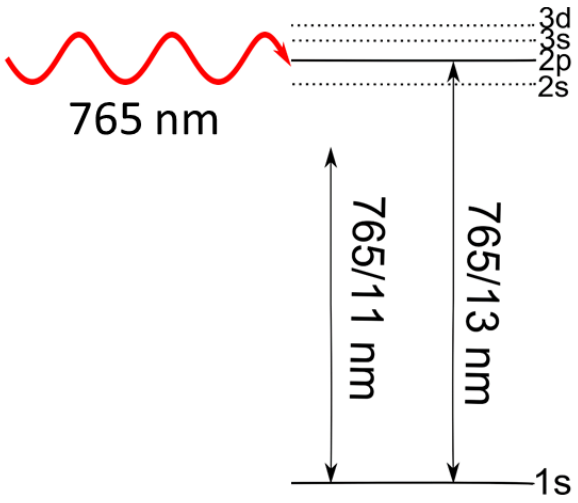

Figure 30. Relevant energy levels of helium, simultaneously interacting with Ti:Sa laser field and its 11-th and 13-th harmonics under the conditions of experiment [22]. The black vertical arrows symbolize energies (and wavelengths) of the harmonic photons, while the red oscillating curve represents the Ti:Sa-laser radiation. The horizontal lines correspond to position of the unperturbed atomic energy levels.

The ratio of the intensities of the 11-th and 13-th harmonics, required to achieve transparency of the medium, as well as the preferable frequencies of the fundamental laser field and its harmonics can be calculated within different models of the atomic system with a different accuracy. At the laser intensity $I_{IR} = 4 \times 10^{12}\,\mathrm{W/cm^2}$, used in the experiment, the reasonable estimate can be obtained from the five-level model, which takes into

account the $1s^2$ and 1s2p resonant atomic states as well as the 1s2s, 1s3s and 1s3d states, which are strongly mixed with the resonantly populated 1s2p state by the IR field, see Figure 30. Following the procedure described in the previous section, we find four Floquet states, composed from the 1s2s, 1s2p, 1s3s and 1s3d bare atomic states coupled by the IR field. Since only one state of four excited states coupled by the IR field (namely, the 1s2p state) interacts with the XUV field, for the purpose of calculation of an atomic excitation each Floquet state can be replaced by the corresponding quasi-energy level periodically modulated in time with a double frequency of the IR field (as it was shown in the previous section). The time dependencies of all four energies (obtained from $\Phi(\tau)$) for the parameters of the experiment [22] are shown in Figure 31. It turns out that for the laser wavelength $\lambda = 765\,\mathrm{nm}$, one of the four quasi-energy levels (which energy is shown in Figure 31 by the bold blue line) plays the dominant role for the atomic excitation, while transitions to the others quasi-energy levels are either far detuned from the resonance with both the 13-th and the 11-th harmonics or have a small dipole moment. For the dominant level, modulation of the magnitude of a dipole moment $A(\tau)$ is much weaker than modulation of its energy. The condition of the perfect MIT for this level is $a_0^{2p} / a_{-2}^{2p} \approx 19.6/1$, corresponding to the ratio of the harmonic intensities $I_{11} / I_{13} \approx 380:1$, which is reasonably close to the original result, $I_{11} / I_{13} = 256:1$ [22], based on the numerical solution of the time-dependent Schrodinger equation. More precise results, as compared to the five-level model, can be obtained if all the bare excited states of He are taken into account in a calculation of the dressed Floquet states on the basis of the non-Hermitian Floquet formalism [88,152,153]. The results of such a calculation are presented

in Figure 32. The effective potential used for calculation is taken from [138] and optimized to better reproduce the excited levels of helium. As it can been seen from Figure 32, at the ratio of intensities $I_{11}:I_{13}=4:1$ used in the experiment [22] the ionization yield suppression is rather small (ratio of the minimum ionization yield to the maximum ionization yield is approximately 0.7). It is in accordance with an experimental result [22]. As it can be seen from Figure 32, a ratio of intensities, leading to nearly full transparency is $I_{11}:I_{13}=256:1$. It is the same as calculated in [22]. It is very challenging to realize experimentally such a high ratio of harmonics intensities and hence to achieve high transparency in the described experiment. However, nearly perfect MIT with comparable intensities of resonant and nonresonant harmonics could be easily achieved using a lower frequency IR field, as it was discussed in Sec. VI.5.

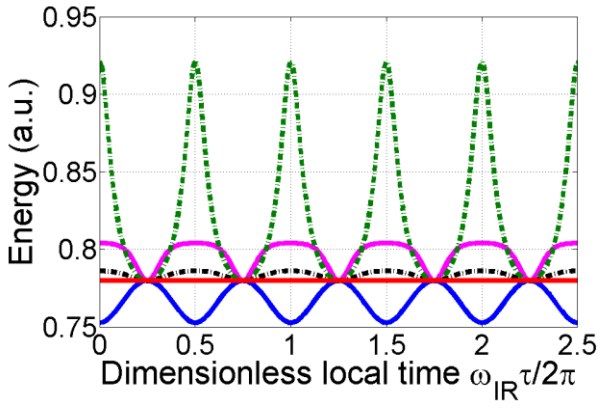

Figure 31. The local-time-dependencies of the instantaneous energies, corresponding to the different Floquet states, and originating from mixture of the 1s2p state with the 1s2s, 1s3s and 1s3d states of helium produced by the Ti:Sa laser radiation under the conditions of experiment [22]. The local time $\tau = t - x / V_M$ is normalized to the laser period. The energies are plotted in atomic units. The bold red horizontal line shows the position of the resonantly populated 1s2p energy level of helium in the absence of the laser field.

Finally, it is worth to emphasize that a simple effective two-level model involving the ground atomic state and just one dressed excited state with modulated energy allows to determine the optimal conditions for transparency rather well and provides their simple intuitive physical interpretation. In particular, it clarifies the role of an IR field as not just adding the IR photons to high harmonics fields and not just mixing, splitting and shifting excited levels, but primarily modulating the frequency of the quasi-resonant dressed transition. It is this modulation that results in an inelastic Raman type Stokes and anti-Stokes scattering of the 11-th harmonic. A destructive interference between the contributions of the 13-th harmonic and anti-Stokes sideband of the 11-th harmonic into the resonant polarization, occurring under the appropriate IR field delay, leads to decrease and/or full elimination of an absorption.

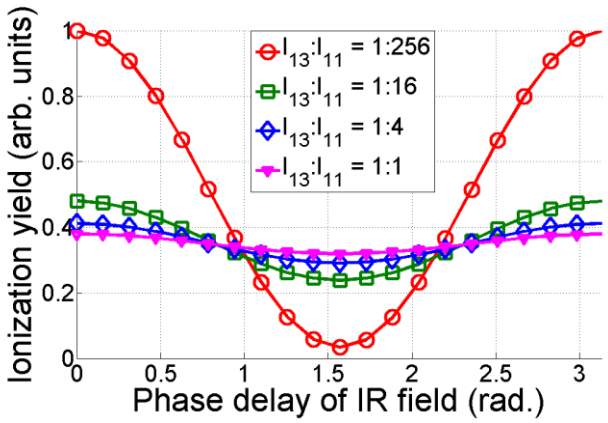

Figure 32. The ionization yield of helium atoms, simultaneously irradiated by the Ti:Sa laser radiation and its 11-th and 13-th harmonics, versus the phase shift of the laser field with respect to the harmonic signal. The ionization yield is normalized to its maximum value. Different colors correspond to the different values of the ratio between intensities of the 11-th and 13-th harmonics. The calculations are performed for the conditions of experiment [22].

VI.7 Conclusion

We found rather general analytical solution describing transformation of a weak HF radiation propagating through the quasi-resonant two-level medium with periodically modulated frequency and decoherence rate of the resonant transition. Compared to the case of the stationary parameters, where the transformation of the field as a result of its propagation is solely defined by an interference between an incident and elastically scatted field, the main new feature inherent to the modulated medium is an inelastic Raman scattering, leading to formation of Stokes and anti-Stokes sidebands at the frequencies multiple to the modulation frequency. As a result, the additional interference between elastically and inelastically scattered spectral components occurs when these sidebands overlap with the spectral components of a single or multi-frequency incident field. Such interference at the atomic resonance frequency leads to enhancement or suppression of the

resonant absorption depending on the phase difference between the relative phase of the interfering components of the field and the modulation phase. With a proper selection of the amplitudes of the incident spectral components (dependent on the modulation amplitude), it leads to complete suppression of the scattered field, resulting in phenomenon of the modulation induced transparency (MIT), i.e., elimination of the medium's effect on the HF field.

We have proven that it is essentially the same simple physically intuitive picture described above which lays the basis for the two different physical processes: coherent forward scattering of γ-ray radiation in the vibrating nuclear targets and propagation of an XUV field through the atomic gases in the presence of the moderately strong IR field. In the first system it is vibration of the medium, while in the second case it is an IR field which causes the modulation of the parameters of the resonant transition. Moreover, under certain conditions, both systems are described by the identical equations having the same solution. It allows to conclude that some effects experimentally demonstrated in one system can be realized in the other one and vice versa. For example, a partial MIT observed in the case of quasi-monochromatic field in γ-ray scattering can be observed in the case of a quasi-monochromatic XUV field (which should be a particular high harmonic of IR field) propagation in atomic gases in the presence of an IR field, while partial MIT observed in the case of two component XUV propagation can be realized in the case of coherent forward γ-ray scattering in the vibrated nuclear absorber. Moreover, perfect MIT may be achieved in all these cases. Similarly, the ultrashort pulse formation realized in γ-

ray range via nuclear absorber vibration [142] can be realized in the XUV range in the presence of an IR field [38,40-42].

In connection with MIT caused by IR field it is insightful to compare three different types of transparency of a medium for HF probe radiation resonant to 1-3 transition in the presence of a strong LF driving field coupled to an adjacent 2-3 transition: (1) electromagnetically-induced transparency (EIT), (2) Autler-Townes transparency (ATT) and (3) MIT. The first two types of transparency imply quasi-resonant driving of a LF $|2\rangle - |3\rangle$ transition with the Rabi frequency substantially smaller than its carrier frequency [6]. EIT is due to the resonant excitation of the specific two-photon atomic coherent superposition state ("dark state") uncoupled to the excited state [3,6]. It requires a two-photon resonance condition $\omega_{31} - \omega_{HF} = \omega_{32} - \omega_{LF}$, and a moderately strong LF driving field: $\gamma_{12} < d_{23}E_{IR}/\hbar < \gamma_{13}$, where γ_{12} and γ_{13} are the coherences decay rates at $|1\rangle - |2\rangle$ and $|1\rangle - |3\rangle$ transitions. The last condition naturally implies: $\gamma_{12} < \gamma_{13}$, which is difficult to achieve in the hot or dense atomic gases where the linewidths of both $|1\rangle - |3\rangle$ and $|1\rangle - |2\rangle$ transitions are typically defined by collisional or Doppler broadening and have comparable magnitude. ATT originates from Autler-Townes splitting of the absorption line (determined by the Rabi frequency of the driving field) into the two spectrally separated Lorentz contours and hence implies: $d_{23}E_{IR}/\hbar > \gamma_{13}$. Compared to both EIT and ATT, MIT implies much stronger LF driving field with the Rabi frequency of the same order or higher than its carrier frequency: $d_{23}E_{IR}/\hbar \sim \omega_{LF}$. Contrary to the ATT and EIT, MIT generally implies also either two- or multi-component HF probe radiation with

frequency interval between the components, equal/multiple to the doubled frequency of the driving field. MIT originates not from excitation of the atomic coherence at the two-photon transition $|1\rangle - |2\rangle$ nor from the Autler-Townes splitting, but from a modulation of the parameters of the quasi-energy HF transition leading to the destructive interference of the coherently scattered fields produced by the different spectral components of the incoming radiation in a modulated medium. MIT can be achieved by a proper choice of incident fields' relative amplitudes and phases.

Along with the indicated differences we would like to point out some analogy between MIT and EIT. Indeed, both MIT and EIT result from destructive interference between the different pathways of atomic excitation. Modulation of the properties of an atomic transition in MIT plays the same role as quantum coherence at the two-photon transition in EIT.

The possible applications of MIT include coherent control and manipulation of the bound [22,24] and auto-ionizing [36] atomic states and shaping of the XUV radiation pulses [26,29,30,154], as well as controlling and optimizing of HHG in the spectral regions, where absorption of XUV radiation by either outer- or inner-shell atomic electrons plays an important role [34,126]. It can be also viewed as a prospective mechanism of controlling chemical reactions on ultrafast time-scale [22,155]. Fundamentally, understanding and controlling light absorption is a basic requirement for the light-wave electronics [55].

CHAPTER VII

FORMATION AND AMPLIFICATION OF SUB-FEMTOSECOND X-RAY PULSES IN A PLASMA MEDIUM OF THE HYDROGEN-LIKE IONS WITH A MODULATED RESONANT TRANSITION[7]

VII.1 Introduction

Coherent intense sub-femtosecond (sub-fs) soft x-ray pulses would open extremely wide applications for dynamical, element-specific microscopy and diffraction imaging in chemistry, biology, medicine, nanoscience and material science, providing unique combination of the unprecedented high spatial and temporal resolution, ultimately determined by the nm carrier wavelength and attosecond (as) pulse duration accordingly (see reviews on x-ray lasers [43-52] and attosecond physics [53-61]). Production of the bright ultrafast coherent sources in a "water window" range (between the C and O K-shell absorption edges at 284–540 eV, i.e. 4.4–2.3 nm), is considered to be especially important for imaging of the protein dynamics in the living cells [44-68].

Currently there are three types of coherent sources in the soft x-ray wavelength range: free-electron lasers [69-76], x-ray plasma-based lasers [46-48,50,77,78] and high harmonic generation (HHG) sources [65-68]. Free-electron lasers present themselves large-scale state-of-the-art expensive facilities and there are only few of them available in

[7] The related work "Formation and amplification of sub-femtosecond X-ray pulses in a plasma medium of the hydrogen-like ions with a modulated resonant transition" by T.R. Akhmedzhanov et al. will be submitted to journal publication soon.

the world. They produce high energy pulses, but the pulse duration is currently limited by fs and pulses are typically not transform limited due to the short noise.

Table-top soft x-ray plasma-based lasers produce relatively high energy pulses (up to several mJ) but of rather long pico-second (ps) duration. The HHG sources allow producing thousands of high harmonics stretching well into x-ray range. However, the individual harmonics energy in the soft x-ray range, in particular, in a water window range, does not exceed nJ due to the low (less than 10^{-7}) conversion efficiency. The duration of a single harmonic is in a range of tens to hundreds fs. Potentially, the set of harmonics could constitute the attosecond x-ray pulses (under condition of an attochirp compensation) but the energy of such pulses would be still limited by nJ [65,67].

This work aims on theoretical study and comparison of two possible paths to coherent intense sub-fs x-ray sources, namely, (i) via efficient compression of picosecond radiation of x-ray plasma lasers into attosecond pulse trains without essential loss of the energy; (i) via amplification of an individual high-harmonic radiation in an active medium of x-ray lasers accompanied by formation of attosecond pulses.

We show that both paths can be realized by using essentially the same technique recently theoretically developed by our group [37,38,41,42]. The basic idea is to use an interaction of the x-ray plasma laser or high-harmonic radiation with the plasma medium consisting hydrogen-like ions (accordingly, without or with a population inversion) at the resonant transition which frequency is modulated by the infrared (IR) laser field.

The outline of the paper is as follows. In Sec.VII.2 we formulate the basic set of the density matrix and wave equations, describing formation of sub-fs pulses in a plasma

of hydrogen-like ions in a presence of a moderately strong IR field. In Sec. VII.3 we study the possibility of an efficient compression of the quasi-monochormatic radiation of X-ray plasma lasers into the trains of sub-fs pulses in the passive (non-inverted) plasma of hydrogen-like ions modulated by an IR field. In Sec. VII.4 we analyze the possibility of amplification of an individual X-ray high harmonic radiation, accompanied by the sub-fs pulses formation in an active inverted plasma of hydrogen-like ions modulated by an IR field. We suggest also an experimental realization of both techniques in LiIII (Li^{2+}ions) and CVI (C^{5+}) ions in the vicinity of the wavelengths 13.5nm and 3.4 nm, corresponding to the resonant transitions from the first excited to the ground state in these ions, modulated by the IR laser fields, and determine the ultimate pulses durations and intensities which can be achieved by those techniques.

In Conclusions we summarize the major results and give a comparative analysis of two suggested techniques, pointing out their advantages and disadvantages, as well as the prospects for extension of these techniques to plasmas of non-hydrogen ions.

VII.2 Propagation of X-ray radiation through modulated medium of hydrogen-like ions

Let us consider propagation of X-ray radiation along x-axis through a medium of neutral plasma of hydrogen-like ions. At the entrance to the medium, x=0, the radiation is quasi-monochromatic and has the form

$$\vec{E}_{X-ray,inc}(t) = \frac{1}{2}\vec{z}_0\tilde{E}_0(t)\exp\{-i\omega_0 t\} + \text{c.c.}, \qquad \text{(VII.1)}$$

where E_0 is the slowly varying envelope of incident radiation, ω_0 is its carrier frequencies, and c.c. stands for complex conjugation. The radiation (VII.1) is chosen to be near-resonant to a transition from the ground state $|1\rangle$ to the first excited bound atomic state, $\omega_0 \approx \omega_{21}^0$ (where ω_{21}^0 is the unperturbed frequency of the resonant transition).

The medium is simultaneously irradiated by a moderately strong z-polarized IR laser field propagating in x direction with a phase velocity determined by the plasma refractive index:

$$\vec{E}_{IR}(t) = \vec{z}_0 \tilde{E}_{IR} \cos\left\{-i\,\Omega\left(t - x n_{pl}/c\right)\right\} \qquad \text{(VII.2)}$$

where $\tilde{E}_{IR}$ is the amplitude of the IR field, Ω is its angular frequency, $n_{pl} = \sqrt{1 - \frac{\omega_{pl}^2}{\Omega^2}}$ is plasma index of refraction, $\omega_{pl}^2 = \frac{4\pi n_e e^2}{m_e}$ (n_e, m_e, e are electrons concentration, electron mass and electron charge) and *c* is the speed of light in vacuum. IR field is far-detuned from the relevant atomic resonances, and it traverses the medium without appreciable distortions.

Since X-ray radiation is z-polarized and it's frequency is close to resonance between ground state and first excited state of hydrogen-like ion, we take into account only two excited states, namely, states: $|2\rangle = (|2s\rangle + |2p,m=0\rangle)/\sqrt{2}$ and $|3\rangle = (|2s\rangle - |2p,m=0\rangle)/\sqrt{2}$ (which energies are harmonically modulated by z-polarized IR field due to the linear Stark effect field, as it may be seen from the density matrix equations below). We do not take into account two other excited states $|4\rangle = |2p,m=1\rangle$, and

$|5\rangle=|2p,m=-1\rangle$ (which are not perturbed by an IR field). In the case of passive (noninverted) medium, studied in Sec. VII.3, these excited states do not influence in any way a propagation of z-polarized field because they have dipole transition moments only for y-polarized X-ray field. In the case of active (inverted) medium, a possibility to use a three-level approximation is obvious only when transitions $|4\rangle$-$|1\rangle$ and $|5\rangle$-$1\rangle$ remain unsaturated by a y-polarized field. It is due to the fact that gain for z-polarized and y-polarized fields originates from the different populated excited levels. Thus y-polarized field does not influence gain for z-polarized field till it appreciably changes a population of a ground state. A possibility to use it for analysis of sufficiently short seeding pulses amplification in the case of sufficiently high gain for the y-polarized field (even when the last one saturates $|4\rangle$-$|1\rangle$ and $|5\rangle$-$1\rangle$ transitions) is proved in an Appendix D, where the equations for populations of those levels and polarizations of the corresponding transitions, as well as the wave equation for y-component of the quasi-resonant X-ray field are taken into account. As for the higher excited states, they may be safely neglected, when both frequency and intensity of an IR field are sufficiently small, as it was studied in details in [156]. Within this approximation, the resonant polarization is defined by density matrix elements, ρ_{ij}:

$$\vec{P}(\vec{r},t) = N\left(\vec{d}_{12}\rho_{21} + \vec{d}_{13}\rho_{31} + c.c.\right) \qquad \text{(VII.3)}$$

where N is ions concentration and $\vec{d}_{ij}$ is dipole moment between states $|i\rangle$ and $|j\rangle$. Within 3-level model, all the non-zero dipole moments are given by:

$$\vec{d}_{12} = \vec{d}_{1s\leftrightarrow 2p,m=0}/\sqrt{2} = \vec{z}_0 d_{\|}, \quad \vec{d}_{13} = -\vec{d}_{1s\leftrightarrow 2p,m=0}/\sqrt{2} = -\vec{z}_0 d_{\|},$$
$$\vec{d}_{22} = \vec{d}_{2s\leftrightarrow 2p,m=0} = \vec{z}_0 d_{av}, \quad \vec{d}_{33} = -\vec{d}_{2s\leftrightarrow 2p,m=0} = -\vec{z}_0 d_{av} \qquad \text{(VII.4)}$$

In atomic units $d_{\|} = \frac{2^7}{3^5 Z}$, and $d_{av} = 3/Z$, where Z is an atomic number. Under the action of both X-ray and IR field, the evolution of density matrix elements is given by:

$$\dot{\rho}_{11} = +\gamma_{11}(\rho_{22} + \rho_{33}) - i\left[\mathrm{H}, \rho\right]_{11}$$
$$\dot{\rho}_{ij} = -\gamma_{ij}\rho_{ij} - i\left[\mathrm{H}, \rho\right]_{ij}, ij \neq 11$$
$$\mathrm{H} = \begin{pmatrix} \omega_1 & -E_z d_{\|} & E_z d_{\|} \\ -E_z d_{\|} & \omega_2 - \tilde{E}_{IR} d_{av} \cos\left\{-i\Omega\left(t - x n_{pl}/c\right)\right\} & 0 \\ E_z d_{\|} & 0 & \omega_3 + \tilde{E}_{IR} d_{av} \cos\left\{-i\Omega\left(t - x n_{pl}/c\right)\right\} \end{pmatrix} \qquad \text{(VII.5)}$$

Here ω_i is energy of atomic level $|i\rangle$. With quadratic Stark effect taken into account, $\omega_1 = -\frac{Z^2}{2}\left(1 + \frac{9}{256}F_c^2\right), \omega_2 = \omega_3 = -\frac{Z^2}{8}\left(1 + \frac{7}{4}F_c^2\right)$ where $F_c = \left(\frac{2}{Z}\right)^3 \tilde{E}_{IR}$ [113].

The decay rates γ_{ij} are defined as $\gamma_{12} \approx \gamma_{13} \approx \gamma_{coll} + \Gamma_{ion}/2 + \Gamma_{radiative}/2$, $\gamma_{23} \approx \gamma_{coll} + \Gamma_{ion} + \Gamma_{radiative}$, $\gamma_{22} \approx \gamma_{33} \approx \Gamma_{ion} + \Gamma_{radiative}$, $\gamma_{11} \approx \Gamma_{radiative}$, where γ_{coll} and Γ_{ion} are collisional broadening and ionization decay rates correspondingly. $\Gamma_{radiative}$ are radiative decay rates, which could be found in [157].Collisional broadening was estimated according to [158], $\Gamma_{ion} \approx \frac{Z^2}{16}\sqrt{\frac{3F_c}{\pi}}\left[\left(\frac{4}{F_c}\right)e^{+3} + \left(\frac{4}{F_c}\right)^3 e^{-3}\right]\exp\left\{-\frac{2}{3F_c}\right\}$ [113].We neglect Doppler broadening of transitions since we consider ion temperatures on the order of 1 eV as it is typical in recombination X-ray plasma lasers [77], resulting in Doppler broadening

comparable or less than collisional broadening. It is worth noting that for parameters we consider in the paper, $\gamma_{ij} \ll \Omega$.

Let us seek for a partial solution in the form

$$\begin{aligned}
&\vec{E}(x,t) = \frac{1}{2}\vec{z}_0\tilde{E}_z(x,t)e^{-i(\omega t-kx)} + \text{c.c.} \\
&\rho_{12}(\vec{r},t) = \tilde{\rho}_{12}(\vec{r},t)e^{i\omega t-ikx}, \\
&\rho_{13}(\vec{r},t) = \tilde{\rho}_{13}(\vec{r},t)e^{i\omega t-ikx}, \\
&\rho_{ij}(\vec{r},t) = \tilde{\rho}_{ij}(\vec{r},t), ij \neq 12,13
\end{aligned} \quad , \qquad \text{(VII.6)}$$

where $\tilde{E}(\vec{r},t)$ and $\tilde{\rho}_{ij}(\vec{r},t)$ are the slowly-varying amplitudes of the field and decay matrix elements, respectively, that is $\left|\frac{1}{\tilde{E}}\frac{\partial\tilde{E}}{\partial t}\right| \ll \omega$, $\left|\frac{1}{\tilde{E}}\frac{\partial}{\partial x}\tilde{E}\right| \ll k$, and $\left|\frac{1}{\tilde{\rho}_{ij}(\vec{r},t)}\frac{\partial\tilde{\rho}_{ij}(\vec{r},t)}{\partial t}\right| \ll \omega$, $\left|\frac{1}{\tilde{\rho}_{ij}(\vec{r},t)}\frac{\partial}{\partial x}\tilde{\rho}_{ij}(\vec{r},t)\right| \ll k$. In such a case, within the rotating wave approximation and approximation of plane waves, we get

$$\frac{\partial\tilde{E}}{\partial x} = i4\pi\frac{\omega N d_{\parallel}}{c\sqrt{\varepsilon}}\left(\rho_{21}-\rho_{31}\right), \qquad \text{(VII.7)}$$

and

$$\begin{aligned}
&\dot{\tilde{\rho}}_{11} = +\gamma_{11}(\tilde{\rho}_{22}+\tilde{\rho}_{33}) + \frac{i\tilde{E}^* d_{\parallel}}{2}(\tilde{\rho}_{21}-\tilde{\rho}_{31}) + \frac{i\tilde{E} d_{\parallel}}{2}(\tilde{\rho}_{13}-\tilde{\rho}_{12}) \\
&\dot{\tilde{\rho}}_{22} = -\gamma_{22}\tilde{\rho}_{22} + \frac{i\tilde{E}\, d_{\parallel}}{2}\tilde{\rho}_{12} - \frac{i\tilde{E}^* d_{\parallel}}{2}\tilde{\rho}_{21} \\
&\dot{\tilde{\rho}}_{33} = -\gamma_{33}\tilde{\rho}_{33} + \frac{i\tilde{E}^* d_{\parallel}}{2}\rho_{31} - \frac{i\tilde{E}\, d_{\parallel}}{2}\rho_{13} \\
&\dot{\tilde{\rho}}_{12} = -\gamma_{12}\tilde{\rho}_{12} - i\tilde{\rho}_{12}(\omega_1-\omega_2+\omega+\tilde{E}_{IR}d_{av}\cos\left(\Omega\left[\tau+\left(1-n_{pl}\right)x/c\right]\right)) - \frac{i\tilde{E}^* d_{\parallel}}{2}\left(\rho_{32}-\rho_{22}+\rho_{11}\right) \\
&\dot{\tilde{\rho}}_{13} = -\gamma_{13}\tilde{\rho}_{13} - i\tilde{\rho}_{13}(\omega_1-\omega_3+\omega-\tilde{E}_{IR}d_{av}\cos\left(\Omega\left[\tau+\left(1-n_{pl}\right)x/c\right]\right)) - \frac{i\tilde{E}^* d_{\parallel}}{2}\left(-\rho_{23}+\rho_{33}-\rho_{11}\right) \\
&\dot{\tilde{\rho}}_{23} = -\gamma_{23}\tilde{\rho}_{23} - i\tilde{\rho}_{23}(\omega_2-\omega_3-2\tilde{E}_{IR}d_{av}\cos\left(\Omega\left[\tau+\left(1-n_{pl}\right)x/c\right]\right)) + \frac{i\tilde{E}^* d_{\parallel}}{2}\tilde{\rho}_{21} + \frac{i\tilde{E}\, d_{\parallel}}{2}\tilde{\rho}_{13}
\end{aligned} \quad , \qquad \text{(VII.8)}$$

where we have introduced local time $\tau = t - x/c$. Equations (VII.7) and (VII.8) along with initial conditions

$$\tilde{\rho}_{ij}(x, t=0) = \tilde{\rho}_{ij}^{(0)}, \tag{VII.9}$$

and boundary conditions (VII.1) describe propagation of a z-polarized X-ray field in *x*-direction.

In the case of passive (non-inverted) medium, which is discussed in the next section, initial conditions are:

$$\tilde{\rho}_{11}(x, t=0) = 1, \tilde{\rho}_{ij}(x, t=0) = 0, ij \neq 11. \tag{VII.10}$$

In order to model amplification of incident X-ray field (VII.1) through inverted medium of X-ray plasma based lasers (considered in section VII.4) we assume at the moment $t = 0$ all the ions have equal probability to be in the excited states $|2\rangle, |3\rangle, |4\rangle, |5\rangle$ and there are no coherencies. Namely, initial conditions (VII.10) become:

$$\tilde{\rho}_{22}(x, t=0) = \tilde{\rho}_{33}(x, t=0) = 0.25, \tilde{\rho}_{ij}(x, t=0) = 0, ij \neq 22, 33 \tag{VII.11}$$

Incident X-ray field (VII.1) is considered to be a z-polarized quasi-monochromatic pulse resonant to transitions $|1\rangle \leftrightarrow |2\rangle$ and $|1\rangle \leftrightarrow |3\rangle$.

As it can be seen from Eqns. (VII.8) for diagonal matrix elements ρ_{12}, ρ_{13}, under the action of the IR field the instantaneous transition frequency of transitions $|1\rangle \leftrightarrow |2\rangle, |1\rangle \leftrightarrow |3\rangle$ is periodically modulated with period equal to the period of the IR field. Physically it corresponds to linear AC Stark effect, Figure 33, (where plasma dispersion

is neglected, i.e. n_{pl} is assumed to be equal to 1). Since transitions $|1\rangle \leftrightarrow |2\rangle, |1\rangle \leftrightarrow |3\rangle$ have non-zero component of dipole moment along z direction, modulation of the transition frequencies will result in modulated polarization leading to appearance of the sidebands in z-polarized field propagating in x-direction. The neighboring sidebands are separated by the double IR field frequency due to the atomic symmetry (Figure 33). Both the phases and the amplitudes of the sidebands depend on the modulation amplitude and length of the medium. With a proper choice of these parameters it appears to be possible to have the sidebands in phase with each other as well as with a resonant component and an incident field at the exit of the medium. As a result, a train of the sub-fs pulses may be formed.

In the next sections we consider the formation of such sub-fs pulses in the passive (non-inverted) and active (inverted) plasma of the hydrogen-like ions accordingly.

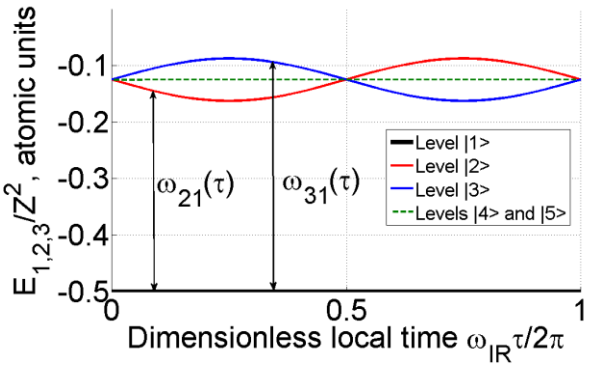

Figure 33. Energy levels of the ground and first excited state of the hydrogen like-ion dressed by an IR field.

VII.3 Efficient transformation of x-ray plasma laser radiation into a train of sub-fs pulses in plasma of non-inverted hydrogen–like ions modulated by an IR laser field

In the case of passive (non-inverted) optically thin resonant medium, when plasma dispersion can be neglected, a set of equations (VII.1), (VII.7), (VII.8), (VII.10) has a simple analytical solution studied in [38]. The amplitudes and phases of the sidebands in this case are defined by the Bessel functions of the modulation index $J_{2n}(P_\omega)$, $P_\omega = \frac{d_{av}\tilde{E}_{IR}}{\Omega}, n = 0, \pm 1, \pm 2...$ In particular, at the modulation index $2.40 < P_\omega < 5.14$ all sidebands are in phase with respect each other and with an incident field (which dominates an anti-phased resonant scattering component) [38]. As a result a train of short pulses can be formed after suppression of an incident field to the level of the sidebands. With an increase of the optical thickness of the medium the amplitudes of the sidebands grow up, while an amplitude of an incident field decreases both due to transformation into the sidebands and the resonant absorption. It was shown that an efficiency of transformation of an incident quasi-monochromatic radiation into the train of the short pulses can be quite high. For example, an efficiency of transformation of quasi-monochromatic VUV radiation with the wavelength 122.1nm into the train of 3.2fs pulses in atomic hydrogen modulated with an IR field with the wavelength 10.65 μm and intensity $1.4 \times 10^{12} W/cm^2$ (corresponding to $P_\omega=4.45$) was shown to be ~ 76% .

In this section we consider the possibility of application of this technique for transformation of quasi-monochromatic X-ray radiation into the trains of sub-fs pulses. High frequency of radiation implies using a plasma of hydrogen-like ions. Plasma dispersion results in increase of the phase velocity of an IR field with respect to the X-ray

field. As a result, the phase shifts between the neighboring sidebands determined by the phase difference between X-ray and IR field varies with the propagation distance. As a result the sidebands formed at different points of medium become out of phase with each other, which increases the pulse duration. Obviously, it leads to a trade-off between pulse duration and efficiency.

Let us consider possible experimental realization of this technique for transformation of quasi-monochromatic x-ray radiation (i) with a frequency in the vicinity of 13.5nm in LiIII and (ii) with a frequency in the vicinity of 4nm in CVI into a train of sub-fs pulses and determine its limiting possibilities in terms of the achievable pulse duration and transformation efficiency, taking into account the effect of the plasma dispersion.

In the case of Li III (i.e. Li^{2+}) ions we consider the concentrations of ions and electrons to be equal $N = 1.5 \times 10^{17} cm^{-3}, n_e = 2N$ at ion temperature ~1 eV and electron temperature ~2eV. (These parameters are chosen to be the same as in the case of active plasma, considered in the next section, for convenient comparison of passive and active cases. In its turn, the parameters for an active plasma are chosen to be close with those used in experimental realization of recombination laser at 2p-1s transition in LIII [87]). The relaxation times (which are inverse of decay rates) under such plasma parameters are estimated as: $\tau_{collision} \approx 0.425 ps, \tau_{radiative} \approx 19.7 ps$. In the case of CVI (i.e. C^{5+}) ions we consider the concentrations of ions N= $1 \times 10^{17} cm^{-3}$ and $5N$ electrons at ion temperature ~3 eV and electron temperature ~5 eV. The relaxation times are $\tau_{collision} \approx 0.56 ps, \tau_{radiative} \approx 1.23 ps$.

The plasma dispersion destroys the pulses after some critical length L_{crit}, when the phase difference between neighboring sidebands phase shifts formed at the entrance and at the exit of medium becomes on the order of π.: $\Omega L_{crit}(1-n_{plasma})/c \sim \pi$. (An estimate of this critical length in Li III gives L_{crit} =2 mm and in CVI L_{crit} =4.5 mm.) Thus, in order to achieve the shortest possible duration of pulses, the condition $\Omega L(1-n_{plasma}) \le \pi c$ needs to be satisfied. For $n_{plasma} \approx 1, \Omega(1-n_{plasma}) \sim 1/\Omega$ and decreases linearly with increasing Ω. On the other hand, in order to form sidebands with amplitudes comparable with the amplitude of the incident field, the effective optical thickness of the medium with physical length L should be on the order of 1. Since effective optical thickness of the medium is inversely proportional to decay rate and decay rate grows exponentially with increasing Ω when index of modulation P_ω is fixed, the required physical length L grows approximately exponentially with increasing Ω. Thus, requirement $\Omega L(1-n_{plasma}) \le \pi c$ limits from the below the wavelength of the modulating laser. For the considered Li III and C VI ions, it implies wavelength of the IR field larger than approximately 1400 nm for Li III and 400 nm for C VI. The minimum possible wavelength of a modulating laser, in its turn, for the fixed modulation index, determines the minimum pulse duration to be achieved. The minimum achievable pulse duration can be estimated as half of period of an IR field divided by the number of sidebands of comparable amplitudes. For the above wavelengths and P_ω= 4.45, the estimate gives 330 as in Li III and 100 as in C VI.

An estimate of intensity of the driving field required to realize a modulation index P_ω=4.45 for those wavelength gives $I_\Omega = 7.3\times10^{14} W/cm^2$ and $I_\Omega = 3.6\times10^{16} W/cm^2$ for LiIII and CVI accordingly.

For considered mechanism of the pulses formation the ionization rate should satisfy the condition $\Gamma_{ion} \ll \Omega$ in order the upper levels would not be depleted by tunneling ionization in the interval between the neighboring maxima of a modulating field. For chosen parameters of a modulating field this condition is fulfilled.

A frequency of an incident X-ray field is chosen to be shifted from the resonant unperturbed by an IR field transition by a magnitude of the quadratic Stark shift. At the chosen field intensities of an IR field this shift is equal to 0.16eV in LiIII and 0.56eV in CVI. A peak intensity of an incident X-ray field is chosen as $1\times10^{8} W/cm^2$.

The incident X-ray field envelope is chosen in the form:

$$\tilde{E}_z(x=0,t) = \tilde{E}_{z,0} f(t),$$
$$f(t) = \begin{cases} \sin^2\left(\dfrac{\pi t}{2t_{ramp}}\right), & 0 < t < t_{ramp} \\ 1, & t_{ramp} < t < T - t_{ramp} \\ \sin^2\left(\dfrac{\pi(T-t)}{2t_{ramp}}\right), & T - t_{ramp} < t < T \end{cases}, \qquad \text{(VII.12)}$$

where $t_{ramp} = 25\,fs$, while T =350 fs for Li III and 250 fs for C VI (see Figure 34 (a) and Figure 35 (a)). Its duration is a chosen to be the on same order of magnitude as decay time. Such field can be produced by X-ray plasma laser seeded with a single high harmonic radiation [159,160] or by x-ray free-electron laser.

The numerical solution of the Eqns. (VII.1), (VII.7), (VII.8), (VII.10) for the described above set of the parameters shows that trains of pulses with duration of 490 as could be formed in Li III plasma and trains of pulses with duration of 120 as could be formed in C VI plasma. Efficiency of transformation, defined as ratio of incident X-ray field energy to output field energy, for the propagation length 0.6 mm in LiIII is 67 % and for the propagation length of 1.0 mm in C VI is 72 %.

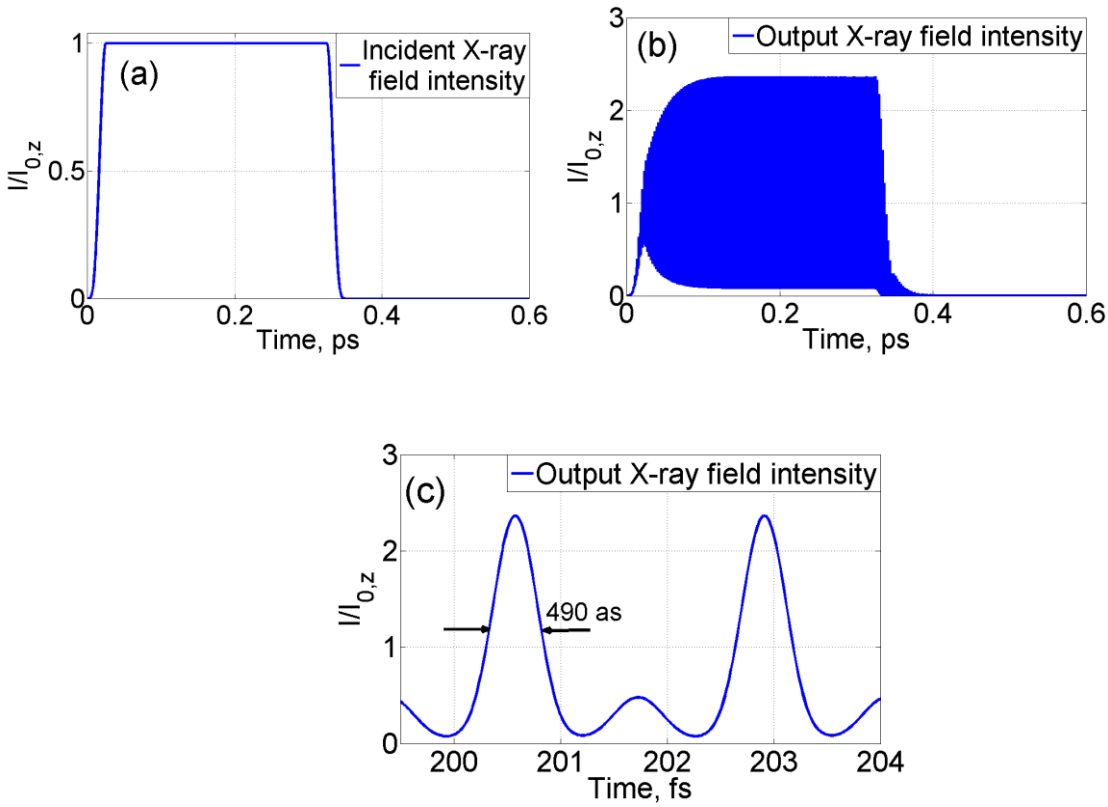

Figure 34. Time-dependence of an X-ray radiation intensity. (a) Incident X-ray field, (b) Output field. (c) The same as (b), but showing only a small part of the whole envelope). The parameters of the Li III plasma, an IR field and an incident XUV field are provided in the text of the paper.

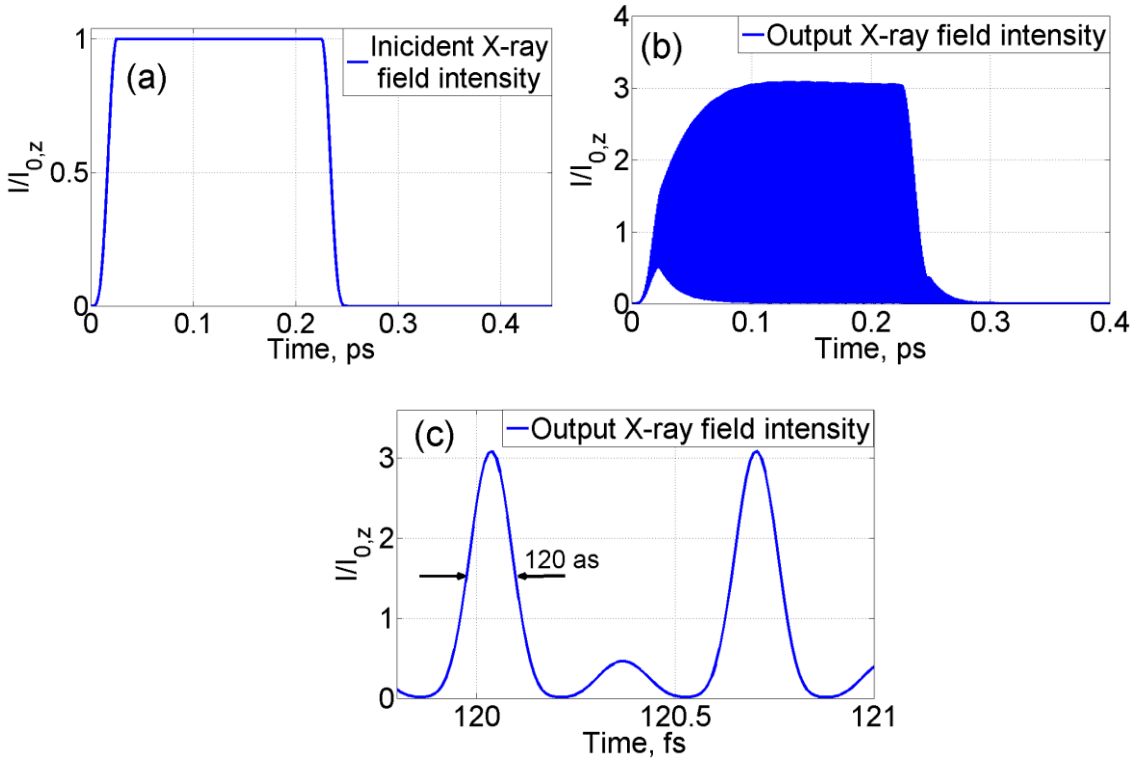

Figure 35. Time-dependence of an X-ray radiation intensity. (a) Incident X-ray field. (b) Output field. (c) The same as (b), but showing only a small part of the whole envelope. The parameters of the C VI plasma, an IR field and an incident XUV field are provided in the text of the paper.

VII.4 Amplification of an individual high harmonic radiation with its simultaneous transformation into the train of attosecond pulses in an active medium of hydrogen-like recombination X-ray plasma lasers modulated by an IR laser field

In this section we study the possibility of amplification of a relatively weak incident X-ray radiation produced by a single high-harmonic generation in the inverted hydrogen-like medium accompanied by attosecond pulses formation due to modulation of an inverted transition by moderately strong quasi-monochromatic IR pulse.

Similar to the case of passive medium, let us consider the possibility of realization of the suggested technique in Li III and C VI with the same parameters of the plasma as

in the passive medium, but under assumption that all ions are fully inverted. It is worth noting that lasing on the considered transition in Li III was theoretically studied [161] and experimentally demonstrated [87]. The chosen above parameters closely correspond to those at which X-ray lasing was realized [87]. An inversion at the operating transition was achieved via fast three-body recombination process in the presence of intense laser pumping. Lasing at the considered transition in C V was theoretically predicted by Princeton's group [77] and currently is studied experimentally by the same group.

As it was discussed in the previous section the pulses duration scales as $1/\Omega$ with IR field frequency. Thus, increasing modulating field frequency might lead to formation of shorter pulses. However, there is a physical limit to it. Namely, keeping of the same modulation index $P_\omega = \frac{d_{av}\tilde{E}_{IR}}{\Omega}$ requires an increase in the IR field intensity with an increase of Ω, which leads to faster ionization of population of the excited levels of ions and vanishing of amplification for X-ray field. The ionization rate from excited states Γ_{ion} grows exponentially with IR field strength and, for $P_\omega = 4.45$, it reaches the magnitude of inverse incident X-ray pulse duration for IR wavelength of approximately 1660 nm in Li III and 440 nm in C VI. With further decrease of IR field wavelength, the extremely large ionization rate leads to fast depletion of excited levels of atom and pulses amplification becomes impossible. This sets the lower limit for the formed pulses duration via this technique in an active medium.

We consider dressing of Li III ions by quasi-monochromatic 1900 nm IR field with intensity $4\times10^{14} W/cm^2$ and driving of CVI ions by a quasi-monochromatic 500 nm laser

field with intensity $2.3\times10^{16}W/cm^2$. The chosen parameters both in LiIII and CVI correspond to the value of a modulation index $P_\omega = 4.45$.

Eqns. (VII.1), (VII.7), (VII.8), (VII.11) are numerically solved for the chosen parameters. Contrary to the case of a passive medium where all sidebands were in phase with respect each other as well as with resonant component (since an incident field dominated an anti-phased resonant scattering component), in an active medium there is a significant phase difference between spectral components of X-ray field for $P_\omega = 4.45$. The plasma dispersion allows to compensate this phase shift at the specific lengths of the medium. As a result well shaped amplified trains of attosecond pulses can be formed at the optimal length of the medium. A train of 960 as pulses with peak intensity about 20 times higher than a peak intensity of the incident pulse can be formed at the length $L = 1.25mm$ in Li III (Figure 36). A train of 290 as pulses with peak intensity about 10 times higher than a peak intensity of an incident field can be formed at the length $L = 2.7mm$ (Figure 37).

More general case when incident field consists of both z- and y-polarized components and a saturation of the 4-1 and 5-1 transition by y-polarized field takes place is studied in Appendix D. It is shown, that a presence of strongly amplified y-polarized component of an X-ray field does not produce any essential effect on amplification of a seed z-polarized pulse. It is due to the fact that this amplification originates from different populated excited states, the duration of an seed incident pulse is shorter than the gain duration while the peak of a strongly amplified y-polarized component delays as compared to a seeded pulse due to the superradiant character of a y-polarized field amplification.

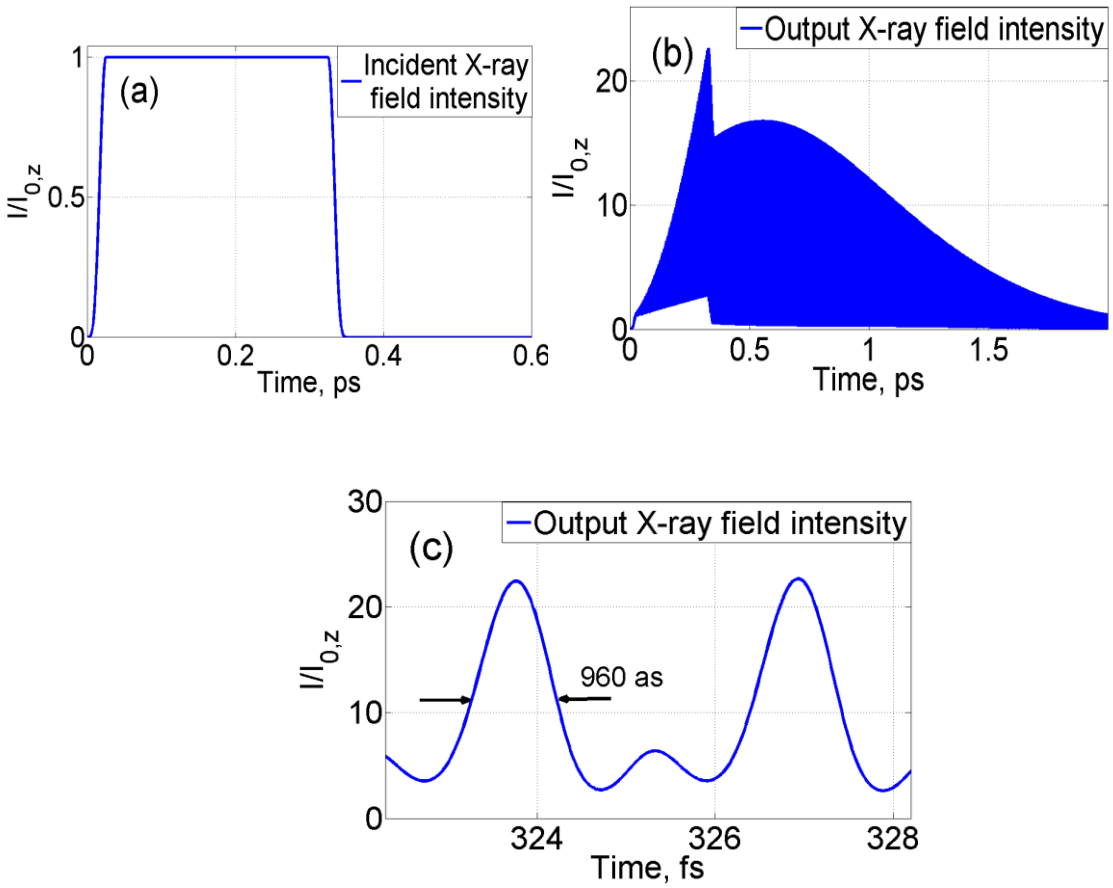

Figure 36. Time-dependence of an X-ray radiation intensity. (a) Incident X-ray field, (b) Output field. (c) The same as (b), but showing only a small part of the whole envelope). The parameters of the inverted Li III plasma, an IR field and an incident XUV field, provided in the text of the paper. An abrupt decrease in amplification at about 350 fs duration is due to the shortness of a seed pulse duration compared to the gain duration.

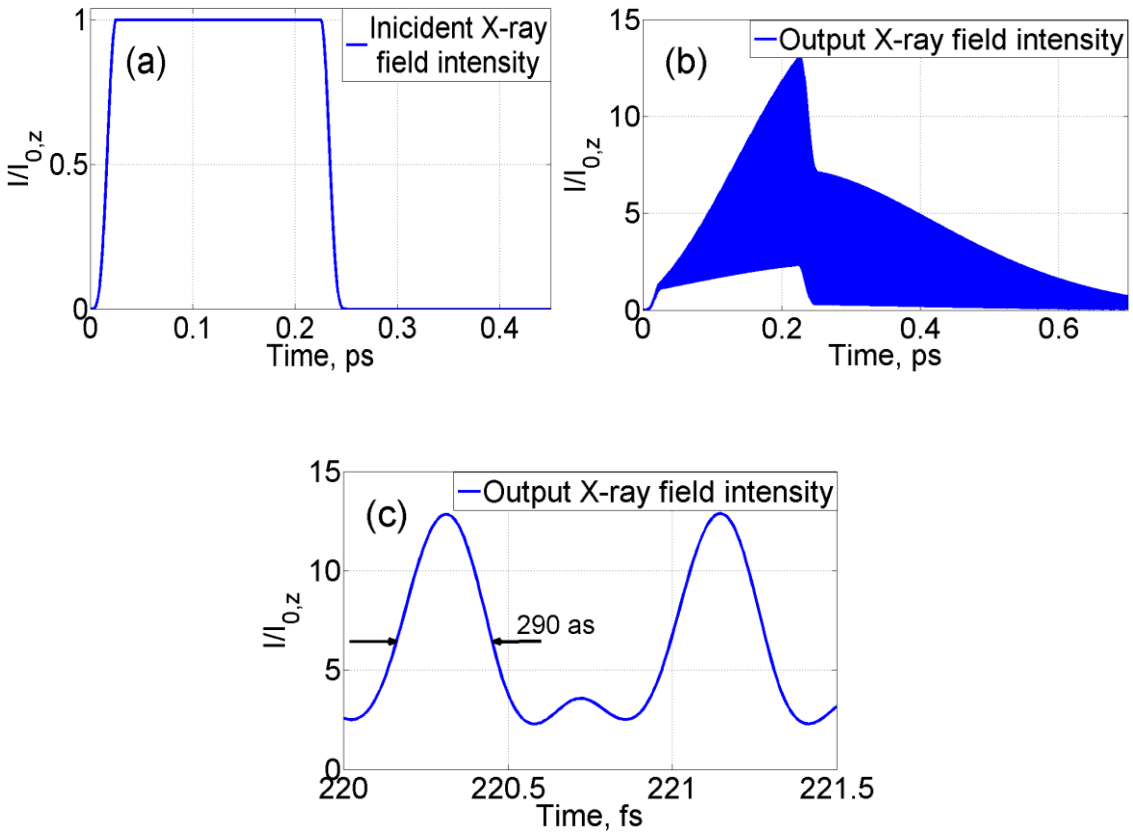

Figure 37. Time-dependence of an X-ray radiation intensity. (a) Incident X-ray field, (b) Output field. (c) The same as (b), but showing only a small part of the whole envelope). The parameters of the inverted CVI plasma, an IR field and an incident XUV field are provided in the text of the paper. An abrupt decrease in amplification at about 250 fs duration is due to the shortness of a seed pulse duration compared to the gain duration.

VII.5 Conclusion

We studied two different paths on the way to producing of intense coherent sub-fs X-ray radiation: (i) via efficient temporal compression of intense x-ray lasers radiation into the trains of sub-fs pulses and (ii) via amplification of the single high harmonic radiation accompanied by formation of sub-fs pulses. We have shown that both paths can be implemented by using the same technique, namely, via interaction of x-ray radiation with a plasma of the hydrogen-like ions with a modulated resonant transition. The first

path implies using of non-inverted medium, while the second path requires using of an inverted medium.

Since a limitation on the maximum intensity of the modulated field (and accordingly minimum modulation frequency for given modulation index) turns out to be less stringent in the passive medium with respect to an active medium, shorter pulses can achieved via the first path.

It would be interesting to extend the obtained results to the wider range of ions, i.e. to the case of non-hydrogen like ions. Indeed, in the case of non-hydrogen-like ions dressing by an IR field is not reduced to a shift and modulation of the frequency if an excited state. However, it results in an effective modulation of the dipole moment of the effective dressed transition [90] which, it was shown also allows for very efficient transformation of a few hundred fs radiation of X-ray lasers into the trains of sub-fs pulses in a passive medium of He or He-like ions [162]. One may expect that similar results can be obtained also in the active medium.

Another interesting extension of this work would be a seeding of an X-ray laser with a set of high harmonics rather than a single harmonic. Indeed, modulation of an active medium should allow for amplification of the whole set of harmonics within the linewidth of an active medium.

CHAPTER VIII

CONCLUSION

Interplay between relatively weak XUV and strong IR fields under their interaction with medium has been widely studied recently. Such studies aim on physical understanding of the corresponding processes, development of new coherent sources of XUV and X-ray radiation, determination of the medium characteristics, control of chemical reactions, ionization and conductivity, etc. Many interesting physical effects, for example, high harmonic generation, adiabatic Stark effect in the IR field, modification of the XUV absorption/gain profiles in the presence of an IR field, modulation of an ionization rate, etc. have been predicted and experimentally demonstrated.

In particular, the possibility to transfer the quasi-monochromatic XUV radiation into the trains of attosecond pulses in atomic hydrogen and hydrogen-like ions in the presence of an IR field was theoretically predicted in the previous works of our group on the bases of numerical calculations within three-level atomic model.

In this dissertation, I further developed and broadened this concept. Several goals were achieved.

The method of pulses formation was generalized and deeply studied both numerically and analytically. Namely, the approach based on modulation of the quasi-resonant excited atomic state by nonionizing IR field was generalized to non-hydrogen-like medium. For the regime of pulses formation based on interruption of the resonant interaction due to rapid excited-state tunneling ionization, the analytical solution was derived. Ultimate capabilities of both methods were studied numerically and an advanced

analytical solution describing the transition between two regimes was derived. All this work opens up straightforward way to experimental realization of the suggested technique.

A deep physical analogy between coherent forward scattering of γ-ray radiation in the vibrating quasi-resonant nuclear absorber and the XUV field propagation in the quasi-resonant atomic medium in the presence of the moderately strong IR field was established. It allows to conclude that some effects experimentally demonstrated in one system can be realized in the other one and vice versa. The experiment studying modulated induced transparency of the vibrating quasi-resonant nuclear absorber is currently being conducted by our group.

Finally, I suggested the new application of the proposed technique for producing of intense coherent attosecond sources of soft-X-ray radiation via two different paths, namely, (i) via efficient compression of picosecond radiation of x-ray plasma lasers into attosecond pulse trains without essential loss of the energy; (ii) via amplification of an individual high-harmonic radiation in an active medium of x-ray lasers accompanied by formation of attosecond pulses. Such pulses might find multiple applications in element specific microscopy and diffraction imaging in chemistry, biology and material science.

REFERENCES

[1] O. Kocharovskaya, Physics Reports **219**, 175 (1992).

[2] E. Arimondo, in *Progress in Optics*, edited by E. Wolf (Elsevier, 1996), pp. 257.

[3] S. E. Harris, Phys. Today **50** 36 (1997).

[4] M. O. Scully and M. S. Zubairy, *Quantum Optics* (Cambridge University Press, Cambridge, 1997).

[5] A. B. Matsko, O. kocharovskaya, Y. Rostovtsev, G. R. Welch, A. S. Zibrov, and M. O. Scully, in *Advances In Atomic, Molecular, and Optical Physics*, edited by B. Benjamin, and W. Herbert (Academic Press, 2001), pp. 191.

[6] M. Fleischhauer, A. Imamoglu, and J. P. Marangos, Rev. Mod. Phys. **77**, 633 (2005).

[7] M. D. Lukin, Reviews of Modern Physics **75**, 457 (2003).

[8] Y. Rostovtsev, O. Kocharovskaya, G. R. Welch, and M. O. Scully, Opt. Photon. News **13**, 44 (2002).

[9] D. Budker, W. Gawlik, D. F. Kimball, S. M. Rochester, V. V. Yashchuk, and A. Weis, Reviews of Modern Physics **74**, 1153 (2002).

[10] D. Budker, D. F. Kimball, S. M. Rochester, and V. V. Yashchuk, Physical Review Letters **83**, 1767 (1999).

[11] V. A. Sautenkov, M. D. Lukin, C. J. Bednar, I. Novikova, E. Mikhailov, M. Fleischhauer, V. L. Velichansky, G. R. Welch, and M. O. Scully, Physical Review A **62**, 023810 (2000).

[12] M. Jain, H. Xia, G. Y. Yin, A. J. Merriam, and S. E. Harris, Physical Review Letters **77**, 4326 (1996).

[13] C. Dorman and J. P. Marangos, Physical Review A **58**, 4121 (1998).

[14] A. J. Merriam, S. J. Sharpe, H. Xia, D. Manuszak, G. Y. Yin, and S. E. Harris, Optics Letters **24**, 625 (1999).

[15] M. D. Lukin, M. Fleischhauer, A. S. Zibrov, H. G. Robinson, V. L. Velichansky, L. Hollberg, and M. O. Scully, Physical Review Letters **79**, 2959 (1997).

[16] D. A. Braje, V. Balić, S. Goda, G. Y. Yin, and S. E. Harris, Physical Review Letters **93**, 183601 (2004).

[17] S. E. Harris and L. V. Hau, Physical Review Letters **82**, 4611 (1999).

[18] M. Fleischhauer and M. D. Lukin, Physical Review Letters **84**, 5094 (2000).

[19] D. F. Phillips, A. Fleischhauer, A. Mair, R. L. Walsworth, and M. D. Lukin, Physical Review Letters **86**, 783 (2001).

[20] C. Liu, Z. Dutton, C. H. Behroozi, and L. V. Hau, Nature **409**, 490 (2001).

[21] M. D. Eisaman, M. Fleischhauer, M. D. Lukin, and A. S. Zibrov, Opt. Photon. News **17**, 22 (2006).

[22] P. Ranitovic, X. M. Tong, C. W. Hogle, X. Zhou, Y. Liu, N. Toshima, M. M. Murnane, and H. C. Kapteyn, Phys. Rev. Lett. **106**, 193008 (2011).

[23] P. Ranitovic *et al.*, New J. Phys. **12**, 013008 (2010).

[24] M. Chini, X. Wang, Y. Cheng, Y. Wu, D. Zhao, D. A. Telnov, S. I. Chuandand, and Z. Chang, Sci. Rep. **3**, 1105 (2013).

[25] M. Chini, B. Zhao, H. Wang, Y. Cheng, S. X. Hu, and Z. Chang, Phys. Rev. Lett. **109**, 073601 (2012).

[26] M. Holler, F. Schapper, L. Gallmann, and U. Keller, Phys. Rev. Lett. **106**, 123601 (2011).

[27] C. Ott, A. Kaldun, P. Raith, K. Meyer, M. Laux, J. Evers, C. H. Keitel, C. H. Greene, and T. Pfeifer, Science **340**, 716 (2013).

[28] M. Swoboda *et al.*, Phys. Rev. Lett. **104**, 103003 (2010).

[29] A. N. Pfeiffer and S. R. Leone, Phys. Rev. A **85**, 053422 (2012).

[30] C. Buth, R. Santra, and L. Young, Phys. Rev. Lett. **98**, 253001 (2007).

[31] L. Yuan, D. Wang, A. A. Svidzinsky, H. Xia, O. Kocharovskaya, A. Sokolov, G. R. Welch, S. Suckewer, and M. O. Scully, Phys. Rev. A **89**, 013814 (2014).

[32] A. A. Svidzinsky, L. Yuan, and M. O. Scully, Phys. Rev. X **3**, 041001 (2013).

[33] K. J. Schafer, M. B. Gaarde, A. Heinrich, J. Biegert, and U. Keller, Phys. Rev. Lett. **92**, 023003 (2004).

[34] P. Johnsson, J. Mauritsson, T. Remetter, A. L'Huillier, and K. J. Schafer, Phys. Rev. Lett. **99**, 233001 (2007).

[35] N. Shivaram, H. Timmers, X. M. Tong, and A. Sandhu, Phys. Rev. Lett. **108**, 193002 (2012).

[36] S. Gilbertson, M. Chini, X. Feng, S. Khan, Y. Wu, and Z. Chang, Phys. Rev. Lett. **105**, 263003 (2010).

[37] V. A. Antonov, Y. V. Radeonychev, and O. Kocharovskaya, Phys. Rev. Lett. **110**, 213903 (2013).

[38] V. A. Antonov, Y. V. Radeonychev, and O. Kocharovskaya, Phys. Rev. A **88**, 053849 (2013).

[39] Y. V. Radeonychev, V. A. Antonov, and O. A. Kocharovskaya, Laser Physics **23**, 085303 (2013).

[40] V. A. Antonov, T. R. Akhmedzhanov, Y. V. Radeonychev, and O. Kocharovskaya, Phys. Rev. A **91**, 023830 (2015).

[41] Y. V. Radeonychev, V. A. Polovinkin, and O. Kocharovskaya, Phys. Rev. Lett. **105**, 183902 (2010).

[42] V. A. Polovinkin, Y. V. Radeonychev, and O. Kocharovskaya, Opt. Lett. **36**, 2296 (2011).

[43] D. Attwood, *Soft X-Rays and Extreme Ultraviolet Radiation: Principles and Applications* (Cambridge University Press, 2007).

[44] J. J. Rocca, Rev. Sci. Instrum. **70**, 3799 (1999).

[45] H. Daido, Reports on Progress in Physics **65**, 1513 (2002).

[46] S. Suckewer and P. Jaegle, Laser Phys. Lett. **6**, 411 (2009).

[47] M. Nishikino and T. Kawachi, Nat Photon **8**, 352 (2014).

[48] B. A. Reagan *et al.*, in *Springer proceedings in physics;169*, edited by J. J. Rocca, C. Menoni, and M. Marconi (Springer, Cham, 2016), p. 11.

[49] I. Kuznetsov *et al.*, in *Springer proceedings in physics;169*, edited by J. J. Rocca, C. Menoni, and M. Marconi (Springer, Cham, 2016), p. 225.

[50] Y. Luo, A. Morozov, D. Gordon, P. Sprangle, A. Svidzinsky, H. Xia, M. Scully, and S. Suckewer, in *Springer proceedings in physics;169*, edited by J. J. Rocca, C. Menoni, and M. Marconi (Springer, Cham, 2016), p. 21.

[51] O. Guilbaud *et al.*, in *Springer proceedings in physics;169*, edited by J. J. Rocca, C. Menoni, and M. Marconi (Springer, Cham, 2016), p. 61.

[52] P. Agostini and L. F. DiMauro, Reports on Progress in Physics **67**, 813 (2004).

[53] A. Scrinzi, M. Y. Ivanov, R. Kienberger, and D. M. Villeneuve, Journal of Physics B: Atomic, Molecular and Optical Physics **39**, R1 (2006).

[54] P. B. Corkum and F. Krausz, Nat. Phys. **3**, 381 (2007).

[55] E. Goulielmakis, V. S. Yakovlev, A. L. Cavalieri, M. Uiberacker, V. Pervak, A. Apolonski, R. Kienberger, U. Kleineberg, and F. Krausz, Science **317**, 769 (2007).

[56] F. Krausz and M. Ivanov, Reviews of Modern Physics **81**, 163 (2009).

[57] L. Gallmann, C. Cirelli, and U. Keller, Annual Review of Physical Chemistry **63**, 447 (2012).

[58] P. Salières, A. Maquet, S. Haessler, J. Caillat, and R. Taïeb, Reports on Progress in Physics **75**, 062401 (2012).

[59] M. Chini, K. Zhao, and Z. Chang, Nat Photon **8**, 178 (2014).

[60] R. Pazourek, S. Nagele, and J. Burgdörfer, Reviews of Modern Physics **87**, 765 (2015).

[61] D. Fabris *et al.*, Nat. Photonics **9**, 383 (2015).

[62] B. J. MacGowan *et al.*, Physical Review Letters **65**, 420 (1990).

[63] P. W. Wachulak, A. Bartnik, H. Fiedorowicz, P. Rudawski, R. Jarocki, J. Kostecki, and M. Szczurek, Nucl. Instr. Meth. B **268**, 1692 (2010).

[64] M. Zepf, B. Dromey, M. Landreman, P. Foster, and S. M. Hooker, Physical Review Letters **99**, 143901 (2007).

[65] T. Popmintchev *et al.*, Science **336**, 1287 (2012).

[66] D. Popmintchev *et al.*, Science **350**, 1225 (2015).

[67] M.-C. Chen, P. Arpin, T. Popmintchev, M. Gerrity, B. Zhang, M. Seaberg, D. Popmintchev, M. M. Murnane, and H. C. Kapteyn, Phys. Rev. Lett. **105**, 173901 (2010).

[68] J. Li, X. Ren, Y. Yin, Y. Cheng, E. Cunningham, Y. Wu, and Z. Chang, Applied Physics Letters **108**, 231102 (2016).

[69] V. Ayvazyan *et al.*, The European Physical Journal D - Atomic, Molecular, Optical and Plasma Physics **37**, 297 (2006).

[70] W. Ackermann *et al.*, Nature Photonics **1**, 336 (2007).

[71] C. Bostedt *et al.*, Journal of Physics B: Atomic, Molecular and Optical Physics **46**, 164003 (2013).

[72] LINAC Coherent Light Source, SLAC National Accelerator Laboratory, https://lcls.slac.stanford.edu/, (Accessed 02/01/2017).

[73] SACLAXFEL, X-ray Free Electron Laser, http://xfel.riken.jp/eng/, (Accessed 02/01/2017).

[74] DESY-FLASH Free Electron Laser FLASH, Deutsches Elektronen-Synchrotron, https://flash.desy.de/, (Accessed 02/01/2017).

[75] Elettra Sincrotrone Trieste, Elettra-Sincrotrone Trieste S.C.p.A. di interesse nazionale, https://www.elettra.trieste.it/lightsources/fermi.html, (02/01/2017).

[76] SPring-8-II Conceptual Design Report, 2014.

[77] Y. Avitzour and S. Suckewer, J. Opt. Soc. Am. B **24**, 819 (2007).

[78] B. A. Reagan, M. Berrill, K. A. Wernsing, C. Baumgarten, M. Woolston, and J. J. Rocca, Phys. Rev. A **89**, 053820 (2014).

[79] A. Cavalleri, M. Rini, H. H. W. Chong, S. Fourmaux, T. E. Glover, P. A. Heimann, J. C. Kieffer, and R. W. Schoenlein, Phys. Rev. Lett. **95**, 067405 (2005).

[80] K. Hoffmann, B. Murphy, B. Erk, A. Helal, N. Kandadai, J. Keto, and T. Ditmire, High Energ. Dens. Phys. **6**, 185 (2010).

[81] L. Yue and L. B. Madsen, Phys. Rev. Lett. **115**, 033001 (2015).

[82] S. Mathias, M. Bauer, M. Aeschlimann, L. Miaja-Avila, H. C. Kapteyn, and M. M. Murnane, in *Dynamics at Solid State Surfaces and Interfaces: Current Developments*, edited by U. Bovensiepen, H. Petek, and M. Wolf (Wiley-VCH Verlag GmbH & Co. KGaA, Weinheim, Germany, 2010), pp. 501.

[83] P. M. Paul, E. S. Toma, P. Breger, G. Mullot, F. Auge, P. Balcou, H. G. Muller, and P. Agostini, Science **292**, 1689 (2001).

[84] K. Zhao, Q. Zhang, M. Chini, Y. Wu, X. Wang, and Z. Chang, Opt. Lett. **37**, 3891 (2012).

[85] S. Schreiber, in *33rd International Free Electron Laser Conference*, edited by Z. Zhao, and D. Wang (SINAP, Shanghai, China, 2011), p. 164.

[86] C. Pellegrini *et al.*, Nucl. Instr. Meth. A **321**, 223 (1993).

[87] D. V. Korobkin, C. H. Nam, S. Suckewer, and A. Goltsov, Phys. Rev. Lett. **77**, 5206 (1996).

[88] S. I. Chu and D. A. Telnov, Phys. Rep. **390**, 1 (2004).

[89] S. H. Autler and C. H. Townes, Phys. Rev. **100**, 703 (1955).

[90] T. R. Akhmedzhanov, V. A. Antonov, and O. Kocharovskaya, J. Phys. B: At. Mol. Opt. Phys. **49**, 205602 (2016).

[91] N. Kaiser, S. Yulin, M. Perske, and T. Feigl, Proc. SPIE **7101**, 71010Z (2008).

[92] S. A. Bogachev, N. I. Chkhalo, S. V. Kuzin, D. E. Pariev, V. N. Polkovnikov, N. N. Salashchenko, S. V. Shestov, and S. Y. Zuev, Appl. Opt. **55**, 2126 (2016).

[93] X. M. Tong and S. I. Chu, Chem. Phys. **217**, 119 (1997).

[94] P.-C. Li, C. Laughlin, and S. I. Chu, Phys. Rev. A **89**, 023431 (2014).

[95] G. Demeter, Comput. Phys. Commun. **184**, 1203 (2012).

[96] R. A. Ganeev *et al.*, Phys. Rev. A **74**, 063824 (2006).

[97] R. A. Ganeev, in *High-order Harmonic Generation in Laser Plasma Plumes* (Imperial College Press, London, 2012), p. 46.

[98] W. L. Wiesse and J. R. Fuhr, J. Phys. Chem. Ref. Data **38**, 565 (2009).

[99] P. L. Shkolnikov and A. E. Kaplan, J. Opt. Soc. Am. B **9**, 2128 (1992).

[100] K. Lan, E. E. Fill, and J. Meyer-ter-Vehn, Europhys. Lett. **64**, 454 (2003).

[101] K. E. Lan, E. Fill, and J. Meyer-ter-Vehn, Laser Part. Beams **22**, 261 (2004).

[102] Y. Nagata, K. Midorikawa, S. Kubodera, M. Obara, H. Tashiro, and K. Toyoda, Phys. Rev. Lett. **71**, 3774 (1993).

[103] S. A. George, W. Silfvast, K. Takenoshita, R. Bernath, C.-S. Koay, G. Shimkaveg, and M. Richardson, Proc. SPIE **6151**, 615143 (2006).

[104] M. S. Dimitrijevic and S. Sahal-Bréchot, Phys. Scr. **54**, 50 (1996).

[105] N. Konjevic, Phys. Rep. **316**, 339 (1999).

[106] N. Shivaram, H. Timmers, X.-M. Tong, and A. Sandhu, Chem. Phys. **414**, 139 (2013).

[107] Y. V. Radeonychev, V. A. Polovinkin, and O. Kocharovskaya, Laser Physics **21**, 1243 (2011).

[108] Y. V. Radeonychev, V. A. Polovinkin, and O. A. Kocharovskaya, Laser Physics **22**, 1547 (2012).

[109] T. R. Akhmedzhanov, V. A. Antonov, O. Kocharovskaya, and unpublished.

[110] G. Andriukaitis, T. Balčiūnas, S. Ališauskas, A. Pugžlys, A. Baltuška, T. Popmintchev, M.-C. Chen, M. M. Murnane, and H. C. Kapteyn, Opt. Lett. **36**, 2755 (2011).

[111] V. V. Apollonov, P. B. Corkum, R. S. Taylor, A. J. Alcock, and H. A. Baldis, Optics Letters **5**, 333 (1980).

[112] V. S. Popov, Phys.-Usp. **47**, 855 (2004).

[113] R. J. Damburg and V. V. Kolosov, in *Rydberg States of Atoms and Molecules*, edited by R. F. Stebbings, and F. B. Dunning (Cambridge University Press, Cambridge, England, 1983).

[114] E. V. Vanin, A. V. Kim, A. M. Sergeev, and M. C. Downer, JETP Lett. **58**, 900 (1993).

[115] T. Brabec and F. Krausz, Physical Review Letters **78**, 3282 (1997).

[116] M. V. Frolov, N. L. Manakov, T. S. Sarantseva, M. Y. Emelin, M. Y. Ryabikin, and A. F. Starace, Physical Review Letters **102**, 243901 (2009).

[117] R. Loudon, *The quantum theory of light* (Clarendon Press, Oxford, 1994).

[118] M. Hentschel *et al.*, Nature **414**, 509 (2001).

[119] L. Gallmann, J. Herrmann, R. Locher, M. Sabbar, A. Ludwig, M. Lucchini, and U. Keller, Molecular Physics **111**, 2243 (2013).

[120] S. R. Leone *et al.*, Nat Photon **8**, 162 (2014).

[121] F. Krausz and M. I. Stockman, Nat Photon **8**, 205 (2014).

[122] A. H. Zewail, The Journal of Physical Chemistry A **104**, 5660 (2000).

[123] X. M. Tong, P. Ranitovic, C. L. Cocke, and N. Toshima, Phys. Rev. A **81**, 021404(R) (2010).

[124] E. J. Takahashi, P. Lan, O. D. Mücke, Y. Nabekawa, and K. Midorikawa, Nature Communications **4**, 2691 (2013).

[125] M. Chini *et al.*, Nat Photon **8**, 437 (2014).

[126] D. C. Yost, T. R. Schibli, J. Ye, J. L. Tate, J. Hostetter, M. B. Gaarde, and K. J. Schafer, Nature Phys. **5**, 815 (2009).

[127] R. A. Ganeev, L. B. Elouga Bom, T. Ozaki, and P. V. Redkin, Journal of the Optical Society of America B **24**, 2770 (2007).

[128] N. B. Delone and V. P. Krainov, Phys. Usp. **42**, 669 (1999).

[129] S. V. Popruzhenko, Journal of Physics B: Atomic, Molecular and Optical Physics **47**, 204001 (2014).

[130] Y. Mairesse *et al.*, Science **302**, 1540 (2003).

[131] P. Tzallas, E. Skantzakis, L. A. A. Nikolopoulos, G. D. Tsakiris, and D. Charalambidis, Nat Phys **7**, 781 (2011).

[132] O. J. Luiten, H. G. C. Werij, M. W. Reynolds, I. D. Setija, T. W. Hijmans, and J. T. M. Walraven, Applied Physics B **59**, 311 (1994).

[133] C. E. M. Strauss and D. J. Funk, Optics Letters **16**, 1192 (1991).

[134] L. Benassi and V. Grecchi, Journal of Physics B: Atomic and Molecular Physics **13**, 911 (1980).

[135] V. V. Kolosov, Journal of Physics B: Atomic and Molecular Physics **16**, 25 (1983).

[136] G. L. Yudin and M. Y. Ivanov, Physical Review A **64**, 013409 (2001).

[137] D. Bauer and P. Mulser, Physical Review A **59**, 569 (1999).

[138] X. M. Tong and C. D. Lin, J. Phys. B: At. Mol. Opt. Phys. **38**, 2593 (2005).

[139] S. L. Ruby and D. I. Bolef, Phys. Rev. Lett. **5**, 5 (1960).

[140] P. Helistö, E. Ikonen, and T. Katila, Phys. Rev. B **34**, 3458 (1986).

[141] Y. V. Shvyd'ko and G. V. Smirnov, J. Phys.: Condens. Matter **4**, 2663 (1992).

[142] F. Vagizov, V. Antonov, Y. V. Radeonychev, R. N. Shakhmuratov, and O. Kocharovskaya, Nature **508**, 80 (2014).

[143] R. N. Shakhmuratov, F. G. Vagizov, V. A. Antonov, Y. V. Radeonychev, M. O. Scully, and O. Kocharovskaya, Phys. Rev. A **92**, 023836 (2015).

[144] Y. V. Radeonychev, M. D. Tokman, A. G. Litvak, and O. Kocharovskaya, Phys. Rev. Lett. **96**, 093602 (2006).

[145] C. Buth and R. Santra, Phys. Rev. A **75**, 033412 (2007).

[146] Z.-H. Loh, C. H. Greene, and S. R. Leone, Chem. Phys. **350**, 7 (2008).

[147] X. M. Tong and N. Toshima, Phys. Rev. A **81**, 063403 (2010).

[148] S. Chen, K. J. Schafer, and M. B. Gaarde, Opt. Lett. **37**, 2211 (2012).

[149] W.-C. Chu, S.-F. Zhao, and C. D. Lin, Phys. Rev. A **84**, 033426 (2011).

[150] M. D. Crisp, Phys. Rev. A **1**, 1604 (1970).

[151] Y. Kagan, A. M. Afanas'ev, and V. G. Kohn, J. Phys. C: Solid State Phys. **12**, 615 (1979).

[152] N. Moiseyev, *Non-Hermitian Quantum Mechanics* (Cambridge University Press, New York, 2011).

[153] H. O. Karlsson, J. Chem. Phys., 9366 (1998).

[154] C. Buth and R. Santra, Phys. Rev. A **78**, 043409 (2008).

[155] M. F. Kling and M. J. J. Vrakking, Annu. Rev. Phys. Chem. **59**, 463 (2008).

[156] V. A. Polovinkin, *PhD Thesis* (Institure of Applied Physics of the Russian Academy of Sciences, Nizhny Novgrod, Russia, 2012), Vol. PhD

[157] A. Kramida, Y. Ralchenko, J. Reader, and NIST ASD Team (2015), (NIST Atomic Spectra Database (ver. 5.3), [Online]. Available: http://physics.nist.gov/asd [2017, January 1], National Institute of Standards and Technology, Gaithersburg, MD.

[158] H. R. Griem, *Spectral line broadening by plasmas* (Academic Press, New York, 1974).

[159] P. Zeitoun *et al.*, Nature **431**, 426 (2004).

[160] A. Depresseux *et al.*, Physical Review Letters **115**, 083901 (2015).

[161] Y. Avitzour and S. Suckewer, Journal of the Optical Society of America B **23**, 925 (2006).

[162] T. R. Akhmedzhanov, V. A. Antonov, and O. Kocharovskaya, Phys. Rev. A **94**, 023821 (2016).

[163] B. H. Bransden and C. J. Joachain, *Physics of Atoms and Molecules* (Prentice Hall, New York, 2003), 2nd edn.

APPENDIX A

TRANSFORMATION OF ELECTROMAGNETIC FIELD DURING ITS PROPAGATION THROUGH TWO-LEVEL MEDIUM WITH HARMONICALLY MODULATED PARAMETERS OF THE RESONANT TRANSITION [8]

In this appendix we consider a particular case of harmonic modulation of the atomic transition frequency and decoherence rate,

$$\begin{cases} \omega_{21}(\tau) = \bar{\omega}_{21} + \Delta_\omega \cos(\Omega\tau + \varphi_M), \\ \gamma_{21}(\tau) = \bar{\gamma}_{21} + \Delta_\gamma \cos(\Omega\tau + \varphi_M). \end{cases} \tag{A.1}$$

In this case Eq. (VI.21), describing transformation of the HF field as a result of its propagation through the medium, takes the form

$$\tilde{E}_{out,lab} = \sum_n \tilde{E}_n \exp\{-\mathrm{i}n\Omega\tau\} + \left(\sum_n \tilde{E}_n e^{\mathrm{i}n\varphi_M} \sum_j \mathrm{i}^j I_j(P_\gamma) J_{j+n}(P_\omega) \right) \times$$
$$\times (e^{-\alpha_B L/2} - 1) \sum_{k,m=-\infty}^{+\infty} \mathrm{i}^m I_m(P_\gamma) J_k(P_\omega) \mathrm{e}^{\mathrm{i}(m-k)(\Omega\tau+\varphi_M)}. \tag{A.2}$$

Here $P_\omega = \Delta_\omega/\Omega$ and $P_\gamma = \Delta_\gamma/\Omega$ are modulation indices of the atomic transition frequency and the decoherence decay rate, respectively. Modulation indices are defined as amplitudes of modulation of the transition frequency/decoherence rate, normalized to the frequency of modulation. $J_n(P_\omega)$ and $I_n(P_\gamma)$ are the Bessel function and the modified Bessel function of the first kind of an order *n*.

---

[8] Reprinted with permission from "Coherent forward scattering of gamma-ray and XUV radiation in the medium with the modulated quasi-resonant transition" by T.R. Akhmedzhanov, V.A. Antonov and O. Kocharovskaya, 2016, J. Phys. B: At. Mol. Opt. Phys., vol. 49**,** pp. 205602, Copyright [2016] by IOP Publishing.

The MIT condition for the monochromatic incident field, $a_n = 0$ is given by an equality

$$\sum_n \mathrm{i}^n I_n(P_\gamma) J_n(P_\omega) = 0. \tag{A.3}$$

In this case, the transparency condition is insensitive to the phase of modulation (A.1), φ_M, and is solely determined by the values of the modulation indices. In particular, if only the frequency of transition is modulated (P_γ =0), transparency takes place for $J_n(P_\omega) = 0$. For $n = 0$ transparency occurs when $P_\omega = 2.40, 5.52, ...$

In the case of a bichromatic incident radiation, $\tilde{E}(z=0,t) = \tilde{E}_0 + \tilde{E}_k \exp\{-\mathrm{i}k\Omega t\}$, and harmonic modulation of the atomic transition frequency and/or decoherence rate (A.1), MIT condition (VI.22) takes the form

$$\tilde{E}_0 \sum_n \mathrm{i}^n I_n(P_\gamma) J_n(P_\omega) + \tilde{E}_k \exp(\mathrm{i}k\varphi_M) \sum_n \mathrm{i}^n I_n(P_\gamma) J_{n+k}(P_\omega) = 0. \tag{A.4}$$

If only the frequency of transition is modulated the Eq. (VI.25) takes the form:

$$\tilde{I}(x) = \frac{c}{8\pi}\left(\left|\tilde{E}_0\right|^2 + \left|\tilde{E}_k\right|^2 - \left|\tilde{E}_0 J_0(P_\omega) + \tilde{E}_k \exp(\mathrm{i}k\varphi_M) J_k(P_\omega)\right|^2 \left(1 - \exp(-\alpha x)\right)\right) \tag{A.5}$$

and the MIT condition (A.4) reduces to

$$\tilde{E}_0 J_0(P_\omega) + \tilde{E}_k \exp(\mathrm{i}k\varphi_M) J_k(P_\omega) = 0. \tag{A.6}$$

Unlike the case of the monochromatic incident field, for the bichromatic radiation, the MIT is highly sensitive on the phase difference between the relative phase of the resonant spectral components of the incident effective field (i.e. resonant spectral components of the elastically and inelastically scattered fields) and the modulation phase φ_M. In general, an interference term in (A.5) results in a periodic variation of the

transmitted radiation as a function of the modulation phase φ_M. The ratio of spectral components amplitudes of an effective incident field at the given modulation amplitude determines a range of such variation, i.e. the maximum and minimum values of the resonant absorption. When MIT condition (A.6) is fulfilled, the minimum value reaches zero, corresponding to fully destructive interference of the resonant components of the effective fields (i.e. resonant spectral components of the elastically and inelastically scattered fields).

APPENDIX B

MULTI-LEVEL ATOMS COUPLED TO IR FIELD: PERTURBATION THEORY AND AN EFFECTIVE TWO-LEVEL MODEL WITH MODULATED PARAMETERS OF THE RESONANT TRANSITION [9]

In this appendix we consider the case of a relatively weak IR field $E_{IR}(x,t) = \tilde{E}_{IR}\cos(\omega_{IR}t - kx)$, which is far-off-resonance with any atomic transition from both the ground, $|1\rangle$, and excited, $|2\rangle$, states, so that the ground state is unperturbed by the IR field and the following conditions are satisfied:

$$\left| \frac{d_{k2}\tilde{E}_{IR}}{2\hbar} / (\omega_{IR} \pm \omega_{k2}) \right| \ll 1, k \in N, k \neq 2, \tag{B.1}$$

where d_{k2} and ω_{k2} are the dipole moment and the frequency of atomic transition between the states $|k\rangle$ and $|2\rangle$, respectively. Eq. (B.1) means that the IR field is not too strong, so that most of the initial population of the state $|2\rangle$ remains in this state at every moment of time. When the conditions (B.1) are fulfilled, and ionization from the state $|2\rangle$ by the IR field is negligible, space-time modulation of state $|2\rangle$ is correctly described by the second-order perturbation theory. In such a case, atomic wave function may be written as [25,163]:

$$|\psi\rangle \approx c_1|1\rangle + c_2 \exp\left(-i\bar{E}_2\tau\right)\left(1 + a_2\exp(-2i\omega_{IR}\tau) + a_{-2}\exp(2i\omega_{IR}\tau)\right)|2\rangle + \ldots, \tag{B.2}$$

---

[9] Reprinted with permission from "Coherent forward scattering of gamma-ray and XUV radiation in the medium with the modulated quasi-resonant transition" by T.R. Akhmedzhanov, V.A. Antonov and O. Kocharovskaya, 2016, J. Phys. B: At. Mol. Opt. Phys., vol. 49**,** pp. 205602, Copyright [2016] by IOP Publishing.

where omitted terms contain excited states other than the state $|2\rangle$, $\bar{E}_2 = E_2 - \frac{\tilde{E}_{IR}^2}{2\hbar}\sum_{k\neq 2}\frac{|d_{2k}|^2\omega_{k2}}{\omega_{k2}^2-\omega_{IR}^{\ 2}}$ is an energy of the state $|2\rangle$ that includes the constant Stark shift, $a_2 = \frac{\tilde{E}_{IR}^2}{8\hbar\omega_{IR}}\sum_{k\neq 2}\frac{|d_{2k}|^2}{\omega_{k2}^2-\omega_{IR}^{\ 2}}(\omega_{2k}-\omega_{IR})$, $a_{-2} = -\frac{\tilde{E}_{IR}^2}{8\hbar\omega_{IR}}\sum_{k\neq 2}\frac{|d_{2k}|^2}{\omega_{k2}^2-\omega_{IR}^{\ 2}}(\omega_{2k}+\omega_{IR})$. The amplitude of excitation of the state $|2\rangle$ by the XUV field (VI.1) is:

$$\begin{aligned} &c_2 \approx \frac{\mathrm{i}d_{21}}{\hbar}\int_{-\infty}^{\tau}\exp\left(\mathrm{i}\left(\bar{E}_2-\omega\right)\tau'\right)\times \\ &\times\left(1+a_2^{\ *}\exp(2\mathrm{i}\omega_{IR}\tau')+a_{-2}*\exp(-2\mathrm{i}\omega_{IR}\tau')\right)\tilde{E}_{XUV}(\tau')d\tau',, \\ &c_1 \approx 1 \end{aligned} \tag{B.3}$$

Accordingly, the resonant polarization of the medium is given by:

$$\begin{aligned} &\tilde{P}(\tau) \approx \frac{\mathrm{i}N|d_{21}|^2}{\hbar}e^{-\mathrm{i}\left(\bar{E}_2-\omega\right)\tau}\left(1+a_2\exp(-2\mathrm{i}\omega_{IR}\tau)+a_{-2}\exp(2\mathrm{i}\omega_{IR}\tau)\right)\times \\ &\int_{-\infty}^{\tau}\exp\left(\mathrm{i}\left(\bar{E}_2-\omega\right)\tau'\right)\left(1+a_2^{\ *}\exp(2\mathrm{i}\omega_{IR}\tau')+a_{-2}*\exp(-2\mathrm{i}\omega_{IR}\tau')\right)\tilde{E}_{XUV}(\tau')d\tau' \end{aligned} \tag{B.4}$$

.

It is worth noting, that the same polarization would be excited and described by Eqs. (VI.3)-(VI.5) if we consider propagation of the same XUV field through a medium of two-level atoms with the ground state $|1\rangle$, the excited state $|2\rangle$, the constant transition frequency $\bar{\omega}_{21} = \bar{E}_2/\hbar$ and , the effective space-time modulated dipole moment:

$$\tilde{d}_{21} = d_{21}\left(1+a_2^{\ *}\exp(2\mathrm{i}\omega_{IR}\tau)+a_{-2}*\exp(-2\mathrm{i}\omega_{IR}\tau)\right). \tag{B.5}$$

Thus, the interaction of the XUV field with the IR-dressed atoms is equivalent to the interaction of this field with the two-level atoms, possessing space-time modulated

dipole moments. Generally, both the phase and the absolute value of the dipole moment are modulated: $\tilde{d}_{21} = d_{21}\exp(-\int_{-\infty}^{\tau}\tilde{\gamma}(\tau')d\tau')\exp\left\{i\int_{-\infty}^{\tau}\Delta\omega_{21}(\tau')d\tau'\right\}$, where $\tilde{\gamma}(\tau)$ and $\Delta\omega_{21}(\tau)$ are real functions:

$$\begin{aligned}\tilde{\gamma}(\tau) &\approx -\frac{\tilde{E}_{IR}^2\omega_{IR}}{2\hbar}\sum_{k\neq 2}\frac{|d_{2k}|^2}{\omega_{k2}^2-\omega_{IR}{}^2}\sin(2\omega_{IR}\tau),\\ \Delta\omega_{21}(\tau) &\approx -\frac{\tilde{E}_{IR}^2}{2\hbar^2}\sum_{k\neq 2}\frac{|d_{2k}|^2\omega_{k2}}{\omega_{k2}^2-\omega_{IR}{}^2}\cos(2\omega_{IR}\tau).\end{aligned} \tag{B.6}$$

The phase modulation of the effective dipole moment, in its turn, is equivalent to the transition frequency modulation, i.e. calculation of polarization according to Eqs. (VI.3)-(VI.4), using $\omega_{21}(\tau) = \bar{E}_2/\hbar + \Delta\omega_{21}(\tau)$ and $\tilde{d}_{21} = d_{21}\exp(-\int\tilde{\gamma}(\tau')d\tau')$ gives the same result as using (B.5) and constant transition frequency $\bar{\omega}_{21} = \bar{E}_2/\hbar$. At the same time, it is worth to point out the modulation of the magnitude of dipole moment is not equivalent to the modulation of the decay rate of an effective dressed transition, i.e. calculation of polarization according Eqs.(VI.3)-(VI.4) using $\omega_{21}(\tau) = \bar{E}_2/\hbar + \Delta\omega_{21}(\tau)$ and $\gamma_{21}(\tau) = \tilde{\gamma}(\tau)$ does not give the same result as using the effective dipole moment, given by Eqs. (B.5). Hence, in a general case, the problem cannot be reduced to an interaction of the XUV field with the effective dressed two-level transition, possessing the modulated frequency and modulated decay rate.

In an adiabatic approximation, when the frequency of the IR field is much lower than the frequencies of transitions between the excited atomic states, the modulation of a magnitude of the dipole moment is negligible in comparison with the modulation of the

transition frequency, see Eq. (B.6). In such a case, an interaction of the XUV field with the IR-driven atoms is reduced to its interaction with the dressed two-level system with a space-time dependent transition frequency. The average frequency of the dressed transition and the modulation index are as follows:

$$\bar{\omega}_{21} = \omega_{21} - \frac{\tilde{E}_{IR}^2}{2\hbar^2} \sum_{k\neq 2} \frac{|d_{2k}|^2}{\omega_{k2}}, \tag{B.7}$$

$$P_\omega = \frac{\tilde{E}_{IR}^2}{4\hbar^2 \omega_{IR}} \left| \sum_{k\neq 2} \frac{|d_{2k}|^2}{\omega_{k2}} \right|. \tag{B.8}$$

Thus an IR field shifts the energy of an upper state and, the most importantly, periodically (in this case harmonically) modulates it. Propagation of an XUV field is described by the Eqs. (VI.3)-(VI.5) with $\Omega = 2\omega_{IR}$, $\omega_{21}(\tau)$, determined by the first Eq. in the set of Eqs. (A.1), where an average frequency and modulation amplitudes, $\bar{\omega}_{21}$ and $\Delta_\omega = 2\omega_{IR} P_\omega$, are defined by Eqs. (B.7) and (B.8) accordingly. If phase velocities of XUV and IR fields are almost equal to each other, so that the phase-matching condition (VI.10) is fulfilled, the analytical solutions (VI.12)-(VI.14) of these equations are directly applicable. Thus, the problem of propagation of the XUV field in multilevel atoms in the considered case becomes exactly equivalent to the problem of coherent forward scattering of γ-radiation analyzed in Section VI.3. In particular, for the monochromatic incident field, MIT implies $J_n(P_\omega) = 0$ (that is, $P_\omega = 2.40, 5.52, \ldots$ at resonant tuning), while for a bichromatic field MIT condition is given by Eq. (VI.22). As it was discussed above, the last condition corresponds to zero value of an effective field "seen" by unperturbed atoms or, equivalently, to zero value of excited resonant polarization caused by a destructive

interference of contributions from different spectral components via the elastic and inelastic (due to modulation) scattering processes.

It is worth to note, that the modulation index of the resonant transition is inversely proportional to the frequency of the IR field. Thus, lowering the modulation frequency results in a deeper modulation of the atomic transition. Physically, an atomic electron trajectory is perturbed by the force due to the electric field. This force is acting in one direction for a half of the field period, then switches its direction to the opposite one. As a result, in the lower frequency field the electron is experiencing the force acting in one direction for a longer time, which leads to a large deflection of an electron from a stationary orbit.

The experiment aimed on direct observation of such sub-laser-cycle harmonic modulation of the 1s3p and 1s4p energy levels of helium by means of the attosecond transient absorption spectroscopy was performed in [25]. It was the first demonstration of the sub-laser-cycle modulation of the Stark shift. At the same time, it should be noted, that the conditions for the validity of the perturbation theory, Eq. (B.1), were not fulfilled in that experiment, as it was already discussed in [24]. (The IR field was strong and close to the resonances between 1s3p, 1s4p, and the neighboring energy levels (1s2s, 1s3s, 1s3d, etc.), so the excited states were severely mixed, rather than slightly perturbed, by the laser radiation.)

It is worth to note that the harmonic modulation of energy of the excited 1s2p state of helium, taking place within the perturbation theory, can be directly observed if both lower frequency and lower intensity IR field is used, satisfying the conditions (B.1). An

example is the IR field with intensity $I = 3\times10^{11}\,\mathrm{W/cm^2}$ and wavelength $\lambda = 3.91\,\mu\mathrm{m}$ [110]. In this case, for the $1s^2 \leftrightarrow 1s2p$ transition of helium $|a_{-2}| \approx 0.06$. Let us further consider the case of the XUV radiation, consisting of the two high-order harmonics of the IR field, one of which is resonant to $1s^2 \leftrightarrow 1s2p$ transition of helium dressed by the IR field (with the unperturbed wavelength 58.4 nm), while the other one is detuned from the resonance by the doubled frequency of the fundamental field. In such a case, the slowly-varying amplitude of the XUV radiation is $\tilde{E} = \tilde{E}_0 \exp(i\varphi_0) + \tilde{E}_{-2} \exp(\mathrm{i}\varphi_{-2}) \exp(2\mathrm{i}\omega_{IR}\tau)$, where $\tilde{E}_0$ and $\tilde{E}_{-2}$ are the amplitudes of the resonant and off-resonant harmonics, respectively, while φ_0 and φ_{-2} are their phases. For 3.91 μm laser radiation, E_0 and E_{-2} correspond to the 67th and 65th harmonics, respectively. Amplitude of excitation of 1s2p state will be $c_{2p}(\tau) \sim \int_{-\infty}^{\tau} \left(a_0 \tilde{E}_0 \exp(\mathrm{i}\varphi_0) + a_{-2}\tilde{E}_{-2} \exp(\mathrm{i}\varphi_{-2}) \right) d\tau'$. Under these conditions, for the intensity of the IR field equal to $I_{IR} = 3\times10^{11}\,\mathrm{W/cm^2}$, an implementation of MIT requires the following ratio between the amplitudes of the XUV spectral components $\tilde{E}_0 / \tilde{E}_{-2} \approx 1{:}14$.

APPENDIX C

THE THREE-LEVEL ATOMS COUPLED TO IR FIELD: RESONANCE POLARIZATION AND EXCITATION PROBABILITY IN FLO-QUET FORMALISM[10]

In this appendix, we find the high frequency polarization and the probability of atomic excitation from the ground state (which determines the ionization yield in the combined IR+XUV radiation) for three-level atoms using Floquet formalism.

Selection rules for a dipole transition put some restrictions on the states $|1\rangle$, $|2\rangle$ and $|3\rangle$, for which such model is applicable. Let us assume that the ground state has an orbital quantum number l. For the case of the linearly polarized fields, it means that one of the excited states, for example, the state $|3\rangle$, should have the orbital quantum number equal to $l \pm 1$ in order that state to be coupled to the ground state by the HF XUV field. Then the state $|2\rangle$ should have the orbital quantum number equal to $l \pm 2$ or l in order to be coupled to the state $|3\rangle$ by the IR field. For example, let us consider a linearly polarized XUV field, which, according to the selection rule $\Delta l = \pm 1$, couples the ground state $1s^2$ ($l = 0$) with the $1s2p$ ($l = 1$) state of helium, and the linearly polarized IR field with relatively low frequency, which couples that excited $1s2p$ state only to the close-by excited state $1s2s$ ($l = 0$). In this case, $|1\rangle = 1s^2$, $|2\rangle = 1s2s$, $|3\rangle = 1s2p$.

---

[10] Reprinted with permission from "Coherent forward scattering of gamma-ray and XUV radiation in the medium with the modulated quasi-resonant transition" by T.R. Akhmedzhanov, V.A. Antonov and O. Kocharovskaya, 2016, J. Phys. B: At. Mol. Opt. Phys., vol. 49**,** pp. 205602, Copyright [2016] by IOP Publishing.

The IR field mixing up two excited levels leads to appearance of two Floquet states. According to Eqs (VI.27), the wave function of the IR-field-dressed atom can be represented in the Floquet basis as follows:

$$\left|\psi\right\rangle = c_1\left|1\right\rangle + \sum_{i=1,2} c_{\lambda_i} \exp(-\mathrm{i}\lambda_i(\tau + \varphi_M / \omega_{IR}))\left|\Phi_{\lambda_i}(\tau)\right\rangle. \tag{C.1}$$

Here λ_i is the quasi-energy of the i^{th} Floquet state

$$\left|\Phi_{\lambda_i}(\tau)\right\rangle = \sum_{m=-\infty}^{+\infty} \exp(-\mathrm{i}m(\omega_{IR}\tau + \varphi_M))\left(a_m^{i;2}\left|2\right\rangle + a_m^{i;3}\left|3\right\rangle\right), \tag{C.2}$$

c_{λ_i} is its amplitude, and φ_M is the phase of the IR field. In the first order of the perturbation theory, according to Eqs. (VI.29), the amplitudes of excitation of the corresponding Floquet states under the action of the XUV field can be calculated as follows:

$$c_{\lambda_i} = \frac{\mathrm{i}}{\hbar}\int_{-\infty}^{\tau} \exp(\mathrm{i}\lambda_i\tau')\left\langle\Phi_{\lambda_i}\left|H_{HF}(\tau')\right|1\right\rangle d\tau',\ c_1 \approx 1, \tag{C.3}$$

where $H_{HF} = \frac{1}{2}\exp(-\mathrm{i}\omega\tau)\tilde{E}_{XUV}(\tau)\sum_3 d_{31}\left|3\right\rangle\left\langle 1\right|$ is the Hamiltonian describing excitation of the atom by XUV field in rotating wave approximation (RWA) and XUV field is assumed to be of finite duration. According to Eqs. (VI.30) and (VI.31), the high frequency polarization and the probability of atomic excitation from the ground state (which determines the ionization yield in the combined IR+XUV radiation), are as follows:

$$\tilde{P}(\tau) = \frac{\mathrm{i}N\left|d_{31}\right|^2}{\hbar}\sum_i e^{-\mathrm{i}(\lambda_i-\omega)\tau}\left\langle 3\middle|\Phi_{\lambda_i}\right\rangle\int_{-\infty}^{\tau}\exp(\mathrm{i}(\lambda_i-\omega)\tau')\tilde{E}_{XUV}(\tau)\left\langle\Phi_{\lambda_i}\middle|3\right\rangle d\tau' \tag{C.4}$$

,

$$P_{excitation} = \sum_i \left| \frac{\mathrm{i}d_{31}}{2\hbar} \int_{-\infty}^{\tau} \exp(\mathrm{i}(\lambda_i - \omega)\tau') \tilde{E}_{XUV}(\tau) \left\langle \Phi_{\lambda_i} \middle| 3 \right\rangle d\tau' \right|^2, \quad \text{(C.5)}$$

where $\left\langle 3 \middle| \Phi_{\lambda_i} \right\rangle = \sum_m \exp(-\mathrm{i}m(\omega_{IR}\tau + \varphi_M)) a_m^{i;3}$. Combining equation for polarization (C.4) with the wave equation for the field envelope in Eq. (VI.5), one can analyze the dynamics of XUV field during its propagation through the dressed medium.

Neighboring "steps" of each ladder (i.e. the closest spectral components of the same Floquet state) are separated by frequency of the IR field, ω_{IR}. Due to the dipole transition selection rules, $a_m^{i;2}$ are not zeroes only for the odd m and $a_m^{i;3}$ are not zeroes only for the even m [24]. In other words, "even" steps of each Floquet state contain only the state $|3\rangle = 1s2p$, while "odd" steps contain only the state $|2\rangle = 1s2s$. Therefore, neighboring "steps" of the same parity are separated by doubled frequency of the IR field.

Considering the incident XUV field in the form of a spectral comb, $E_{HF} = \frac{1}{2}\sum_n \tilde{E}_{2n}(\tau)\exp(-\mathrm{i}(\omega + 2n\omega_{IR})\tau) + \text{c.c.}$, with a characteristic duration of each XUV spectral component much larger than the IR-field-cycle, $\tau_{XUV,env} \gg 1/\omega_{IR}$, we have

$$\tilde{P}(\tau) = \frac{\mathrm{i}N|d_{31}|^2}{\hbar} \sum_i e^{-\mathrm{i}(\lambda_i - \omega)\tau} \left(\sum_m a_{2m}^{i,3} \exp(-2\mathrm{i}m(\omega_{IR}\tau + \varphi_M)) \right) \times \int_{-\infty}^{\tau} \exp(\mathrm{i}(\lambda_i - \omega)\tau') \sum_n \tilde{E}_{-2n}(\tau') \exp(-2\mathrm{i}n\varphi_M) \left(a_{-2n}^{i,3} \right)^* d\tau', \quad \text{(C.6)}$$

$$P_{excitation} = \sum_i \left| \int_{-\infty}^{\infty} \frac{d_{31}}{2\hbar} \exp(\mathrm{i}(\lambda_i - \omega)\tau') \sum_n \tilde{E}_{-2n}(\tau') \exp(-2\mathrm{i}n\varphi_M) \left(a_{-2n}^{i,3} \right)^* d\tau' \right|^2 \quad \text{(C.7)}$$

.

APPENDIX D

GENERAL CASE OF AN ARBITRARY POLARIZED INCIDENT FIELD[11]

It is worth noting that the transitions $|1\rangle \leftrightarrow |4\rangle, |1\rangle \leftrightarrow |5\rangle$, which are not modulated by a z-polarized IR field, have non-zero dipole moment along y direction. They lead to amplification of a y-polarized component of an incident field, however, without formation of the sub-fs pulses, since the frequencies of these transitions are not affected by z-polarized IR field. It is worth to emphasize that modulation of $|1\rangle \leftrightarrow |2\rangle, |1\rangle \leftrightarrow |3\rangle$ transitions effectively reduces their dipole moments as compared to $|1\rangle \leftrightarrow |4\rangle, |1\rangle \leftrightarrow |5\rangle$ transitions, resulting in smaller magnitude of the gain at that transitions. For considered above value of modulation index $P_\omega = 4.45$ the effective dipole moment at the modulated transitions is approximately 3 times smaller compared to unperturbed transitions. It results in approximately 9 times lower gain and in approximately 9 times higher saturation intensity for the modulated transition. Thus, even in the case of high ratio between of the z-polarized over y-polarized components in the incident field, a saturation of the unmodulated transitions occurs at the shorter distances than at the modulated transitions. The saturation of the unmodulated transition leads to increase the ground state population due to population depletion of levels $|4\rangle$ and $|5\rangle$, resulting in decrease of population inversion at each of two transitions $|1\rangle \leftrightarrow |2\rangle$ and $|1\rangle \leftrightarrow |3\rangle$ and, accordingly, to further reduced gain for a z-polarized component of an incident X-ray radiation.

---

[11]The related work "Formation and amplification of sub-femtosecond X-ray pulses in a plasma medium of the hydrogen-like ions with a modulated resonant transition" by T.R. Akhmedzhanov et al. will be submitted to journal publication soon..

Therefore, it is important to investigate an influence of a y-polarized component on amplification of a z-polarized component within a general 5-level model, including all four excited degenerate levels.

Let us assume now that at the entrance to the medium, x=0, the X-ray radiation has the form

$$\vec{E}_{X-ray,inc}(t) = \frac{1}{2}\vec{z}_0\tilde{E}_{z,0}(t)\exp\left\{-i\,\omega_{z,0}t\right\} + \text{c.c.} + \frac{1}{2}\vec{y}_0\tilde{E}_{y,0}(t)\exp\left\{-i\,\omega_{y,0}t\right\} + \text{c.c.} \qquad \text{(D.1)}$$

,

where $E_{z,0}$ and $E_{y,0}$ are the slowly varying envelopes of z-polarized and y-polarized components of incident radiation, $\omega_{z,0}$ and $\omega_{y,0}$ are their carrier frequencies, and c.c. stands for complex conjugation. The radiation (D.1) is chosen to be near-resonant to a transition from the ground state |1⟩ to the first excited bound atomic state, $\omega_0 \approx \omega_{21}^0$ (where ω_{21}^0 is the unperturbed frequency of the resonant transition).

Propagation of X-ray radiation through medium is described by wave equation

$$\frac{\partial^2\vec{E}_{X-ray}}{\partial x^2} - \frac{\varepsilon}{c^2}\frac{\partial^2\vec{E}_{X-ray}}{\partial t^2} = \frac{4\pi}{c^2}\frac{\partial^2\vec{P}}{\partial t^2}\ , \qquad \text{(D.2)}$$

where $\vec{E}_{X-ray} = \vec{z}_0E_z + \vec{y}_0E_y$ is X-ray field strength, $\vec{P}$ is the resonant polarization.

We take into account now the following states of atomic hydrogen: the ground state |1s⟩, denoted as |1⟩, and four degenerate first excited states: |2⟩= (|2s⟩+|2p,m=0⟩)/√2, |3⟩==(|2s⟩–|2p,m=0⟩)/√2, |4⟩==|2p,m=1⟩, |5⟩==|2p,m=–1⟩. Within this approximation, the resonant polarization is defined by density matrix elements ρ_{ij}:

$$\vec{P}(\vec{r},t) = N\left(\vec{d}_{12}\rho_{21} + \vec{d}_{13}\rho_{31} + \vec{d}_{14}\rho_{41} + \vec{d}_{15}\rho_{51} + \text{c.c.}\right), \tag{D.3}$$

where N is ions concentration and $\vec{d}_{ij}$ is dipole moment between states $|i\rangle$ and $|j\rangle$. Within 5 level model, all the non-zero dipole moments are given by:

$$\begin{gathered}
\vec{d}_{12} = \vec{d}_{1s\leftrightarrow 2p,m=0}\Big/\sqrt{2} = \vec{z}_0 d_{\|}, \quad \vec{d}_{13} = -\vec{d}_{1s\leftrightarrow 2p,m=0}\Big/\sqrt{2} = -\vec{z}_0 d_{\|}, \\
\vec{d}_{22} = \vec{d}_{2s\leftrightarrow 2p,m=0} = \vec{z}_0 d_{av}, \quad \vec{d}_{33} = -\vec{d}_{2s\leftrightarrow 2p,m=0} = -\vec{z}_0 d_{av}, \\
\vec{d}_{14} = \vec{d}_{1s\leftrightarrow 2p,m=1} = i\vec{y}_0 d_{\perp}, \quad \vec{d}_{15} = \vec{d}_{1s\leftrightarrow 2p,m=-1} = i\vec{y}_0 d_{\perp}, \\
\vec{d}_{ij} = \vec{d}^{*}_{ji}
\end{gathered} \tag{D.4}$$

In atomic units $d_{\|} = d_{\perp} = \dfrac{2^7}{3^5 Z} \equiv d$, and $d_{av} = 3/Z$, where Z is ion nucleus charge.

Under the action of both X-ray and IR field, the evolution of density matrix elements is given by:

$$\begin{gathered}
\dot{\rho}_{11} = +\gamma_{11}(\rho_{22} + \rho_{33} + \rho_{44} + \rho_{55}) - i\left[\mathrm{H},\rho\right]_{11} \\
\dot{\rho}_{ij} = -\gamma_{ij}\rho_{ij} - i\left[\mathrm{H},\rho\right]_{ij}, ij \neq 11 \\
\mathrm{H} = \begin{pmatrix}
\omega_1 & -E_z d_{\|} & E_z d_{\|} & iE_y d_{\perp} & iE_y d_{\perp} \\
-E_z d_{\|} & \omega_2 - \tilde{E}_{IR}\cos\left\{-i\Omega\left(t - xn_{pl}/c\right)\right\} & 0 & 0 & 0 \\
E_z d_{\|} & 0 & \omega_3 + \tilde{E}_{IR}\cos\left\{-i\Omega\left(t - xn_{pl}/c\right)\right\} & 0 & 0 \\
-iE_y d_{\perp} & 0 & 0 & \omega_4 & 0 \\
-iE_y d_{\perp} & 0 & 0 & 0 & \omega_5
\end{pmatrix}
\end{gathered} \tag{D.5}$$

Here ω_i is energy of atomic level $|i\rangle$. With quadratic Stark effect taken into account,

$\omega_1 = -\dfrac{Z^2}{2}\left(1 + \dfrac{9}{256}F_c^2\right), \omega_2 = \omega_3 = -\dfrac{Z^2}{8}\left(1 + \dfrac{7}{4}F_c^2\right), \omega_4 = \omega_5 = -\dfrac{Z^2}{8}\left(1 + \dfrac{39}{8}F_c^2\right)$ where

$F_c = \left(\dfrac{2}{Z}\right)^3 \tilde{E}_{IR}$ [113].

The decay rates γ_{ij} are defined as $\gamma_{12} \approx \gamma_{13} \approx \gamma_{coll} + \Gamma_{ion}/2 + \Gamma_{radiative}/2$, $\gamma_{14} \approx \gamma_{15} \approx \gamma_{coll} + \Gamma_{ion,2}/2 + \Gamma_{radiative}/2$, $\gamma_{23} \approx \gamma_{coll} + \Gamma_{ion} + \Gamma_{radiative}$, $\gamma_{24} = \gamma_{25} = \gamma_{34} = \gamma_{35} \approx \gamma_{coll} + \Gamma_{ion}/2 + \Gamma_{ion,2}/2 + \Gamma_{radiative}$, $\gamma_{45} \approx \gamma_{coll} + \Gamma_{ion,2} + \Gamma_{radiative}$, $\gamma_{22} \approx \gamma_{33} \approx \Gamma_{ion} + \Gamma_{radiative}$, $\gamma_{44} = \gamma_{55} \approx \approx \Gamma_{ion,2} + \Gamma_{radiative}$, $\gamma_{11} \approx \Gamma_{radiative}$, where γ_{coll} and Γ_{ion} are collisional broadening and ionization decay rates correspondingly. $\Gamma_{radiative}$ are radiative decay rates, which could be found in [157].Collisional broadening was estimated according to [158], $\Gamma_{ion} \approx \frac{Z^2}{16}\sqrt{\frac{3F_c}{\pi}}\left[\left(\frac{4}{F_c}\right)e^{+3} + \left(\frac{4}{F_c}\right)^3 e^{-3}\right]\exp\left\{-\frac{2}{3F_c}\right\}$ [113]. $\Gamma_{ion,2}$ can be found using Popov-Perelomov-Terentiev equations [112]We neglect Doppler broadening of transitions since we consider ion temperatures on the order of 1 eV as it is typical in recombination X-ray plasma lasers [77], resulting in Doppler broadening comparable or less than collisional broadening. It is worth noting that for parameters we consider in the paper, $\gamma_{ij} \ll \Omega$.

Let us seek for a partial solution in the form

$$\begin{aligned}
&\vec{E}(x,t) = \frac{1}{2}\left(\vec{y}_0\tilde{E}_y(x,t) + \vec{z}_0\tilde{E}_z(x,t)\right)e^{-i(\omega t - kx)} + \text{c.c.} \\
&\rho_{12}(x,t) = \tilde{\rho}_{12}(x,t)e^{i\omega t - ikx}, \\
&\rho_{13}(x,t) = \tilde{\rho}_{13}(x,t)e^{i\omega t - ikx}, \\
&\rho_{14}(x,t) = \tilde{\rho}_{14}(x,t)e^{i\omega t - ikx}, \\
&\rho_{15}(x,t) = \tilde{\rho}_{15}(x,t)e^{i\omega t - ikx}, \\
&\rho_{ij}(x,t) = \tilde{\rho}_{ij}(x,t), ij \neq 12,13,14,15
\end{aligned} \quad , \qquad \text{(D.6)}$$

where $\tilde{E}_v(x,t)$, $v = \overline{y,z}$, and $\tilde{\rho}_{ij}(x,t)$ are the slowly-varying amplitudes of the field and decay matrix elements, respectively, that is $\left|\frac{1}{\tilde{E}_v}\frac{\partial \tilde{E}_v}{\partial t}\right| \ll \omega$, $\left|\frac{1}{\tilde{E}_v}\frac{\partial}{\partial x}\tilde{E}_v\right| \ll k$, and

$\left|\frac{1}{\tilde{\rho}_{ij}(\vec{r},t)}\frac{\partial\tilde{\rho}_{ij}(\vec{r},t)}{\partial t}\right| \ll \omega, \left|\frac{1}{\tilde{\rho}_{ij}(\vec{r},t)}\frac{\partial}{\partial x}\tilde{\rho}_{ij}(\vec{r},t)\right| \ll k$. In such a case, within the rotating wave approximation and approximation of plane waves, we get

$$
\begin{aligned}
&k = \frac{\omega}{c},\\
&\frac{\partial\tilde{E}_z}{\partial x} = i4\pi\frac{\omega N d_{\parallel}}{c\sqrt{\varepsilon}}\left(\rho_{21}-\rho_{31}\right),,\\
&\frac{\partial\tilde{E}_y}{\partial x} = -4\pi\frac{\omega N d_{\perp}}{c\sqrt{\varepsilon}}\left(\rho_{41}+\rho_{51}\right)
\end{aligned}
\qquad \text{(D.7)}
$$

and

$$
\begin{aligned}
\dot{\tilde{\rho}}_{11} &= +\gamma_{11}(\tilde{\rho}_{22}+\tilde{\rho}_{33}+\tilde{\rho}_{44}+\tilde{\rho}_{55})+\frac{i\tilde{E}_z^* d_{\parallel}}{2}\left(\tilde{\rho}_{21}-\tilde{\rho}_{31}\right)+\frac{i\tilde{E}_z d_{\parallel}}{2}\left(\tilde{\rho}_{13}-\tilde{\rho}_{12}\right)-\frac{\tilde{E}_y d_{\perp}}{2}\left(\rho_{14}+\rho_{15}\right)-\frac{\tilde{E}_y^* d_{\perp}}{2}\left(\rho_{41}+\rho_{51}\right)\\
\dot{\tilde{\rho}}_{22} &= -\gamma_{22}\tilde{\rho}_{22}+\frac{i\tilde{E}_z d_{\parallel}}{2}\tilde{\rho}_{12}-\frac{i\tilde{E}_z^* d_{\parallel}}{2}\tilde{\rho}_{21}\\
\dot{\tilde{\rho}}_{33} &= -\gamma_{33}\tilde{\rho}_{33}+\frac{i\tilde{E}_z^* d_{\parallel}}{2}\rho_{31}-\frac{i\tilde{E}_z d_{\parallel}}{2}\rho_{13}\\
\dot{\tilde{\rho}}_{44} &= -\gamma_{44}\tilde{\rho}_{44}-i\tilde{\rho}_{14}\frac{i\tilde{E}_y d_{\perp}}{2}-i\tilde{\rho}_{41}\frac{i\tilde{E}_y^* d_{\perp}}{2}\\
\dot{\tilde{\rho}}_{55} &= -\gamma_{55}\tilde{\rho}_{55}-i\tilde{\rho}_{15}\frac{i\tilde{E}_y d_{\perp}}{2}-i\tilde{\rho}_{51}\frac{i\tilde{E}_y^* d_{\perp}}{2}\\
\dot{\tilde{\rho}}_{12} &= -\gamma_{12}\tilde{\rho}_{12}-i\tilde{\rho}_{12}(\omega_1-\omega_2+\omega+\tilde{E}_{IR}d_{av}\cos\left(\Omega\left[\tau+\left(1-n_{pl}\right)x/c\right]\right))-\frac{i\tilde{E}_z^* d_{\parallel}}{2}\left(\rho_{32}-\rho_{22}+\rho_{11}\right)+\frac{i\tilde{E}_y^* d_{\perp}}{2}\left(i\rho_{52}+i\rho_{42}\right)\\
\dot{\tilde{\rho}}_{13} &= -\gamma_{13}\tilde{\rho}_{13}-i\tilde{\rho}_{13}(\omega_1-\omega_3+\omega-\tilde{E}_{IR}d_{av}\cos\left(\Omega\left[\tau+\left(1-n_{pl}\right)x/c\right]\right))-\frac{i\tilde{E}_z^* d_{\parallel}}{2}\left(-\rho_{23}+\rho_{33}-\rho_{11}\right)+\frac{i\tilde{E}_y^* d_{\perp}}{2}\left(i\rho_{53}+i\rho_{43}\right)\\
\dot{\tilde{\rho}}_{14} &= -\gamma_{14}\tilde{\rho}_{14}-i\tilde{\rho}_{14}(\omega_1-\omega_4+\omega)-\frac{i\tilde{E}_z^* d_{\parallel}}{2}\left(-\rho_{24}+\rho_{34}\right)+\frac{i\tilde{E}_y^* d_{\perp}}{2}\left(i\rho_{44}+i\rho_{54}-i\rho_{11}\right)\\
\dot{\tilde{\rho}}_{15} &= -\gamma_{15}\tilde{\rho}_{15}-i\tilde{\rho}_{15}(\omega_1-\omega_5+\omega)-\frac{i\tilde{E}_z^* d_{\parallel}}{2}\left(-\rho_{25}+\rho_{35}\right)+\frac{i\tilde{E}_y^* d_{\perp}}{2}\left(i\rho_{55}+i\rho_{45}-i\rho_{11}\right)\\
\dot{\tilde{\rho}}_{23} &= -\gamma_{23}\tilde{\rho}_{23}-i\tilde{\rho}_{23}(\omega_2-\omega_3-2\tilde{E}_{IR}d_{av}\cos\left(\Omega\left[\tau+\left(1-n_{pl}\right)x/c\right]\right))+\frac{i\tilde{E}_z^* d_{\parallel}}{2}\tilde{\rho}_{21}+\frac{i\tilde{E}_z d_{\parallel}}{2}\tilde{\rho}_{13}\\
\dot{\tilde{\rho}}_{24} &= -\gamma_{24}\tilde{\rho}_{24}-i\tilde{\rho}_{24}(\omega_2-\omega_4-\tilde{E}_{IR}d_{av}\cos\left(\Omega\left[\tau+\left(1-n_{pl}\right)x/c\right]\right))+\frac{i\tilde{E}_z d_{\parallel}\tilde{\rho}_{14}}{2}+\frac{\tilde{E}_y^* d_{\perp}\tilde{\rho}_{21}}{2}\\
\dot{\tilde{\rho}}_{25} &= -\gamma_{25}\tilde{\rho}_{25}-i\tilde{\rho}_{25}(\omega_2-\omega_5-\tilde{E}_{IR}d_{av}\cos\left(\Omega\left[\tau+\left(1-n_{pl}\right)x/c\right]\right))+\frac{i\tilde{E}_z d_{\parallel}\rho_{15}}{2}+\frac{\tilde{E}_y^* d_{\perp}\rho_{21}}{2}\\
\dot{\tilde{\rho}}_{34} &= -\gamma_{34}\tilde{\rho}_{34}-i\tilde{\rho}_{34}(\omega_3-\omega_4+\tilde{E}_{IR}d_{av}\cos\left(\Omega\left[\tau+\left(1-n_{pl}\right)x/c\right]\right))-\frac{i\tilde{E}_z d_{\parallel}\tilde{\rho}_{14}}{2}+\frac{\tilde{E}_y^* d_{\perp}\tilde{\rho}_{31}}{2}\\
\dot{\tilde{\rho}}_{35} &= -\gamma_{35}\tilde{\rho}_{35}-i\tilde{\rho}_{35}(\omega_3-\omega_5+\tilde{E}_{IR}d_{av}\cos\left(\Omega\left[\tau+\left(1-n_{pl}\right)x/c\right]\right))-\frac{i\tilde{E}_z d_{\parallel}\tilde{\rho}_{15}}{2}+\frac{\tilde{E}_y^* d_{\perp}\tilde{\rho}_{31}}{2}\\
\dot{\tilde{\rho}}_{45} &= -\gamma_{45}\tilde{\rho}_{45}-i\tilde{\rho}_{45}(\omega_4-\omega_5)-i\tilde{\rho}_{15}\frac{i\tilde{E}_y d_{\perp}}{2}-i\tilde{\rho}_{41}\frac{i\tilde{E}_y^* d_{\perp}}{2}
\end{aligned}
\qquad \text{(D.8)}
$$

where we have introduced local time $\tau = t - x/c$. Equations (D.7) and (D.8) along with initial conditions

$$\tilde{\rho}_{ij}(x, t=0) = \tilde{\rho}_{ij}^{(0)}, \tag{D.9}$$

and boundary conditions (D.1) describe propagation of the X-ray field in *x*-direction.

In order to model amplification of incident X-ray field (D.1) through inverted medium of X-ray plasma based lasers, we assume at the moment $t = 0$ all the ions have equal probability to be in the excited states $|2\rangle, |3\rangle, |4\rangle, |5\rangle$ and there are no coherencies. Namely, initial conditions (D.9) become:

$$\begin{aligned} &\tilde{\rho}_{22}(x, t=0) = \tilde{\rho}_{33}(x, t=0) = \tilde{\rho}_{44}(x, t=0) = \tilde{\rho}_{55}(x, t=0) = 0.25, \\ &\tilde{\rho}_{ij}(x, t=0) = 0, ij \neq 22, 33, 44, 55 \end{aligned} \tag{D.10}$$

The results of the numerical solution of these set of equations in Li III plasma for the same parameters of the plasma as in Figure 36 and for different values of intensity of an incident y-polarized component are presented in Figure 38.

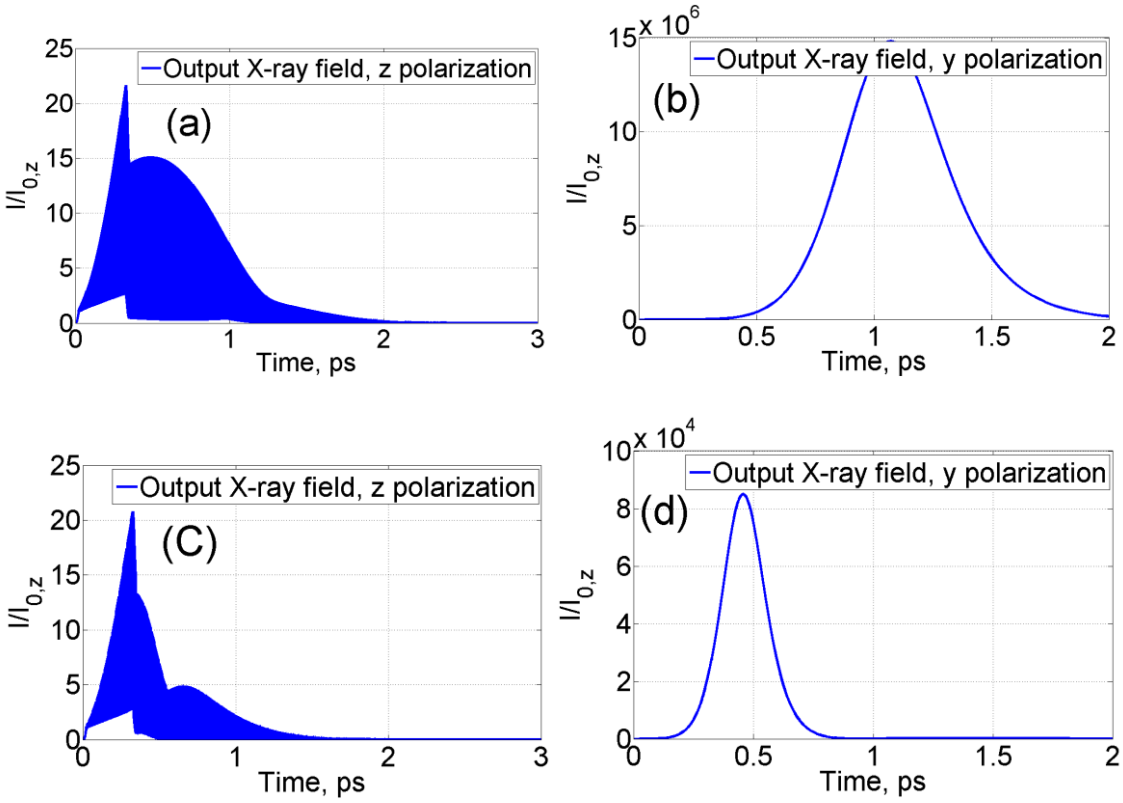

Figure 38. Time-dependence of intensities of z-polarized (a) and b)) and y-polarized (c) and d)) components of X-ray radiation after propagation through 1.25 mm of inverted Li III plasma. The parameters of the plasma, IR field and envelope of the incident field are the same as in Figure 36. (a) and (b) correspond to $I_z(x=0)=I_y(x=0)=10^3 W/cm^2$, (b) and (d) correspond to $I_z(x=0)=I_y(x=0)=10^6 W/cm^2$.

Comparison of Figure 36 (a), Figure 38 (a) and (c) clearly shows that the presence of highly amplified y-polarized component practically does not affect amplification of the seeding z-polarized field, which duration is a few times shorter than a polarization decay time of the resonant transition. The peak of y-polarized field essentially delays as compared to the peak of an amplified the z-polarized seeding pulse. The reason for this delay is that an y-polarized emission occurs in a superradiant (SR) regime. Indeed,

cooperative frequency for chosen parameters of the medium $\Omega_c = \sqrt{\frac{3Nc\gamma_{sp}\lambda_{41}^2}{8\pi}} \approx 1\times 10^{13}\,Hz$ (λ_{41} is $|4\rangle \leftrightarrow |1\rangle$ transition wavelength and γ_{sp} is spontaneous emission decay rate) exceeds the line broadening $2/T_2 \approx 4.7\times 10^{12}\,Hz$. As a result of this delay, saturation of the unmodulated transitions and correspondingly a reduction of gain at the modulated transition influences only an amplified stage of free induction decay of z-polarized radiation. It is worth to note that an increase of an intensity of an y-polarized component of an incident field results in both delay time and SR pulse duration reduction due to induced nature of the superradiant process, enhancing an influence of an amplified y-polarized component on the shape of the amplified free induction decay in the vicinity of the peak of a y-polarized SR pulse (see a cusp in Figure 38 (c)) due to gain reduction, followed by a restoration of a gain at the back edge of the SR pulse. The investigation of the time dependence of z-polarized component both at $I_y(x=0) = 10^3 W/cm^2$ and at $I_y(x=0) = 10^6 W/cm^2$ (Figure 38 (a) and (c)) with much higher resolution reveals the same structure of ultra-short pulse train with duration about 900 as in the case $I_y(x=0) = 0$ (Figure 36(a)). The amplitude of the pulses in the train is defined by the total radiation pulse envelope, according to Figure 38 (a) and (c). The shape of the pulses starts to destroy only in the tail of the envelope pulse in a vicinity of 1ps time.